

A VLA SURVEY FOR FAINT COMPACT RADIO SOURCES IN THE ORION NEBULA CLUSTER

PATRICK D. SHEEHAN¹, JOSH A. EISNER¹, RITA K. MANN², AND JONATHAN P. WILLIAMS³

¹Steward Observatory, University of Arizona, 933 N. Cherry Avenue, Tucson, AZ, 85721

²National Research Council Canada, 5071 West Saanich Road, Victoria, BC, V9E 2E7, Canada and

³Institute for Astronomy, University of Hawaii at Manoa, Honolulu, HI 96822

Draft version February 12, 2022

ABSTRACT

We present Karl G. Jansky Very Large Array (VLA) 1.3 cm, 3.6 cm, and 6 cm continuum maps of compact radio sources in the Orion Nebular Cluster. We mosaicked 34 square arcminutes at 1.3 cm, 70 square arcminutes at 3.6 cm and 109 square arcminutes at 6 cm, containing 778 near-infrared detected YSOs and 190 *HST*-identified proplyds (with significant overlap between those characterizations). We detected radio emission from 175 compact radio sources in the ONC, including 26 sources that were detected for the first time at these wavelengths. For each detected source we fit a simple free-free and dust emission model to characterize the radio emission. We extrapolate the free-free emission spectrum model for each source to ALMA bands to illustrate how these measurements could be used to correctly measure protoplanetary disk dust masses from sub-millimeter flux measurements. Finally, we compare the fluxes measured in this survey with previously measured fluxes for our targets, as well as four separate epochs of 1.3 cm data, to search for and quantify variability of our sources.

Subject headings:

1. INTRODUCTION

The Orion Nebular Cluster (ONC) presents an excellent example of star formation in a richly clustered environment, typical of star formation in our galaxy. Near-infrared surveys of the ONC find >700 YSOs, most of which are likely to harbor protoplanetary disks (Hillenbrand & Carpenter 2000). *Hubble Space Telescope* (*HST*) images of the ONC also reveal ionized disks and dusty disks silhouetted against the backdrop of nebular emission (e.g., O'Dell & Wen 1994; Bally et al. 1998a; Smith et al. 2005; Ricci et al. 2008).

The O6 star θ^1 Ori C, located in the central Trapezium Cluster, produces intense UV radiation that photoevaporates many of the nearby protoplanetary disks. The hot gas ionized by this intense radiation expands freely and flows away at the local sound speed into lower pressure regions (e.g., Henney & Arthur 1998). The ionized winds from the protoplanetary disks emit strong free-free emission at radio wavelengths (e.g., Garay et al. 1987; Churchwell et al. 1987).

Compact radio sources have long been known in the ONC (e.g., Moran et al. 1982; Garay et al. 1987; Churchwell et al. 1987; Felli et al. 1993a; Zapata et al. 2004a,b). They were first identified as free-free emission by Garay et al. (1987), and suggested to be the ionized material evaporated from protostellar disks by Churchwell et al. (1987). Observations of the ONC with the *Hubble Space Telescope* firmly established these compact structures as externally ionized protoplanetary disks (e.g., O'Dell et al. 1993).

Measurements of the masses of protoplanetary disks are crucial for understanding evolution, as well as potential for planet formation. Disk mass measurements are typically made by observing dust continuum emission at long wavelengths, where the emission is optically thin and probes the entirety of the disk (e.g., Beckwith et al.

1990). Towards this end, a host of millimeter interferometric surveys of the ONC have previously been carried out (e.g. Mundy et al. 1995; Bally et al. 1998b; Williams et al. 2005; Eisner & Carpenter 2006; Eisner et al. 2008; Mann & Williams 2009, 2010; Mann et al. 2014).

These surveys are complicated by potential contamination of the millimeter dust continuum emission by free-free emission from ionized disk winds. Disk mass measurements are facilitated at shorter wavelengths, of 1.3 mm or 870 μ m, where the ratio of dust emission to free-free emission is expected to be more favorable. Even here, however, free-free emission can contribute significantly to the observed brightnesses of the sources (e.g., Eisner et al. 2008; Mann & Williams 2009, 2010; Mann et al. 2014).

Observations at longer radio wavelengths can help to constrain the free-free contribution at shorter wavelengths. Free-free emission has a flat spectrum ($F_\nu \propto \nu^{-0.1}$) when optically thin, as is expected to be true at millimeter and centimeter wavelengths (e.g. Eisner et al. 2008; Mann & Williams 2009, 2010; Mann et al. 2014). Optically thick free-free emission can span a range of spectral indices, but the emission usually only becomes optically thick at wavelengths longer than ~ 10 cm (e.g. Eisner et al. 2008). Dust emission, however, has a steep spectral index ($F_\nu \propto \nu^{2+\beta}$, $\beta = 0 - 2$) which falls off rapidly at longer wavelengths. Free-free emission can therefore be constrained at longer radio wavelengths where the contribution from dust emission to the flux is small. Radio fluxes may also in some cases be affected by magnetospheric flaring from young stars, exhibiting gyrosynchrotron emission with a steep negative spectral index when optically thin ($F_\nu \propto \nu^{-0.7}$; e.g. Feigelson & Montmerle 1999; Rivilla et al. 2015), or a steep positive spectral index when optically thick at lower frequencies ($F_\nu \propto \nu^{2.5}$).

Previous studies have used the VLA to search for compact radio sources in the ONC (e.g., Felli et al. 1993a;

TABLE 1

Band	Configuration	Date	Int. Time [min]	RMS [μJy]	Peak RMS [μJy]	Beam	No. Beams	Total Detections	> 6σ Detections	> 4.5σ Detections
1.3 cm	B	Nov. 10, 2013	62	33	~ 93	0.33'' × 0.21''	1.5 × 10 ⁶	79	57	22
6 cm	A	Mar. 3, 2014	7	37	~ 150	0.40'' × 0.28''	3.1 × 10 ⁶	108	87	21
3.6 cm	A	Mar. 3, 2014	9.5	30	~ 70	0.24'' × 0.18''	5.1 × 10 ⁶	98	80	18
1.3 cm	A	Mar. 3, 2014	49	25	~ 50	0.09'' × 0.08''	14.9 × 10 ⁶	70	54	16
1.3 cm	A	Mar. 7, 2014	49	26	~ 100	0.08'' × 0.08''	15.7 × 10 ⁶	73	56	17
1.3 cm	A	May 3, 2014	36.5	22	~ 85	0.10'' × 0.07''	14.6 × 10 ⁶	89	67	22
1.3 cm	A & B combined	12	~ 50	0.09'' × 0.09''	12.4 × 10 ⁶	126	98	28

^a > 6σ Detections refers to the number of sources detected in each map because they pass the blind detection threshold. > 4.5σ Detections refers to the additional sources detected in a catalog driven search, and Total Detections is the sum of those numbers.

Zapata et al. 2004a), and fluxes produced by those studies have been used to correct for free-free contamination in disk mass studies (e.g., Eisner et al. 2008; Mann & Williams 2010; Mann et al. 2014). The expanded capabilities of the VLA correlator (Perley et al. 2009), now enable surveys of much higher sensitivity than were previously possible. More recent surveys have taken advantage of this increase in sensitivity to map star forming regions, including the ONC at 4.5 GHz and 7.5 GHz (Dzib et al. 2013; Kounkel et al. 2014; Forbrich et al. 2016). This enhanced sensitivity is well-matched to the deeper observations now enabled with ALMA.

Here we present new high resolution Karl G. Jansky Very Large Array (henceforth JVLA to avoid confusion with previous surveys using the original VLA) maps of the ONC at 1.3 cm, 3.6 cm, and 6 cm to study the free-free emission from ONC cluster members. In Section 2 we describe our observations and maps of the ONC. In Section 3 we detail our methodology for searching for compact radio sources, as well as our model for characterizing the free-free emission. In Section 4 we compare our results to previous catalogs of compact radio sources in the ONC, discuss the nature of the sources we detect, and show that our measurements are crucial for accurately measuring disk masses of protoplanetary disks from both current and future submillimeter surveys.

2. OBSERVATIONS & DATA REDUCTION

We imaged the Orion Nebula Cluster in 1.3 cm, 3.6 cm, and 6 cm wavelength continuum emission with the JVLA between November 2013 and May 2014. The 3.6 cm and 6 cm maps were observed using the ‘A’ configuration (baselines ranging from 680 m to 36 km), and the 1.3 cm data were taken in three epochs with the ‘A’ configuration and one epoch with the ‘B’ configuration (baselines ranging from 210 m to 11 km). Details of the observations and maps are provided in Table 1.

The 3.6 cm and 6 cm data were taken simultaneously in 32 128 MHz bands, split evenly between 3.6 cm and 6 cm. Each band contained 64 2 MHz channels, and the bands were arranged continuously from 4.488 - 6.512 GHz at 6 cm and from 8.116 - 10.012 GHz at 3.6 cm, for a total of 2 GHz of continuum bandwidth each.

The field of view of the JVLA antenna primary beam at 6 cm, FWHM of 9'', encompasses all 778 YSOs from Hillenbrand & Carpenter (2000), and 196 of the 196 HST detected proplyds (Ricci et al. 2008). 141 of the 196 HST detected proplyds are also detected as sources in Hillenbrand & Carpenter (2000). We therefore use a single pointing to image the field at 6 cm. At 3.6 cm the field of view is 5', so we imaged the field with two pointings

that encompassed 778 YSOs and 187 *HST*-detected proplyds.

For a rectangular mosaic the Nyquist sampling theorem suggests that a pointing spacing of FWHM/2 or better is needed (e.g. Cornwell 1988), but since we are interested in compact sources, Nyquist sampling is not crucial (e.g. Eisner et al. 2008). At 3.6 cm the FWHM/2 is between 2.1' and 2.6' across the band. The two 3.6 cm pointings are separated by 2.4', so the map is sub-Nyquist sampled at the low frequency end of the band, but not at the high frequency end of the band.

The 1.3 cm data were taken in 64 128 MHz bands arranged from 17.976 - 26.024 GHz. Each band was composed of 64 2 MHz channels, for a total of 8 GHz of bandwidth. Most of the data, however, from 17.976 - 22.024 GHz is affected by significant RFI, so we exclude that data from our analysis. The 1.3 cm data therefore has an effective bandwidth of 4 GHz.

A field of view containing 778 YSOs and 193 *HST* detected proplyds was mosaicked using 7 pointings. A two dimensional map is Nyquist sampled if the pointing spacing is FWHM/ $\sqrt{3}$ or better, but since we are interested here in compact sources, Nyquist sampling is, again, not crucial. At 1.3 cm FWHM/ $\sqrt{3}$ is between 1.2' and 1.4' across the band. The mosaic spacings range between 1-2', so the map is largely not Nyquist sampled. We show the field of view of our observations for each band in Figure 1.

The data were calibrated and imaged using the CASA software package. Antenna-based complex gains were calculated using periodic observations of the quasar J0541-0541. Bandpass solutions for each antenna were calculated from observations of the quasar J0319+4130, and the overall flux density scale was calculated using models included in CASA for 3C48.

We produced maps of the ONC at each frequency by Fourier transforming the complex visibilities, using the mosaicking modes for the 1.3 cm and 3.6 cm maps. We weighted the data with a robust parameter of 0, which provided a good balance between the high sensitivity of normal weighting and the high spatial resolution of uniform weighting. We also used the multi-frequency synthesis option with nterms=1 for no source frequency dependence (Rau & Cornwell 2011). Our goal is to search for compact structures in the Orion Nebula, so we removed baselines shorter than 100 kλ from our data before inverting the visibilities. The spatial scales eliminated by this cut correspond to structures greater than 2'', meaning that large scale structure from the Orion Nebula has been resolved out of our maps. For these observations

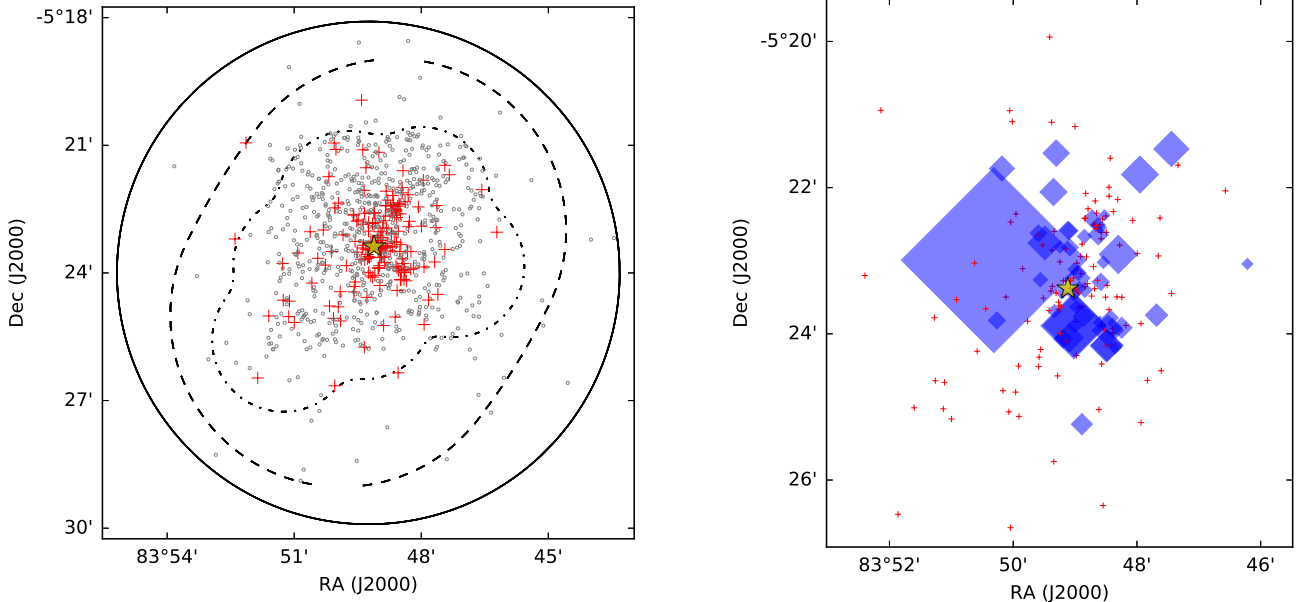


FIG. 1.— The fields we image, out to the 20% gain contour at 6 cm (solid) and the 10% gain contour at 3.6 cm (dashed) and 1.3 cm (dash-dotted) observations, with a yellow star representing the location of θ^1 Ori C. On the left we show all of the sources we detected in at least one of our bands with red plusses and the known sources surveyed but not detected with grey circles. On the right we show sources found to be variable with blue rectangles whose size is proportional to how variable the source is. The largest symbols represent a variability amplitude of 900% while the smallest represent an amplitude of 20%. The detected sources which are not variable are shown again with red plusses.

our reference frequencies are 5.5 GHz for the 6 cm map, 9 GHz for the 3.6 cm map, and 22.5 GHz for the 1.3 cm map. We image the 6 cm data out to the 20% gain contour at 5.5 GHz, and the smaller 3.6 cm and 1.3 cm maps out to the 10% gain contour at 9 GHz and 22 GHz respectively¹. We imaged each 1.3 cm epoch separately to study the variability of the bright sources, and together to increase our sensitivity to look for faint sources in the map.

We CLEANed the images using the Clark algorithm (Clark 1980). Sources above 10σ were initially identified for CLEANing by visual inspection. The maps were CLEANed down to the rms, as measured in source-free regions of the maps, listed in Table 1. Post-source detection, we could re-CLEAN the image using the new detections, however the sidelobes of these sources are low enough to be below the noise level, and the improvement by CLEANing them is minimal and the computational requirements are significant.

We used a single iteration of self-calibration on the 6 cm data, correcting for just the phases of our data from a model produced by an initial CLEANing of the data. This improved the rms ($\sim 50 \mu\text{Jy}$ to $\sim 40 \mu\text{Jy}$) in crowded regions of the map or near bright sources with significant beam artifacts.

We self-calibrated the data using a model produced from both fields simultaneously. We find that self-calibrating the fields separately and then imaging them jointly produced ringing in the image that was removed by self-calibrating the data together. We used two iterations of self-calibration, first solving for the phases from our initial model, and then solving for the amplitudes and

any residual phase errors in a second iteration. We apply amplitude self-calibration because it helps to remove residual artifacts around bright sources in our map. It does not change the flux in our maps markedly. This improved the rms from $\sim 80 \mu\text{Jy}$ near bright sources with significant beam artifacts to $\sim 45 \mu\text{Jy}$.

We self-calibrated fields including the brightest sources together, which is necessary to remove ringing like in the 3.6 cm maps, using a single iteration of self-calibration to correct phase errors in the data. The self-calibration improved the rms by as much as a factor of 3 near bright sources with significant beam artifacts (e.g. $\sim 50 \mu\text{Jy}$ to $\sim 20 \mu\text{Jy}$ for the combined 1.3 cm map, $\sim 100 \mu\text{Jy}$ to $\sim 35 \mu\text{Jy}$ for the 1.3 cm data taken on March 3, 2014).

After CLEANing, each map was corrected for attenuation by the primary beam, using the primary beam at the central frequency of each band. The bandwidth of our observations is a significant fraction of the central frequency, however, so the primary beam correction may vary significantly over the band. We have computed the error induced in wideband fluxes measured when correcting by the primary beam of the central frequency, rather than the appropriate primary beam for each channel, and find that this error is <5% for realistic spectral indices (-0.1-2).

Finally, we restored each map with a CLEAN beam whose size is determined by a Gaussian fit to the central peak of the dirty beam for that map. The size of this beam is given approximately by λ/B_{max} for the map, but the exact size and shape depend on the distribution of baselines in the uv -plane and the choice of weighting function. We list the beam sizes for each map in Table 1. After our initial CLEANing of the data we self-calibrated on the brightest sources in our maps to remove residual beam structure and improve the sensitivity, particularly in crowded regions.

¹ These correspond to the 33 and 10% gain contours for the low and high frequency 6 cm band edges respectively, the 16 and 6% gain contours for the 3.6 cm band edges, and the 14 and 6% gain contours for the 1.3 cm band edges.

3. ANALYSIS

3.1. Source Detection

In each of our VLA maps we search for sources detected above a certain signal-to-noise threshold. Our maps contain $> 10^6$ synthesized beams (see Table 1), so we must employ a relatively conservative threshold to ensure that we do not select noise spikes in the images as real detections. The noise in each map follows a Gaussian distribution (see Figure 2), so we expect $\ll 1$ noise spike to fall above a 6σ detection threshold. We therefore use 6σ as our detection limit.

We can also use catalogs of previously known source positions to target our search. We search our maps at the positions of > 700 near-infrared detected sources (Hillenbrand & Carpenter 2000) and ~ 200 *HST* detected proplyds (Ricci et al. 2008, with an overlap of about ~ 150 of the near-infrared detected sources). We also search the coordinates of known submillimeter sources detected with the SMA, CARMA, and ALMA that lack counterparts at infrared wavelengths (Eisner et al. 2008; Mann & Williams 2010; Mann et al. 2014). Finally, we search for compact radio sources which were detected with the VLA by previous surveys (Felli et al. 1993a; Kounkel et al. 2014). Due to the smaller number of synthesized beams being probed (~ 800), we expect $\ll 1$ noise spike to fall above a 4.5σ level. For each previously identified source we search for a detection above 4.5σ within a radius of $0.5''$, typical of the sizes of beams from these previous studies.

The rms at each pixel is calculated from a 128 by 128 pixel box surrounding that pixel in the residual map. The rms in the map is generally low ($\sim 25 \mu\text{Jy}$ in the 1.3 cm maps, $\sim 30 \mu\text{Jy}$ at 3.6 cm, and $\sim 37 \mu\text{Jy}$ at 6 cm). However, the central region of each map exhibits beam artifacts from a cluster of bright sources and poor sampling of large scale emission. The rms in these regions can be much higher than the rest of the map ($\sim 100 \mu\text{Jy}$ in the 1.3 cm maps, $\sim 70 \mu\text{Jy}$ at 3.6 cm, and $\sim 150 \mu\text{Jy}$

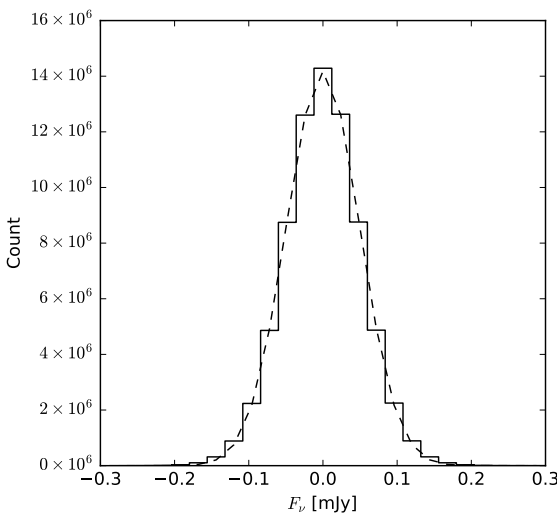


FIG. 2.— We show a histogram of all the pixel values within the 50% gain contour of our 6 cm residual map. We also show the best fit Gaussian to the distribution with the dashed line. Here we show only the 6 cm map, but we have produced similar figures for the 3.6 cm and 1.3 cm maps and find that both of those distributions are also Gaussian, so we can use a σ -cut to confidently distinguish between real sources and noise spikes in our images.

at 6 cm; see Table 1).

We list the total number of sources detected in each map in Table 1. For each map we also provide a breakdown of the number of sources detected in our blind search as well as the additional number of sources detected from the catalog driven search. We detect 108 objects in our 6 cm map, 98 objects in our 3.6 cm map, and a total of 144 objects across all of our 1.3 cm maps. In all we detect 175 distinct sources across all of our maps. We show the position of every detected source in our maps in the left panel of Figure 1.

Of the 175 unique compact radio sources, 120 sources are associated with YSOs detected in near-infrared surveys (e.g. Hillenbrand & Carpenter 2000), and 67 sources are associated with *HST* detected proplyds. 149 have previous radio detections, and 40 have been previously detected at millimeter wavelengths. We also report the detection of 11 sources here for the first time at any wavelength.

We fit every detected source with a two dimensional Gaussian to determine position, extent, and total source flux. For sources identified in the previously mentioned catalogs that are not detected in our maps, we also integrate over a $1''$ aperture centered on the known source position to produce an unbiased estimate of the signal (or noise) towards that position. We include a 10% error on the measurement to account for systematic errors in the band-to-band flux calibration. These intensities, measured towards all cataloged objects in our field of view, are presented in Table 2. The print version of this paper presents only the first page of that table. We also plot images of those sources in Figure 3.

Our catalog of sources, as presented in Table 2 is sorted by right ascension and then given a catalog ‘ID’, which we list in Table 2. We refer to each source by this ID throughout the remainder of the text and figures. In Table 2 we also list the proplyd name, identification from early ONC radio surveys (e.g., Garay et al. 1987; Felli et al. 1993b), identification from Zapata et al. (2004a), or identification from Hillenbrand & Carpenter (2000) when applicable.

3.2. Estimating the Free-Free Emission Spectrum

Evidence suggests that the proplyds are undergoing mass loss from photoevaporation by the nearby O star θ^1 Ori C, so the free-free emission we detect here is likely due to a wind (e.g., Churchwell et al. 1987; Henney & Arthur 1998). For emission from a spherically symmetric wind with an arbitrary $n \propto r^{-\alpha}$ density profile the expected spectral dependence of free-free emission is

$$F_{\nu,ff} = \begin{cases} F_{\nu,turn} \left(\frac{\nu}{\nu_{turn}} \right)^{-0.1} & \nu \geq \nu_{turn} \\ F_{\nu,turn} \left(\frac{\nu}{\nu_{turn}} \right)^{(4\alpha-6.2)/(2\alpha-1)} & \nu < \nu_{turn} \end{cases} \quad (1)$$

(Wright & Barlow 1975). ν_{turn} is the frequency where the wind becomes partially optically thick, and is determined by the radius of the inner boundary of the ionized envelope. High turnover frequencies indicate more compact inner boundaries. When the wind becomes fully optically thick at very low frequencies the spectrum follows the typical $F_\nu \propto \nu^2$ spectrum expected for optically thick thermal emission.

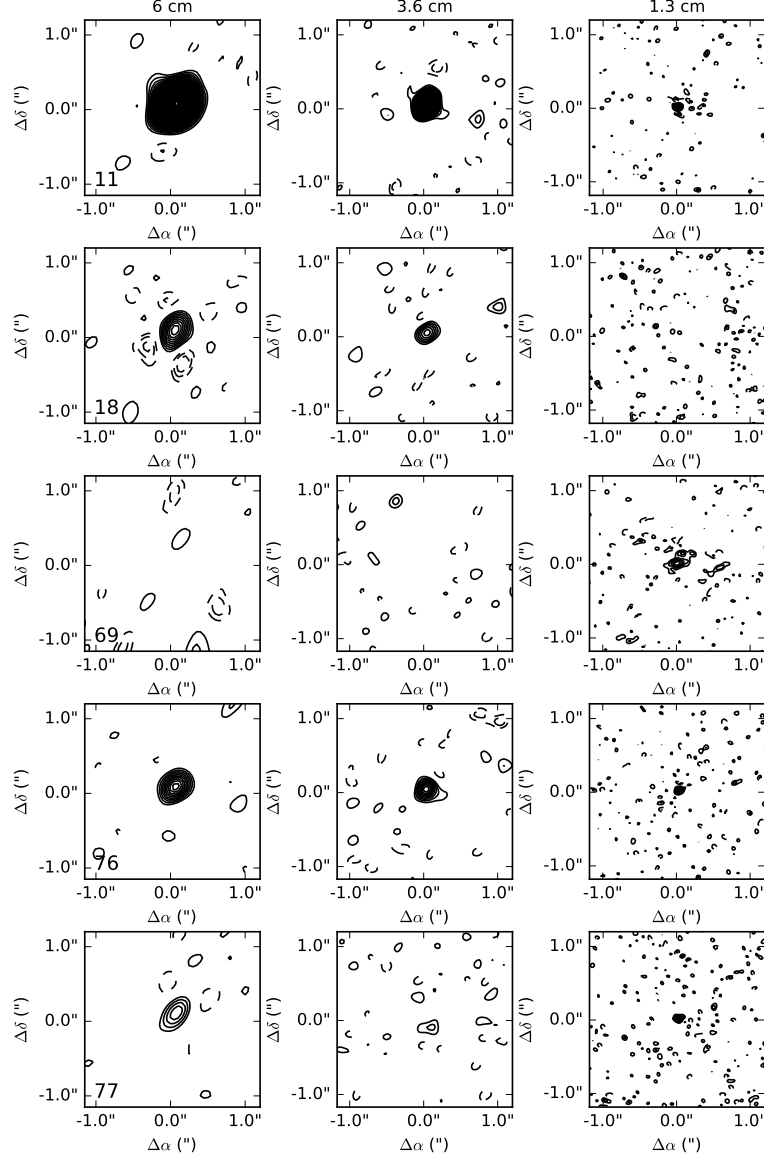


FIG. 3.— Contour images of sources detected in our 6 cm, 3.6 cm or 1.3 cm continuum maps. Each row shows a single source in each band. At 1.3 cm we show only one epoch as a representative image of the source. Contour increments are 1σ , beginning at $\pm 2\sigma$, where σ is determined locally for each object. This figure is continued at the end of the text.

For a fully ionized wind with a constant mass-loss rate we expect $\alpha = 2$ and the spectral dependence of free-free emission is

$$F_{\nu,ff} = \begin{cases} F_{\nu,turn} \left(\frac{\nu}{\nu_{turn}} \right)^{-0.1} & \nu \geq \nu_{turn} \\ F_{\nu,turn} \left(\frac{\nu}{\nu_{turn}} \right)^{0.6} & \nu < \nu_{turn} \end{cases}. \quad (2)$$

Steeper density profiles may lead to steeper spectral dependences below the turnover frequency (e.g., Plambeck et al. 1995). Here, for simplicity, we adopt the solution for a fully ionized wind with a constant mass-loss rate. Many of our sources show evidence for a free-free turnover (see Figure 4), so we adopt a model including a turnover in the spectrum.

At higher frequencies, dust emission is expected to dominate. The differences in the expected spectral slopes between dust and free-free emission allows us to charac-

terize each separately by observing our targets at a range of wavelengths. For each of our detected sources we fit a simple model to the known radio, millimeter, and submillimeter photometry:

$$F_\nu = F_{\nu,ff} + F_{\nu,dust,230GHz} \left(\frac{\nu}{230\text{GHz}} \right)^{2+\beta}. \quad (3)$$

Here we assume $\beta = 0.7$, consistent with previous studies of protoplanetary disks in other star forming regions (e.g., Rodmann et al. 2006; Ricci et al. 2010a,b).

We fit the SED of each source by searching a grid over a large range of parameter space of ν_{turn} , $F_{\nu,turn}$, and $F_{\nu,dust,230GHz}$ for a minimum in χ^2 . We then use a second, finely spaced, grid search based on the initial search to find the best χ^2 fit.

ν_{turn} , $F_{\nu,turn}$ and $F_{\nu,dust,230GHz}$ are left as free parameters in the grid search. If a source has no submillimeter detections (≥ 90 GHz; Eisner et al. 2008;

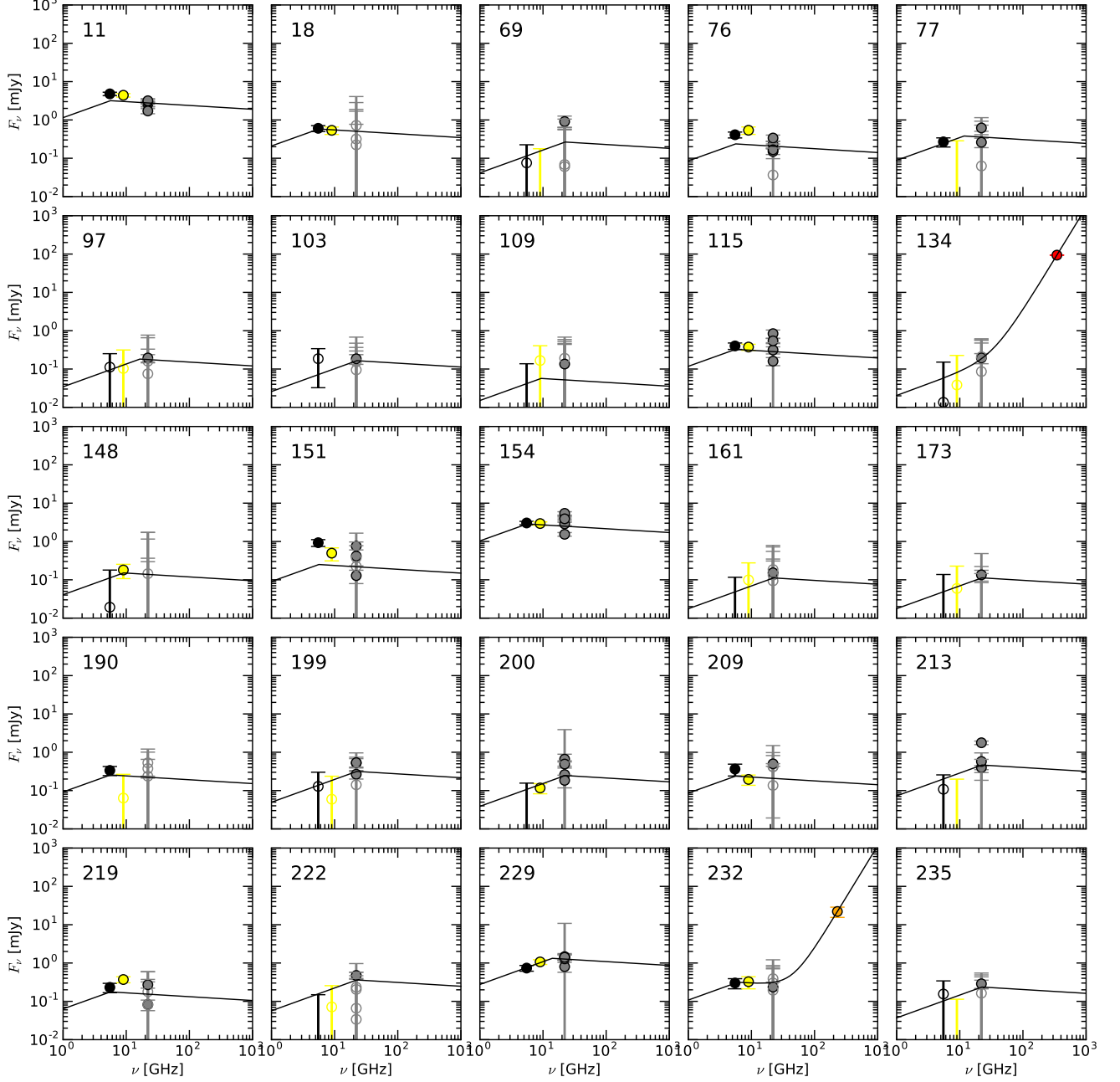


FIG. 4.— The millimeter and radio SEDs for all of the sources detected in our maps. We also show the best fit dust + free-free emission model for each source, as described in Section 3.2. Black, yellow and grey points are the 6 cm, 3.6 cm, and 1.3 cm flux measurements for objects detected in our maps. Circles with colored faces indicate that the source was detected by our search routines, while open face circles are fluxes measured in an aperture around a known source position. Orange data points are 3mm, 1.3 mm, and 870 μ m fluxes from Eisner et al. (2008, and references therein). Green data points are 870 μ m fluxes from Mann & Williams (2010), and red data points are 870 μ m fluxes from Mann et al. (2014). The fluxes shown here are all measured with one of the SMA, CARMA, ALMA, OVRO, or the VLA. This figure is continued at the end of the text.

Mann & Williams 2010; Mann et al. 2014), we assume that $F_{\nu,dust,230GHz} = 0$. In that case we also require $5.5GHz \leq \nu_{turn} \leq 22GHz$, because outside of this range we cannot constrain ν_{turn} . If a source does have submillimeter detections we only require $5.5GHz \leq \nu_{turn}$.

Sources 281, 391, 416, 423, 430, 433, 442, 512, 516, 537, 564, and 595 are all extended sources that are marginally resolved by our 3.6 cm and 6 cm maps, as well as in our B-configuration 1.3 cm observations. In

our A-configuration 1.3 cm observations, however, these sources are very well resolved. In fact, they are so well resolved that much or all of the emission from the source is resolved out. As such we exclude the A-configuration flux measurements from our SED fitting, as flux variations are likely due to structure being resolved out rather than actual variability.

Some of our sources are variable across our multiple epochs of 1.3 cm data (see Section 4.2). We account for

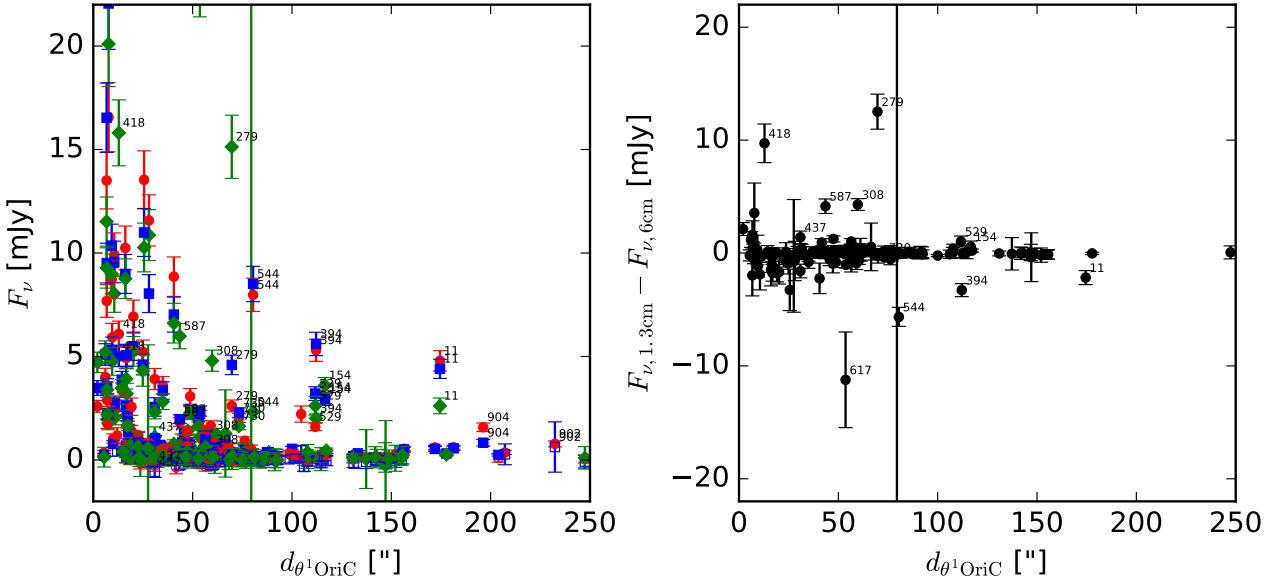


FIG. 5.— (left) The measured radio flux of each of our detected objects at 1.3 cm (green diamonds), 3.6 cm (blue squares), and 6 cm (red circles) as a function of projected distance from θ^1 Ori C. (right) Difference in measured 1.3 cm and 6 cm fluxes as a function of projected distance from θ^1 Ori C. With the exception of a few outliers, we find that radio fluxes for our targets decrease with increasing projected separation, as we would expect for free-free emission driven by the powerful ionizing radiation of θ^1 Ori C. This is also consistent with the difference in 1.3 cm and 6 cm fluxes, which falls near zero for most sources. Optically thin free-free emission is expected to have a roughly flat spectrum at these wavelengths, so we would expect the differences in those measurements to fall near zero. We label the significant outliers with the source ID for reference in future sections.

this variability in our modeling by including the measured flux at each epoch and allowing the variability to influence the uncertainty of our parameter estimation. Sources that are more variable will also have more uncertainty in model fits.

We list the parameters of our best fit models to each source detected in our maps in Table 3. The photometry, along with the best fit model, for each source is plotted in Figure 4.

The origin of the radiation ionizing these sources has been the subject of much debate. Early radio studies of the region disagreed as to whether these sources were externally ionized by radiation from θ^1 Ori C or ionized internally by a young massive star, and as to whether these objects are dense neutral condensations or protoplanetary disks (e.g., Garay et al. 1987; Churchwell et al. 1987), although these studies are complicated by the fact that only projected, and not actual, distances from θ^1 Ori C are known. Since these early studies, *HST* imaging (e.g., O'Dell et al. 1993) and detailed modeling of those images (e.g. Henney & Arthur 1998) has favored protoplanetary disks ionized by θ^1 Ori C.

Free-free emission powered by ionizing radiation from θ^1 Ori C should decrease with increasing separation from θ^1 Ori C. We show the measured flux versus distance in the left panel of Figure 5. For most sources there is a trend of decreasing radio flux with increasing separation, suggesting that they are exhibiting free-free emission from gas ionized by θ^1 Ori C. We also find that the difference in their 1.3 cm and 6 cm flux is close to zero, as expected for optically thin free-free emission, which has a roughly flat spectrum (see the right panel of Figure 5). We note that here we report projected distances. Actual

separations are greater than or equal to this number. We discuss the outliers of these trends below, in Section 4.3.

For this study, we are only concerned with whether these sources are emitting thermal free-free emission or not so that we can characterize the emission and remove it from dust emission for disk mass studies, but on the surface Figure 5 would seem to suggest that these sources are externally ionized by θ^1 Ori C. The detailed structure of these compact objects is beyond the scope of this paper, as the radio emission can be well characterized without that knowledge, but we will revisit the subject in a more detailed study in the future.

4. DISCUSSION

4.1. Comparison with Previous Radio Surveys

Many compact radio sources have previously been identified at a range of wavelengths in the ONC through VLA surveys of the region. The earliest searches for compact radio sources in the ONC were conducted primarily at 20 cm, 6 cm, 2 cm, and 1.3 cm (e.g., Garay et al. 1987; Churchwell et al. 1987; Felli et al. 1993a,b). These surveys were state of the art at the time, with rms as low as $0.18 \text{ mJy beam}^{-1}$ at 2 cm (Churchwell et al. 1987; Felli et al. 1993a), $0.23 \text{ mJy beam}^{-1}$ at 6 cm (Felli et al. 1993b), or $1.0 \text{ mJy beam}^{-1}$ at 1.3 cm (Garay et al. 1987). These searches identified 49 compact radio sources in the ONC.

A more recent survey mapped a $4' \times 4'$ region of the ONC at 3.6 cm using the VLA. This survey achieved a sensitivity of $0.03 \text{ mJy beam}^{-1}$ and uncovered 77 compact radio sources (Zapata et al. 2004a). Of these 77 sources, 38 were previously known from the earlier studies mentioned above, while 39 were new centimeter de-

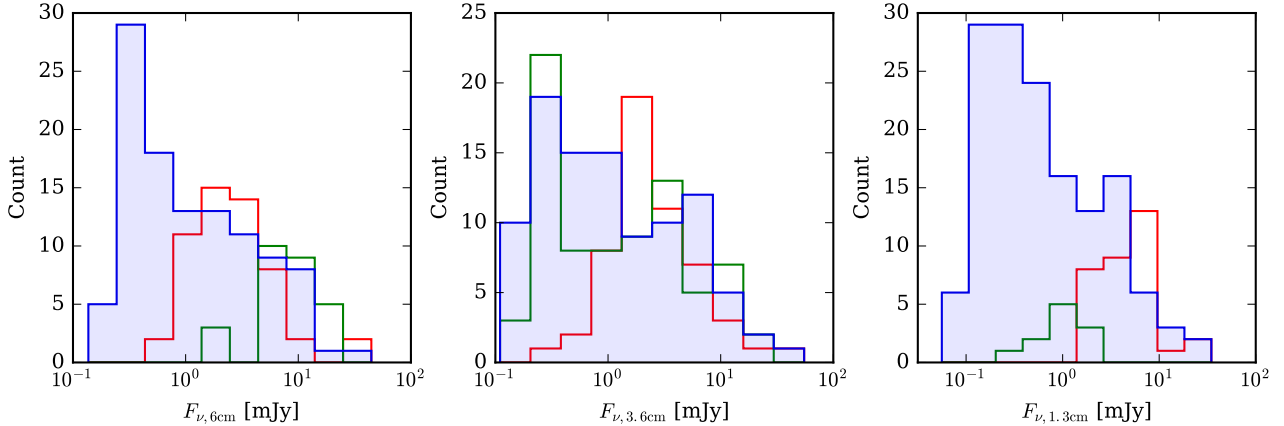


FIG. 6.— Histograms of the fluxes of sources detected in each of our maps. We also show a histogram of the compact radio sources detected in previous studies. Blue shows the histogram of detected sources from this work. Green shows the histograms of detected sources from Felli et al. (1993b) (6 cm), Zapata et al. (2004a) (3.6 cm), and Zapata et al. (2004b) (1.3 cm). Red shows the 4.5 GHz (6 cm) and 7.5 GHz (3.6 cm) detections from Kounkel et al. (2014), and the 2 cm detections from Felli et al. (1993a). We do not show the Forbrich et al. (2016) 6 cm sample, which includes 477 sources fainter than 0.3 mJy.

tectons. Zapata et al. (2004b) also mapped a $30'' \times 30''$ region in OMC-1 South at 1.3 cm with the VLA. They achieved an rms of $0.07 \text{ mJy beam}^{-1}$, but due to the limited area of their maps only detected 11 sources.

A recent survey mapped out a large region encompassing λ Ori, Lynds 1622, NGC 2068, NGC 2071, NGC 2023, NGC 2024, σ Ori, the ONC, and Lynds 1641 with the VLA at 4.5 GHz and 7.5 GHz with a $60 \mu\text{Jy}$ sensitivity (Kounkel et al. 2014). They found > 350 sources over the area of their map, 54 of which overlap with the area we survey. The majority of their detected sources also have spectral indices consistent with flat spectra.

Here we compare these previous surveys with our own JVLA maps. In Figure 6 we plot the distribution of fluxes for compact sources detected in our maps as well as the distribution of fluxes for previously identified compact radio sources at the same wavelength. The most extensive existing studies at 1.3 cm are limited by either survey area or sensitivity so we also compare our 1.3 cm detections with previous 2 cm detections.

Of the 49 compact radio sources detected by initial surveys (e.g. Garay et al. 1987; Churchwell et al. 1987; Felli et al. 1993a,b), we have detected 37 in our maps. We have also recovered 64 of the 77 sources detected by Zapata et al. (2004a), 9 of the 11 sources found by Zapata et al. (2004b), 42 of the 54 sources found by Kounkel et al. (2014), and 144 of the 556 sources found by Forbrich et al. (2016). We detect 29 of the 35 sources that were previously detected at 2 cm. We also report the detection of 135 sources that have not previously been detected at 1.3 cm, 34 at 3.6 cm, 4 at 6 cm, and 26 sources that have not previously been detected at any radio wavelengths. The sources that were previously detected, but that we do not detect in our maps, are likely variable given the deeper sensitivity in our JVLA data.

4.2. Variability

Previous radio studies of the ONC explored multiple epochs of data to search for evidence of source variability. Felli et al. (1993b) monitored the ONC at 2 cm and 6 cm for a period of 7 months and found 13 sources to be variable over that time with flux variability of 20 – 80%. Zapata et al. (2004a) tracked the ONC at 3.6 cm over four

years, and identified 36 sources that are time variable by more than 30%. More recently, Kounkel et al. (2014) mapped a large region of the Gould Belt at 4.5 GHz and 7.5 GHz over three epochs each separated by a month, and found 32 variable sources in the ONC. Furthermore, Rivilla et al. (2015) studied a field in the ONC at 0.7 cm and 0.9 cm and found 19 sources which are variable over long-term (monthly) timescales, and 5 sources which are variable on short timescales (hours to days). Moreover, very short timescale radio flares have been observed towards a number of pre-main sequence stars (e.g., Bower et al. 2003; Forbrich et al. 2008; Rivilla et al. 2015)

Here we compare previously measured fluxes for detected compact radio sources with the fluxes in our maps. Time-baselines are ~ 10 years at 1.3 cm and 3.6 cm and $\gtrsim 20$ years at 6 cm, and we cannot characterize shorter timescales for variability. We thus seek to identify sources that may not have been detected as variable in previous, shorter time-baseline studies (Felli et al. 1993b; Zapata et al. 2004a). We also use our multiple epochs of 1.3 cm data to search for variability on timescales of ~ 7 months, between November 10, 2013 to May 3, 2014.

As we discussed earlier, Sources 281, 391, 416, 423, 430, 433, 442, 512, 516, 537, 564, and 595 are very well resolved with the A-configuration at 1.3 cm. As such we exclude these sources from our variability considerations at 1.3 cm, as flux variations may be due to structure being resolved out rather than actual variability.

We define a variable source as one for which the flux measurements are 3σ discrepant from one epoch to the next, at any observed wavelength. $\Delta F/F$ quantifies how variable a source is, where F is the mean flux of the source and ΔF is the standard deviation of the fluxes. We show the results of this search in Table 4. For the sources detected in Zapata et al. (2004a) and Zapata et al. (2004b) we include a 10% uncertainty on the flux on top of the uncertainties they quote to account for a systematic flux calibration uncertainty across the datasets.

At 1.3 cm we find 30 sources that show some indication of variability, with $\Delta F/F$ ranging from 20–900%. At 3.6 cm we identify 32 sources whose fluxes are variable, including 3 sources not identified as variable in Zapata et al. (2004a), because they were too faint to be

detected in individual epochs. The variability, as defined by $\Delta F/F$, of these sources ranges from 20–200%. Finally, at 6 cm we identify 5 variable sources with $\Delta F/F$ ranging from 50–100%.

There were 13 sources detected by previous radio surveys of the ONC (e.g. Felli et al. 1993a,b). Most of those sources were not detected in the same bands as our observations, and so they are excluded from our variability analysis. However, the 5 variable sources with 6 cm fluxes from Felli et al. (1993b) were undetected in our maps, and have $\Delta F/F$ ranging from 50–100%. Given the high fluxes of the remainder of the sources, we would have expected to detect them in our maps, so those sources likely have similarly high variability amplitudes.

In all, we find that 55 of our sources are variable at one or more wavelengths. Of the variable sources, 11 are characterized as variable at multiple wavelengths. 20 are found to be variable at one wavelength but not another, although many of our constraints on $\Delta F/F$ are not strong. The remaining sources could only be analyzed at a single wavelength.

We show the location of each variable source in the right panel of Figure 1, with the strength of the variability ($\Delta F/F$) represented by the size of the plot symbol. We find that variability amplitude does not follow the same trend as free-free flux, with variability decreasing with increased separation from θ^1 Ori C. Instead we find sources which are significantly variable out to large radii. Some of the most variable objects can be found at large separations.

Variability of radio emission from these sources is likely to arise from a few different mechanisms. It may be the result of gyrosynchrotron emission produced by magnetospheric activity in young stars (e.g., Feigelson & Montmerle 1999). These flares may be the result of magnetic reconnections on the protostellar surface, which would produce radio flares on the timescales of minutes (e.g. Dulk 1985; Bower et al. 2003; Forbrich et al. 2008). Interactions between the magnetic fields of the protostar and its disk could also produce flares on the timescales similar to the rotation periods of young stars, which are typically days to weeks in the ONC (e.g. Shu et al. 1997; Forbrich et al. 2006; Rodríguez-Ledesma et al. 2009).

Free-free emission may also be variable if the density distribution of material being ionized is non-uniform causing the amount of ionized material to vary, or if the incident ionizing radiation is varying. Studies have found that O-type stars have winds that exhibit cyclical variability on timescales of hours to days (see review by Fullerton 2003). The visible, UV and X-ray intensity of θ^1 Ori C varies with a period of 15.4 days (e.g., Stahl et al. 1993, 1996; Caillault et al. 1994; Walborn & Nichols 1994), so the ionization level and therefore free-free flux might be expected to vary on a similar timescale. The ionized region, however, is likely to be many light days across or larger, so this variability may be washed out.

Inhomogeneities in the disk are unlikely to be brought into the ionized region on timescales shorter than the dynamical timescale. For disks, the dynamical timescale varies depending on location in the disk and the mass of the central star (e.g., Kenyon 2001). Inner disk radii for young stars are found to be on the order of 0.1 – 1 AU (e.g., Eisner et al. 2007), so the smallest dynamical

timescales we can expect are on the order of weeks to half a year. Photoevaporation in disks tends to produce winds at radii larger than the critical radius, where the photoionized material has sufficient velocity to escape. For ionization by EUV photons this tends to occur at radii of $\gtrsim 5$ AU (e.g., Hollenbach et al. 1994; Gorti & Hollenbach 2009), corresponding to dynamical timescales of a few years. Non-uniformities in the disk are therefore likely to cause longer term variability in the free-free emission.

Aside from the timescale of variability, the SED of the source at each epoch might be used to distinguish between free-free and synchrotron emission. As described in Section 3.2, free-free emission is characterized by a flat spectrum with $F_\nu \propto \nu^{-0.1}$. Gyrosynchrotron emission however, is expected to have a spectral index that is significantly negative, typically $F_\nu \propto \nu^{-0.7}$. We discuss constraints on the nature of some of these sources in Section 4.3. Further studies with concurrent flux measurements at multiple wavelengths, however, are needed to fully distinguish between these sources of emission.

Here we do not have simultaneous flux measurements at all bands for each epoch of data, so it is difficult to constrain the spectral index of the emission at each epoch. There are, however, a few sources which change flux significantly between the 1.3 cm observations on March 3 and March 7 2014. For example, on March 3, Source 529 had a 1.3 cm flux of 7 mJy, but on March 7 it was down to a flux of 4.5 mJy. By May 7th the flux was all the way down at 0.5 mJy. Such an extreme change in flux may be indicative of gyrosynchrotron emission from a magnetic flare. Source 544 also shows a similar pattern. Source 587 has a flux of 1.7 mJy on March 3, but on March 7 it's flux increased significantly to 22 mJy, again possibly indicative of a magnetic flare. For most sources, however, we do not have sufficient time resolution to distinguish between daily, weekly, or even longer variability timescales.

4.3. Nature of Detected Sources

We detected emission in at least one of our maps from 67 *HST* identified proplyds (Ricci et al. 2008; Mann & Williams 2010; Mann et al. 2014). Furthermore, we have detected radio emission towards 120 sources that have been identified by near-infrared imaging (Hillenbrand & Carpenter 2000). We also detect radio emission from 2 sources dubbed ‘MM’ by Eisner et al. (2008), indicating that they have previously only been detected at wavelengths longer than 1 mm. Finally, we have detected 51 sources that are not associated with a known proplyd or near-infrared detected source.

The majority of our targets, including all of the sources identified as proplyds, are well fit by our free-free and dust emission model, in agreement with previous conclusions that these objects are disks with winds driven by photoevaporation (e.g., Churchwell et al. 1987; Henney & Arthur 1998). We detect a turnover in the free-free emission spectrum for 40 objects, as evidenced by $5.5\text{GHz} < \nu_{turn} < 22\text{GHz}$. There are at least 3 sources (Sources 374, 465, 473) that might even have $\nu_{turn} > 22\text{GHz}$, indicating that our maps are insufficient to fully characterize their emission. With such high turnover frequencies, these objects must have small inner boundaries to their ionized envelopes and are likely very compact and dense.

Further short wavelength observations are necessary to better constrain the free-free emission spectrum.

Some sources have SEDs that appear to be fitted well by our free-free + dust model with some variability included. Fluxes at all three wavelengths were measured concurrently on March 3, 2014, and if we just consider those flux measurements, all of our sources are fitted well by free-free emission models. Without simultaneous 3.6 cm and 6 cm measurements for the other 1.3 cm epochs it is impossible to say whether the SEDs at those epochs remain consistent with free-free emission, although it seems probable.

Below we split the sources whose SEDs are not fitted well by our model and therefore are not indicative of being free-free emission, or do not follow the expected trend of decreasing centimeter flux with increasing separation from θ^1 Ori C:

4.3.1. Strong Free-Free Sources

Source 418 is θ^1 Ori A, a binary system with a B0.5 primary star and a low-mass companion, possibly a T Tauri star (Levato & Abt 1976; Bossi et al. 1989), which is known to be highly variable (e.g., Felli et al. 1993b). Rivilla et al. (2015) suggest that this variability may be twofold, (i) variations in free-free opacity from a stellar wind from the interactions with the companion, and (ii) variations in the non-thermal emission from stellar activity related to the distance between to binary, similar to the case of WR 140 (e.g., Williams et al. 1990). Rivilla et al. (2015) suggest that while the former mechanism may be present, the latter is required to explain previous observations.

Sources 279 and 308 each have radio spectra that are steeper than $\nu^{0.6}$. Source 279 is the Becklin-Neugebauer Object, and is thought to be a runaway B star, ejected from a system with Source I (our Source 308) in an explosive event 500 years ago (e.g., Plambeck et al. 1995; Gómez et al. 2008; Plambeck et al. 2013). The BN Object has a spectral dependence of $\nu^{1.3}$ below 100 GHz, above which it flattens, and is suggested to be free-free emission from a dense, hypercompact HII region. Source I has a spectral dependence of ν^2 and is most easily explained by H⁻ free-free emission in a disk (e.g., Plambeck et al. 2013). Both sources have massive stars driving ionizing circumstellar material and driving the free free emission we detect, explaining their significant fluxes despite their distance from θ^1 Ori C.

4.3.2. Dust-Only Sources

Sources 134, 236, 246, and 301 have millimeter (850 μ m or 1.3mm) detections and are detected at 1.3 cm in our maps, but are undetected at 3.6 cm and 6 cm. The SEDs for all of these sources are well fit by a model that is predominantly dust emission at 1.3 cm (and perhaps a minor contribution from free-free emission). Sources 236 and 246 are identified by Eisner et al. (2008) as “MM” objects (MM21 and MM8 respectively), which lack near-IR counterparts. Source 301 is also identified by Eisner et al. (2008) as LMLA 162. All three of those sources (236, 246, and 301) are among the most massive known sources in the ONC ($> 0.2 M_\odot$ Eisner et al. 2008). They are likely highly embedded young objects, and may be candidate Class 0 or I objects as suggested by Eisner et al. (2008).

4.3.3. Non-Thermal Radio Sources

Sources 11 and 617 each have spectra with steep negative spectral indices (see Figure 5), which may indicate that they are emitting synchrotron radiation. Source 11 is not associated with any previous detections in our reference catalogs, and is not found to not be variable at 3.6 cm. Source 617 has previously been detected, and is commonly referred to as F (e.g., Churchwell et al. 1987; Garay et al. 1987; Felli et al. 1993a). It has previously been found to experience radio flares on timescales as short as hours and possibly as long as months (Rivilla et al. 2015).

Sources 154, 394, 437, 440, 529, 544, 587, and 730 are highly variable sources, showing significant changes in flux over just a few days between our observations on March 3, 2014 and March 7, 2014. All are significant outliers in Figure 5. Source 154 has previously been identified as A (e.g., Churchwell et al. 1987; Garay et al. 1987; Felli et al. 1993a), and Zapata et al. (2004a) find the source to show large percentages of circular polarization, and suggest that the emission may be gyrosynchrotron in nature. Felli et al. (1993b) also classify Source 587, also known as G, as a non-thermal variable emitter. All of these sources are associated with infrared detected objects (Hillenbrand & Carpenter 2000). These sources may be indicative of radio flares of gyrosynchrotron emission, but further observations with concurrent flux measurements at multiple wavelengths are needed to confirm this.

Source 903 is located far from θ^1 Ori C, and is only detected at 6 cm, but it has a high flux given its significant separation (see Figure 5). It is out of the field of view of our 1.3 cm data, and right on the edge of our 3.6 cm map, but undetected. It is associated with the proplyd 281-306, which is a disk seen only in silhouette with HST (Ricci et al. 2008). Radio emission from this source may be attributed to magnetic activity from the young star or free-free emission from material ionized by the star itself, as it is likely too far to be material ionized by θ^1 Ori C.

Source 904 is also located far from θ^1 Ori C, with a high flux given its separation (Figure 5), and is outside the field of view of our 1.3 cm map. Its 6 cm and 3.6 cm fluxes are consistent with free-free emission, but do show indications that the spectral index may be significantly negative. It is unassociated with any previous catalog.

4.3.4. Extragalactic Sources

Given the large survey area of our maps, it is possible that some of our detections are extragalactic in nature. Following Fomalont et al. (1991), at 6 cm we would expect the number of extragalactic contaminants greater than 156 μ Jy (our 6σ threshold) in our 109 arcmin² survey area to be 6.5 ± 2.3 . At 3.6 cm, using Fomalont et al. (2002), we estimate 1.1 ± 0.2 extragalactic sources in our 70 arcmin² survey area to above 216 μ Jy. No similar survey exists at 1.3 cm, so we use the 3.6 cm numbers to estimate that in our 1.3 cm map we would expect 1.8 ± 0.2 contaminants in our 34 arcmin² survey area above 72 μ Jy. As most of these sources show non-thermal emission with negative spectral indices at these wavelengths (Condon 1992) they should be fainter at 1.3 cm than at 3.6 cm and therefore we would expect the

contamination at 1.3 cm to be even smaller than this.

4.4. Free-free Contamination of Sub-millimeter Dust Masses

At submillimeter, millimeter and radio wavelengths, the light emitted by dust grains is expected to be largely optically thin and the flux is directly proportional to the amount of dust present (e.g., Beckwith et al. 1990). As such, submillimeter flux measurements of protoplanetary disks are commonly used to measure the mass of those disks (e.g., Andrews & Williams 2005; Eisner et al. 2008; Mann & Williams 2010; Andrews et al. 2013; Mann et al. 2014). A number of previous surveys across millimeter and submillimeter wavelengths have employed this method to measure disk masses for protoplanetary disks in the ONC (e.g., Mundy et al. 1995; Bally et al. 1998b; Williams et al. 2005; Eisner & Carpenter 2006; Eisner et al. 2008; Mann & Williams 2010; Mann et al. 2014).

The proplyds, however, are located near the Trapezium cluster of young massive stars that are photoevaporating the disks (e.g., Churchwell et al. 1987). The ionized material produced in the proplyds emits free-free emission, which can be bright at the same wavelengths used to measure disk masses. In order to accurately measure disk masses, it is therefore important to separate the dust and free-free contributions to sub-millimeter and millimeter fluxes. This is particularly true with the advent of ALMA, which will detect disks in the ONC much fainter than those that have been previously detected.

In this work we characterized the free-free emission from a collection of compact radio sources in the ONC. In Table 3 we use the best fit free-free emission spectrum model from Section 3.2 to calculate the expected free-free flux at all ALMA bands. This table can be used to correct measured millimeter fluxes for free-free contamination, and accurately measure the sub-millimeter dust flux and thereby the dust mass.

For most sources this extrapolation provides a good estimate of the free-free contribution of the source at ALMA wavelengths. This is not true, however, of sources for which the model fit is poor as was discussed in the previous section. Furthermore, the extrapolation to ALMA bands for sources whose turnover frequency is designated as > 22 GHz is also very uncertain. Many of these sources were only detected at 1.3 cm, and a few have radio photometry that is best fit by a $\nu^{0.6}$ power law. Our extrapolation for these sources assumes $\nu_{turn} = 22$ GHz, but if $\nu_{turn} > 22$ GHz the free-free flux at ALMA bands would be greater than our current prediction. Further radio or millimeter observations are necessary to constrain ν_{turn} before accurate ALMA free-free fluxes can be predicted.

Variability is also a significant source of uncertainty in determining how well free-free emission from disks can be constrained and removed from disk mass measurements, if the free-free flux to dust flux ratio is large. For example, the measured 230 GHz flux of Source 439 is 8.8 mJy and the model free-free flux at 230 GHz is 2.8 mJy, with a variability of 24%. So free-free emission makes up $32 \pm 8\%$ of the total 230 GHz flux. Source 466, however, has a measured 230 GHz flux of 7.7 mJy, 0.3 mJy of which is due to free free emission with 50.8% variability, so the free-free emission makes up $5 \pm 2\%$ of that flux. Because of the smaller free-free flux to total flux ratio of Source

466, the dust flux can be better constrained, even though Source 466 is more variable.

ALMA, however, will be able to detect disks which are much fainter than has previously been possible. For these sources, variability may be a significant problem. Source 469 has a 230 GHz free-free flux of 0.33 mJy with a variability of 108%. Although it has no previous millimeter detections, if it were found to have a millimeter flux of 0.5 mJy, the dust mass calculation would be highly uncertain because the free-free flux would make up $65 \pm 70\%$ of the total 230 GHz flux.

An accurate estimate of the uncertainty associated with variability of our sources, however, likely requires further monitoring of the sources to characterize the timescale and amplitude of the variability. Sources with significant variability may even require concurrent millimeter and radio flux measurements in order to measure the free-free contribution to millimeter flux measurements.

While not important for some objects, the correction for free-free emission is often crucial for correctly measuring disk mass. For example, the free-free emission from sources 391, 408, 416, 418, 421, 423, 430, 438, 439, 442, 446, 460, 465, 484, 491, 494, 499, 512, 516, 518, 535, 537, 555, 564, 605, 612 and 617 contributes $>50\%$ of the measured 3 mm fluxes. Free-free emission also contributes $>40\%$ of the measured 1.3 mm fluxes for sources 408, 416, 418, 421, 423, 438, 442, 460, 465, 484, 491, 494, 499, 516, 518, 535, 564 and 617 and $>30\%$ of the measured 850 μ m fluxes for sources 408, 421, 423, 438, 460, 465, 484, 491, 494, 499 and 617. Without these corrections, disk mass estimates from these sub-millimeter bands would be off by a significant amount.

4.5. Future Work

While our radio dataset is tremendously useful for finding radio sources and characterizing their free-free emission for ALMA disk mass studies in the ONC, the data also has a number of other applications which we will explore in future work.

Due to the high resolution of our maps, particularly at 1.3 cm, many of the sources detected in our maps are well resolved. The morphologies of these objects show interesting features, particularly when matched up with high resolution HST images of the proplyds. For many sources structure in HST maps are well matched with features in our maps.

Furthermore, we can use resolved images to measure mass loss rates for the protoplanetary disks. The free-free emission we detect here originates from ionized cocoons of gas which are flowing away from their associated disks under the intense radiation pressure from the star θ^1 Ori C. The flux of this free free emission coupled with measured sizes of these cocoons of gas is sufficient to measure disk mass-loss rates. Mass loss rates have previously been measured for a handful of disks in the ONC (e.g., Churchwell et al. 1987), but the improved sensitivity and resolution of our maps will allow us to make this measurement for many more sources.

5. CONCLUSIONS

We have produced new high spatial resolution maps of the Orion Nebula at 1.3 cm, 3.6 cm and 6 cm with

significantly improved sensitivities compared with previous radio studies of the region using the JVLA. In these maps we search for compact ($\lesssim 2''$) radio sources, and use these detections to constrain the properties of free-free emission from protoplanetary disks in the ONC. Free-free emission is emitted from the ionized winds driven by the nearby massive star θ^1 Ori C. Constraints on this free-free emission are crucial for studies aiming to measure disk masses for the proplyds from sub-millimeter fluxes.

We detect 144 sources at 1.3 cm, 98 sources at 3.6 cm, and 108 sources at 6 cm, for a total of 175 unique sources. Of these 175 detections, 149 have previously been detected at radio wavelengths, 67 are associated with *HST* detected proplyds, 120 with near-infrared detected YSOs, 40 with sources detected previously at millimeter wavelengths, and 11 are detected for the first time at any wavelength.

For each source detected in our maps we report its position and flux, as measured by fitting a gaussian to the source, in Table 2. For previously identified sources not detected in one or more of our maps we also report the integrated flux in an 1'' aperture measured towards the source. This information is presented in an extended version of Table 2 that is available in the online materials.

We fit each of our source spectra with a combined dust + free-free emission model. The majority of our targets are fitted well by this dust + free-free model, with many showing evidence for a turnover in the free-free emission. Further studies of free-free emission may benefit from longer wavelength flux measurements to better constrain the free-free turnover. Four of our detected sources (134, 236, 246, and 301) have SEDs that are consistent with being produced entirely by dust emission and are likely highly embedded young objects. We also detect the Becklin-Neugebauer Object, it's alleged counterpart Source I, and θ^1 Ori A.

Many of our sources have previously measured radio fluxes, so we can investigate variability. We find that 30 sources are variable at 1.3 cm, 32 at 3.6 cm, and 5 at 6 cm. 55 of our detected sources are variable at one or more wavelengths. For sources that are variable we define a metric, $\Delta F/F$, to quantify the variability, and

find that $\Delta F/F \approx 20 - 900\%$ for our targets. 13 are variable at $> 100\%$, suggesting that any sub-millimeter measurements will be very uncertain. The time sampling is, however, poor, so more dedicated monitoring of our targets is necessary for better understanding this variability.

Finally, the free-free emission properties derived from our modeling can be extrapolated to sub-millimeter wavelengths to estimate the free-free contribution to sub-millimeter fluxes. This is necessary for correctly distinguishing dust emission and free-free emission at sub-millimeter wavelengths, particularly when sub-millimeter fluxes are used to calculate disk dust masses. This will be crucial for future studies of dust emission from protoplanetary disks in the ONC with ALMA. We provide free-free flux estimates for each detected source at each ALMA band in Table 3. Variability is a significant source of uncertainty in correcting millimeter flux measurements for free-free emission if the free-free flux to dust flux ratio is large, so understanding this variability is an important future direction.

In the future we will use this dataset to study the morphologies of the sources resolved in our high resolution VLA maps, particularly as compared with HST images of the proplyds. We will also measure the rate at which material is being photoevaporated and lost from the disks of these sources under the intense radiation and winds from θ^1 Ori C and the Trapezium Cluster, and therefore derive disk lifetimes for the protoplanetary disks in the ONC.

This material is based upon work supported by the National Science Foundation Graduate Research Fellowship under Grant No. 2012115762. This work was supported by NSF AAG grant 1311910. The results reported herein benefitted from collaborations and/or information exchange within NASA's Nexus for Exoplanet System Science (NExSS) research coordination network sponsored by NASA's Science Mission Directorate. The National Radio Astronomy Observatory is a facility of the National Science Foundation operated under cooperative agreement by Associated Universities, Inc.

REFERENCES

- Andrews, S. M., Rosenfeld, K. A., Kraus, A. L., & Wilner, D. J. 2013, ApJ, 771, 129
- Andrews, S. M., & Williams, J. P. 2005, ApJ, 631, 1134
- Bally, J., Sutherland, R. S., Devine, D., & Johnstone, D. 1998a, AJ, 116, 293
- Bally, J., Testi, L., Sargent, A., & Carlstrom, J. 1998b, AJ, 116, 854
- Beckwith, S. V. W., Sargent, A. I., Chini, R. S., & Guesten, R. 1990, AJ, 99, 924
- Bossi, M., Gaspani, A., Scardia, M., & Tadini, M. 1989, A&A, 222, 117
- Bower, G. C., Plambeck, R. L., Bolatto, A., McCrady, N., Graham, J. R., de Pater, I., Liu, M. C., & Baganoff, F. K. 2003, ApJ, 598, 1140
- Caillault, J.-P., Gagné, M., & Stauffer, J. R. 1994, ApJ, 432, 386
- Churchwell, E., Felli, M., Wood, D. O. S., & Massi, M. 1987, ApJ, 321, 516
- Clark, B. G. 1980, A&A, 89, 377
- Condon, J. J. 1992, ARA&A, 30, 575
- Cornwell, T. J. 1988, A&A, 202, 316
- Dulk, G. A. 1985, ARA&A, 23, 169
- Dzib, S. A., Loinard, L., Mioduszewski, A. J., Rodríguez, L. F., Ortiz-León, G. N., et al. 2013, ApJ, 775, 63
- Eisner, J. A., & Carpenter, J. M. 2006, ApJ, 641, 1162
- Eisner, J. A., Hillenbrand, L. A., White, R. J., Bloom, J. S., Akeson, R. L., & Blake, C. H. 2007, ApJ, 669, 1072
- Eisner, J. A., Plambeck, R. L., Carpenter, J. M., Corder, S. A., Qi, C., & Wilner, D. 2008, ApJ, 683, 304
- Feigelson, E. D., & Montmerle, T. 1999, ARA&A, 37, 363
- Felli, M., Churchwell, E., Wilson, T. L., & Taylor, G. B. 1993a, A&AS, 98, 137
- Felli, M., Taylor, G. B., Catarzi, M., Churchwell, E., & Kurtz, S. 1993b, A&AS, 101, 127
- Fomalont, E. B., Kellermann, K. I., Partridge, R. B., Windhorst, R. A., & Richards, E. A. 2002, AJ, 123, 2402
- Fomalont, E. B., Windhorst, R. A., Kristian, J. A., & Kellerman, K. I. 1991, AJ, 102, 1258
- Forbrich, J., Menten, K. M., & Reid, M. J. 2008, A&A, 477, 267
- Forbrich, J., Preibisch, T., & Menten, K. M. 2006, A&A, 446, 155
- Forbrich, J., Rivilla, V. M., Menten, K. M., Reid, M. J., Chandler, C. J., et al. 2016, ArXiv e-prints

- Fullerton, A. W. 2003, in Astronomical Society of the Pacific Conference Series, Vol. 305, Magnetic Fields in O, B and A Stars: Origin and Connection to Pulsation, Rotation and Mass Loss, ed. L. A. Balona, H. F. Henrichs, & R. Medupe, 333
- Garay, G., Moran, J. M., & Reid, M. J. 1987, *ApJ*, 314, 535
- Gómez, L., Rodríguez, L. F., Loinard, L., Lizano, S., Allen, C., Poveda, A., & Menten, K. M. 2008, *ApJ*, 685, 333
- Gorti, U., & Hollenbach, D. 2009, *ApJ*, 690, 1539
- Henney, W. J., & Arthur, S. J. 1998, *AJ*, 116, 322
- Hillenbrand, L. A., & Carpenter, J. M. 2000, *ApJ*, 540, 236
- Hollenbach, D., Johnstone, D., Lizano, S., & Shu, F. 1994, *ApJ*, 428, 654
- Kenyon, S. J. 2001, in Astronomical Society of the Pacific Conference Series, Vol. 231, Tetons 4: Galactic Structure, Stars and the Interstellar Medium, ed. C. E. Woodward, M. D. Bicay, & J. M. Shull, 594
- Kounkel, M., Hartmann, L., Loinard, L., Mioduszewski, A. J., Dzib, S. A., et al. 2014, *ApJ*, 790, 49
- Levato, H., & Abt, H. A. 1976, *PASP*, 88, 712
- Mann, R. K., & Williams, J. P. 2009, *ApJ*, 694, L36
—. 2010, *ApJ*, 725, 430
- Mann, R. K., Di Francesco, J., Johnstone, D., Andrews, S. M., Williams, J. P., et al. 2014, *ApJ*, 784, 82
- Moran, J. M., Garay, G., Reid, M. J., Genzel, R., & Ho, P. T. P. 1982, *Annals of the New York Academy of Sciences*, 395, 204
- Mundy, L. G., Looney, L. W., & Lada, E. A. 1995, *ApJ*, 452, L137
- O'Dell, C. R., & Wen, Z. 1994, *ApJ*, 436, 194
- O'Dell, C. R., Wen, Z., & Hu, X. 1993, *ApJ*, 410, 696
- Perley, R., Napier, P., Jackson, J., Butler, B., Carlson, B., et al. 2009, *IEEE Proceedings*, 97, 1448
- Plambeck, R. L., Wright, M. C. H., Mundy, L. G., & Looney, L. W. 1995, *ApJ*, 455, L189
- Plambeck, R. L., Bolatto, A. D., Carpenter, J. M., Eisner, J. A., Lamb, J. W., et al. 2013, *ApJ*, 765, 40
- Rau, U., & Cornwell, T. J. 2011, *A&A*, 532, A71
- Ricci, L., Robberto, M., & Soderblom, D. R. 2008, *AJ*, 136, 2136
- Ricci, L., Testi, L., Natta, A., & Brooks, K. J. 2010a, *A&A*, 521, A66
- Ricci, L., Testi, L., Natta, A., Neri, R., Cabrit, S., & Herczeg, G. J. 2010b, *A&A*, 512, A15
- Rivilla, V. M., Chandler, C. J., Sanz-Forcada, J., Jiménez-Serra, I., Forbrich, J., & Martín-Pintado, J. 2015, *ApJ*, 808, 146
- Rodmann, J., Henning, T., Chandler, C. J., Mundy, L. G., & Wilner, D. J. 2006, *A&A*, 446, 211
- Rodríguez-Ledesma, M. V., Mundt, R., & Eislöffel, J. 2009, *A&A*, 502, 883
- Shu, F. H., Shang, H., Glassgold, A. E., & Lee, T. 1997, *Science*, 277, 1475
- Smith, N., Bally, J., Shuping, R. Y., Morris, M., & Kassis, M. 2005, *AJ*, 130, 1763
- Stahl, O., Wolf, B., Gang, T., Gummersbach, C. A., Kaufer, A., Kovacs, J., Mandel, H., & Szeifert, T. 1993, *A&A*, 274, L29
- Stahl, O., Kaufer, A., Rivinius, T., Szeifert, T., Wolf, B., et al. 1996, *A&A*, 312, 539
- Walborn, N. R., & Nichols, J. S. 1994, *ApJ*, 425, L29
- Williams, J. P., Andrews, S. M., & Wilner, D. J. 2005, *ApJ*, 634, 495
- Williams, P. M., van der Hucht, K. A., Pollock, A. M. T., Florkowski, D. R., van der Woerd, H., & Wamsteker, W. M. 1990, *MNRAS*, 243, 662
- Wright, A. E., & Barlow, M. J. 1975, *MNRAS*, 170, 41
- Zapata, L. A., Rodríguez, L. F., Kurtz, S. E., & O'Dell, C. R. 2004a, *AJ*, 127, 2252
- Zapata, L. A., Rodríguez, L. F., Kurtz, S. E., O'Dell, C. R., & Ho, P. T. P. 2004b, *ApJ*, 610, L121

TABLE 2

ID	Proplyd Name	HC00 ID	GMR ID	Z04a ID	Other Names	R.A. [J2000]	Dec [J2000]	$F_{\nu, 6\text{cm}}$ [mJy]	$F_{\nu, 3.6\text{cm}}$ [mJy]	$F_{\nu, 1.3\text{cm}, 1^a}$ [mJy]	$F_{\nu, 1.3\text{cm}, 2^a}$ [mJy]	$F_{\nu, 1.3\text{cm}, 3^a}$ [mJy]	$F_{\nu, 1.3\text{cm}, 4^a}$ [mJy]	$F_{\nu, 1.3\text{cm}, mean^a}$ [mJy]
1	4538-311	—	—	—	5h34m53.79s	-5d23m10.73s	0.015 ± 0.567
2	—	—	—	—	5h34m55.97s	-5d23m13.00s	0.269 ± 0.338
3	4582-635	—	—	—	5h34m58.16s	-5d26m35.13s	-0.245 ± 0.409
4	005-514	—	—	—	5h35m00.47s	-5d25m14.34s	0.114 ± 0.233
5	006-439	—	—	—	5h35m00.58s	-5d24m38.79s	-0.008 ± 0.229	-0.049 ± 1.203
6	016-149	—	—	—	5h35m01.60s	-5d21m49.35s	-0.262 ± 0.274	-0.149 ± 0.884
7	038-627	—	—	—	5h35m04.19s	-5d26m27.89s	-0.061 ± 0.237
8	044-527	—	—	—	5h35m04.42s	-5d25m27.40s	0.006 ± 0.174	-0.091 ± 0.609
9	—	—	—	—	5h35m04.55s	-5d20m13.90s	0.255 ± 0.314	-0.843 ± 1.131
10	046-245	—	—	—	5h35m04.63s	-5d22m44.85s	0.022 ± 0.173	0.039 ± 0.368
11	—	—	—	1	5h35m04.86s	-5d23m02.61s	4.790 ± 0.492	4.404 ± 0.463	2.643 ± 0.415	2.990 ± 0.426	3.169 ± 0.425	1.712 ± 0.262	2.554 ± 0.367	...
12	049-143	—	—	—	5h35m04.94s	-5d21m42.99s	0.095 ± 0.225	0.135 ± 0.444
13	053-717	—	—	—	5h35m05.40s	-5d27m16.99s	0.080 ± 0.254
14	057-419	—	—	—	5h35m05.73s	-5d24m18.55s	-0.098 ± 0.220	0.160 ± 0.331	0.116 ± 0.743	-0.019 ± 0.814	-0.064 ± 0.538	0.003 ± 0.178	-0.048 ± 0.267	...
15	061-401	—	508	—	5h35m06.09s	-5d24m00.60s	0.022 ± 0.176	-0.055 ± 0.350	-0.049 ± 0.680	-0.020 ± 0.643	-0.192 ± 0.472	0.021 ± 0.159	-0.029 ± 0.240	...
16	—	601	—	—	5h35m06.18s	-5d22m12.40s	-0.054 ± 0.183	0.181 ± 0.342	0.426 ± 3.794	-0.605 ± 3.254	-0.499 ± 1.532	-0.017 ± 1.483	-0.208 ± 0.854	...
17	—	538	—	—	5h35m06.28s	-5d22m02.63s	-0.068 ± 0.190	0.092 ± 0.367	-0.334 ± 2.154	...	-0.617 ± 1.151	...
18	—	509	—	—	5h35m06.35s	-5d22m11.60s	0.015 ± 0.169	-0.058 ± 0.293	-0.187 ± 2.417	0.170 ± 2.730	-0.020 ± 1.658	-0.356 ± 1.323	0.425 ± 0.730	...
19	—	321	—	—	5h35m06.44s	-5d23m15.30s	0.052 ± 0.161	-0.086 ± 0.314	0.113 ± 1.030	0.164 ± 0.948	0.057 ± 0.640	0.028 ± 0.228	0.093 ± 0.302	...
20	—	526	—	—	5h35m06.45s	-5d22m07.60s	0.038 ± 0.211	0.292 ± 0.343	-0.462 ± 2.676	-0.023 ± 2.732	0.499 ± 1.407	0.026 ± 1.409	0.290 ± 0.756	...
21	—	636	—	—	5h35m06.46s	-5d21m18.80s	0.022 ± 0.222	-0.261 ± 0.429
22	—	99	—	—	5h35m06.53s	-5d24m41.50s	-0.021 ± 0.152	0.114 ± 0.343	0.239 ± 0.837	0.092 ± 0.747	0.072 ± 0.649	-0.092 ± 0.178	-0.178 ± 0.289	...
23	—	116	—	—	5h35m06.53s	-5d24m33.30s	0.043 ± 0.147	0.099 ± 0.295	-0.052 ± 0.760	-0.074 ± 0.848	-0.088 ± 0.528	0.002 ± 0.185	-0.137 ± 0.242	...
24	—	742	—	—	5h35m06.54s	-5d22m28.60s	0.027 ± 0.193	0.014 ± 0.336	-0.804 ± 2.140	0.598 ± 2.413	-0.216 ± 1.313	-0.072 ± 0.753	-0.140 ± 0.605	...
25	—	60	—	—	5h35m06.55s	-5d25m01.70s	0.011 ± 0.163	-0.125 ± 0.423	-0.520 ± 1.617	0.179 ± 1.364	0.067 ± 0.872	-0.021 ± 0.305	-0.044 ± 0.446	...
26	—	066-652	—	—	5h35m06.59s	-5d26m51.99s	-0.017 ± 0.238	0.009 ± 0.999
27	—	741	—	—	5h35m06.67s	-5d22m44.60s	0.055 ± 0.164	0.084 ± 0.282	0.285 ± 1.806	0.340 ± 1.635	-0.072 ± 1.031	0.260 ± 0.586	0.319 ± 0.534	...
28	—	521	—	—	5h35m06.89s	-5d22m09.30s	0.018 ± 0.190	0.084 ± 0.344	0.366 ± 2.157	-0.163 ± 2.072	0.034 ± 1.167	-0.469 ± 0.989	0.026 ± 0.597	...
29	069-601	—	—	—	5h35m06.91s	-5d26m00.60s	-0.030 ± 0.165	0.186 ± 0.533
30	—	497	—	—	5h35m07.04s	-5d22m16.90s	0.035 ± 0.174	-0.020 ± 0.333	-0.164 ± 1.928	-0.081 ± 1.748	-0.248 ± 1.108	0.520 ± 0.872	0.025 ± 0.577	...
31	—	64	—	—	5h35m07.06s	-5d25m00.90s	-0.094 ± 0.178	0.067 ± 0.342	0.236 ± 1.232	-0.420 ± 1.245	-0.151 ± 0.882	-0.069 ± 0.290	-0.034 ± 0.383	...
32	—	715	—	—	5h35m07.17s	-5d24m45.80s	0.074 ± 0.169	0.008 ± 0.304	-0.163 ± 0.841	-0.219 ± 0.777	0.045 ± 0.582	-0.121 ± 0.222	-0.250 ± 0.303	...
33	072-135	603	—	—	5h35m07.21s	-5d21m34.42s	0.111 ± 0.193	-0.037 ± 0.330	1.628 ± 2.702	-0.884 ± 2.385	0.318 ± 1.816	0.024 ± 1.193	0.223 ± 0.751	...
34	—	534	—	—	5h35m07.24s	-5d22m03.90s	0.002 ± 0.198	0.094 ± 0.281	-0.475 ± 1.748	-0.068 ± 1.281	0.075 ± 0.995	-0.044 ± 0.742	0.028 ± 0.494	...
35	073-227	467	—	—	5h35m07.27s	-5d22m26.58s	0.057 ± 0.187	0.119 ± 0.299	0.243 ± 1.646	-0.155 ± 1.259	-0.071 ± 0.990	-0.206 ± 0.790	0.025 ± 0.444	...
36	—	459	—	—	5h35m07.39s	-5d22m29.00s	0.033 ± 0.175	-0.016 ± 0.281	-0.047 ± 1.333	-0.029 ± 1.240	-0.062 ± 0.849	0.187 ± 0.677	-0.031 ± 0.446	...
37	—	1	—	—	5h35m07.41s	-5d25m48.20s	0.001 ± 0.158	-0.038 ± 0.457
38	—	718	—	—	5h35m07.52s	-5d21m45.90s	-0.031 ± 0.200	0.182 ± 0.316	0.676 ± 1.776	-0.464 ± 1.411	-0.200 ± 1.067	-0.125 ± 0.898	-0.0205 ± 0.551	...
39	—	777	—	—	5h35m07.57s	-5d22m00.50s	0.021 ± 0.177	-0.040 ± 0.257	-0.352 ± 1.642	-0.446 ± 1.263	0.027 ± 0.836	0.364 ± 0.809	0.122 ± 0.401	...
40	—	175	—	—	5h35m07.64s	-5d24m00.80s	0.089 ± 0.168	0.174 ± 0.218	0.006 ± 0.491	-0.025 ± 0.462	0.144 ± 0.350	-0.046 ± 0.137	-0.022 ± 0.189	...
41	—	85	—	—	5h35m07.71s	-5d24m53.00s	0.001 ± 0.151	-0.177 ± 0.338	-0.233 ± 0.861	0.083 ± 0.918	0.087 ± 0.639	-0.059 ± 0.192	-0.145 ± 0.301	...
42	—	667	—	—	5h35m07.74s	-5d21m01.50s	0.029 ± 0.210	-0.038 ± 0.381
43	—	625	—	—	5h35m07.74s	-5d21m27.10s	-0.029 ± 0.208	0.086 ± 0.424	-0.541 ± 2.599	-0.427 ± 2.418	-0.156 ± 1.226	-0.479 ± 1.062	-0.084 ± 0.726	...
44	—	670	—	—	5h35m07.84s	-5d21m00.40s	-0.056 ± 0.218	-0.038 ± 0.379
45	—	639	—	—	5h35m07.95s	-5d21m17.20s	-0.078 ± 0.220	-0.019 ± 0.367	-0.763 ± 3.085	-0.279 ± 2.775	0.624 ± 1.847	-0.149 ± 1.322	-0.295 ± 0.896	...
46	—	711	—	—	5h35m07.95s	-5d21m17.80s	-0.113 ± 0.233	0.097 ± 0.361	-0.698 ± 3.107	-0.345 ± 2.838	-0.149 ± 1.584	0.382 ± 1.563	-0.260 ± 0.804	...
47	—	743	—	—	5h35m08.10s	-5d23m15.20s	-0.079 ± 0.166	0.131 ± 0.239	-0.156 ± 0.569	-0.093 ± 0.598	0.177 ± 0.440	0.024 ± 0.178	0.022 ± 0.228	...
48	—	433	—	—	5h35m08.11s	-5d22m37.50s	-0.050 ± 0.201	-0.114 ± 0.231	0.088 ± 1.139	0.028 ± 0.942	-0.036 ± 0.659	0.137 ± 0.476	0.009 ± 0.321	...
49	—	166	—	—	5h35m08.23s	-5d24m03.30s	0.125 ± 0.157	-0.086 ± 0.232	0.027 ± 0.454	0.005 ± 0.434	-0.064 ± 0.339	0.015 ± 0.145	0.074 ± 0.166	...
50	—	693	—	—	5h35m08.23s	-5d22m40.90s	-0.097 ± 0.233	0.136 ± 0.412
51	—	400	—	—	5h35m08.24s	-5d21m00.40s	-0.056 ± 0.218	-0.038 ± 0.379
52	—	725	—	—	5h35m08.27s	-5d23m07.80s	0.048 ± 0.172	0.061 ± 0.233	-0.162 ± 0.786	-0.060 ± 0.647	-0.006 ± 0.505	0.030 ± 0.209	0.038 ± 0.225	...
53	—	115	—	—	5h35m08.31s	-5d24m35.00s	-0.024 ± 0.167	0.052 ± 0.251	0.109 ± 0.616	-0.083 ± 0.616	-0.031 ± 0.430	-0.005 ± 0.140	-0.017 ± 0.210	...
54	—	740	—	—	5h35m08.32s	-5d21m02.40s	0.092 ± 0.230	0.036 ± 0.436	0.115 ± 2.149	-0.232 ± 1.577	0.314 ± 1.429	...
55	—	749	—	—	5h35m08.34s	-5d23m21.90s	-0.035 ± 0.167	0.198 ± 0.206	0.085 ± 0.560	0.034 ± 0.528	0.090 ± 0.457	-0.034 ± 0.142	-0.010 ± 0.237	...
56	—	454	—	—	5h35m08.42s	-5d22m30.30s	-0.059 ± 0.163	-0.141 ± 0.222	-0.281 ± 0.875	0.111 ± 0.877	-0.129 ± 0.587	0.106 ± 0.497	0.073 ± 0.297	...
57	—	634	—	—	5h35m08.43s	-5d21m19.80s	0.158 ± 0.210	0.048 ± 0.329	0.637 ± 2.122	-0.550 ± 2.156	-0.284 ± 1.242	0.537 ± 1.054	0.000 ± 0.608	...
58	—	353	—	—	5h35m08.44s	-5d23m05.00s	0.143 ± 0.186	0.197 ± 0.228	0.062 ± 0.773	0.069 ± 0.705	0.191 ± 0.554	0.015 ± 0.248	0.218 ± 0.276	...
59	—	100	—	—	5h35m08.53s	-5d24m41.70s	-0.028 ± 0.144	0.127 ± 0.284	-0.093 ± 0.647	0.073 ± 0.568	0.157 ± 0.456	-0.008 ± 0.157	0.040 ± 0.210	...
60	—	37	—	—	5h35m08.54s	-5d25m18.10s	-0.054 ± 0.141	0.033 ± 0.303	-0.006 ± 0.204	0.009 ± 1.935	0.190 ± 1.316	-0.004 ± 0.392	-0.076 ± 0.603	...
61	—	102	—	—	5h35m08.58s	-5d24m40.40s	0.020 ± 0.140	0.100 ± 0.264	-0.034 ± 0.626	0.132 ± 0.563	0.016 ± 0.478	-0.043 ± 0.157	-0.038 ± 0.217	...
62	—	290	—	—	5h35m08.62									

TABLE 2 — *Continued*

ID	Proplyd Name	HC00 ID	GMR ID	Z04a ID	Other Names	R.A. [J2000]	Dec [J2000]	$F_{\nu, 6\text{cm}}$ [mJy]	$F_{\nu, 3.6\text{cm}}$ [mJy]	$F_{\nu, 1.3\text{cm}, 1^a}$ [mJy]	$F_{\nu, 1.3\text{cm}, 2^a}$ [mJy]	$F_{\nu, 1.3\text{cm}, 3^a}$ [mJy]	$F_{\nu, 1.3\text{cm}, 4^a}$ [mJy]	$F_{\nu, 1.3\text{cm}, mean^a}$ [mJy]
81	—	723	—	—	5h35m09.91s	-5d24m10.50s	0.050 ± 0.149	-0.009 ± 0.226	-0.080 ± 0.503	0.030 ± 0.460	0.066 ± 0.346	0.005 ± 0.105	0.059 ± 0.199	0.059 ± 0.199
82	—	588	—	—	5h35m09.93s	-5d21m43.40s	0.004 ± 0.178	-0.130 ± 0.271	-0.068 ± 0.749	0.038 ± 0.764	-0.256 ± 0.485	-0.124 ± 0.481	-0.292 ± 0.307	-0.292 ± 0.307
83	—	179	—	—	5h35m09.94s	-5d23m59.00s	-0.071 ± 0.150	0.130 ± 0.219	-0.090 ± 0.453	-0.028 ± 0.414	0.071 ± 0.344	-0.012 ± 0.136	-0.026 ± 0.183	-0.026 ± 0.183
84	—	62	—	—	5h35m10.03s	-5d25m01.50s	-0.019 ± 0.166	-0.046 ± 0.243	-0.195 ± 1.167	0.530 ± 1.128	0.141 ± 0.685	-0.022 ± 0.243	0.060 ± 0.447	0.060 ± 0.447
85	—	173	—	—	5h35m10.04s	-5d24m02.00s	-0.021 ± 0.147	0.139 ± 0.192	0.135 ± 0.411	-0.128 ± 0.410	0.042 ± 0.365	-0.014 ± 0.112	-0.009 ± 0.166	-0.009 ± 0.166
86	—	26	—	—	5h35m10.08s	-5d25m31.50s	0.009 ± 0.172	0.084 ± 0.272	0.171 ± 2.139	-0.189 ± 0.710	-0.013 ± 0.109	-0.013 ± 0.109
87	102-233	445	—	—	5h35m10.14s	-5d22m32.72s	0.106 ± 0.173	0.112 ± 0.199	0.171 ± 0.539	0.274 ± 0.525	-0.038 ± 0.419	0.008 ± 0.461	0.165 ± 0.196	0.165 ± 0.196
88	102-021	—	—	—	5h35m10.19s	-5d20m20.99s	0.131 ± 0.248	0.251 ± 0.517
89	—	671	—	—	5h35m10.20s	-5d21m00.40s	0.025 ± 0.192	-0.293 ± 0.364	-0.462 ± 2.560	-0.738 ± 2.363	0.720 ± 1.405	0.531 ± 1.337	0.047 ± 0.719	0.047 ± 0.719
90	102-322	305	—	—	5h35m10.21s	-5d23m21.58s	0.052 ± 0.176	-0.036 ± 0.206	-0.098 ± 0.606	-0.065 ± 0.508	0.087 ± 0.382	-0.029 ± 0.198	-0.094 ± 0.206	-0.094 ± 0.206
91	—	553	—	—	5h35m10.27s	-5d21m57.20s	-0.141 ± 0.174	-0.017 ± 0.242	-0.034 ± 0.579	-0.014 ± 0.519	0.000 ± 0.395	-0.160 ± 0.438	0.099 ± 0.203	0.099 ± 0.203
92	—	320	—	—	5h35m10.27s	-5d23m16.40s	0.042 ± 0.172	-0.010 ± 0.222	0.104 ± 0.600	-0.045 ± 0.552	0.076 ± 0.428	0.013 ± 0.234	-0.094 ± 0.202	-0.094 ± 0.202
93	—	144	—	—	5h35m10.31s	-5d24m17.50s	0.055 ± 0.154	-0.016 ± 0.170	-0.122 ± 0.473	-0.176 ± 0.493	-0.041 ± 0.381	-0.064 ± 0.129	-0.126 ± 0.192	-0.126 ± 0.192
94	—	647	—	—	5h35m10.32s	-5d21m13.10s	-0.206 ± 0.197	-0.036 ± 0.293	-0.553 ± 1.511	-0.183 ± 1.522	-0.005 ± 1.113	0.027 ± 0.885	0.177 ± 0.382	0.177 ± 0.382
95	—	90	—	—	5h35m10.38s	-5d24m51.60s	0.067 ± 0.162	-0.061 ± 0.204	-0.150 ± 0.895	-0.168 ± 0.831	-0.177 ± 0.567	-0.002 ± 0.201	-0.179 ± 0.346	-0.179 ± 0.346
96	—	374	—	—	5h35m10.39s	-5d22m59.80s	-0.040 ± 0.166	-0.036 ± 0.189	0.103 ± 0.575	-0.073 ± 0.670	-0.022 ± 0.423	-0.043 ± 0.305	-0.074 ± 0.194	-0.074 ± 0.194
97	—	—	—	—	5h35m10.43s	-5d24m30.30s	0.112 ± 0.139	0.103 ± 0.211	0.160 ± 0.607	0.075 ± 0.580	-0.075 ± 0.405	-0.010 ± 0.155	0.194 ± 0.043	0.194 ± 0.043
98	—	605	—	—	5h35m10.43s	-5d21m34.60s	0.088 ± 0.183	-0.005 ± 0.270	-0.234 ± 0.817	0.053 ± 0.765	-0.127 ± 0.650	-0.374 ± 0.689	-0.128 ± 0.314	-0.128 ± 0.314
99	—	466	—	—	5h35m10.45s	-5d22m27.30s	-0.048 ± 0.165	0.086 ± 0.179	0.045 ± 0.508	0.017 ± 0.508	-0.098 ± 0.414	0.006 ± 0.398	-0.122 ± 0.201	-0.122 ± 0.201
100	—	570	—	—	5h35m10.47s	-5d21m49.60s	0.026 ± 0.193	0.109 ± 0.243	-0.024 ± 0.679	0.159 ± 0.622	0.203 ± 0.462	-0.268 ± 0.473	-0.061 ± 0.233	-0.061 ± 0.233
101	—	612	—	—	5h35m10.47s	-5d21m32.50s	0.056 ± 0.195	-0.047 ± 0.272	-0.050 ± 0.969	-0.075 ± 0.776	-0.379 ± 0.619	0.036 ± 0.625	-0.097 ± 0.286	-0.097 ± 0.286
102	—	417	—	3	5h35m10.49s	-5d22m45.75s	0.062 ± 0.132	0.153 ± 0.232	-0.035 ± 0.533	0.041 ± 0.519	-0.082 ± 0.399	-0.029 ± 0.396	0.027 ± 0.212	0.027 ± 0.212
103	—	—	—	—	5h35m10.51s	-5d22m25.01s	0.186 ± 0.154	-0.337 ± 0.210	0.154 ± 0.526	-0.017 ± 0.489	0.185 ± 0.052	-0.027 ± 0.393	0.035 ± 0.201	0.035 ± 0.201
104	—	8	—	—	5h35m10.52s	-5d25m44.60s	-0.071 ± 0.163	-0.166 ± 0.326
105	—	500	—	—	5h35m10.54s	-5d22m16.60s	0.008 ± 0.161	0.164 ± 0.200	-0.027 ± 0.506	-0.169 ± 0.470	0.091 ± 0.433	-0.252 ± 0.399	-0.046 ± 0.208	-0.046 ± 0.208
106	106-417	146	—	—	5h35m10.55s	-5d24m16.75s	0.009 ± 0.149	-0.071 ± 0.196	0.047 ± 0.443	-0.003 ± 0.443	0.016 ± 0.377	-0.023 ± 0.118	-0.010 ± 0.171	-0.010 ± 0.171
107	—	421	—	—	5h35m10.58s	-5d22m44.80s	0.084 ± 0.130	-0.004 ± 0.214	0.004 ± 0.572	0.040 ± 0.529	0.043 ± 0.411	-0.071 ± 0.426	0.025 ± 0.219	0.025 ± 0.219
108	106-156	554	—	—	5h35m10.58s	-5d21m56.27s	0.196 ± 0.199	0.118 ± 0.260	0.145 ± 0.615	0.123 ± 0.522	0.013 ± 0.441	0.369 ± 0.485	0.088 ± 0.260	0.088 ± 0.260
109	—	385	—	—	5h35m10.62s	-5d22m56.06s	-0.028 ± 0.165	0.167 ± 0.239	-0.109 ± 0.634	-0.138 ± 0.577	-0.031 ± 0.494	0.191 ± 0.397	0.035 ± 0.545	0.035 ± 0.545
110	—	2	—	—	5h35m10.63s	-5d25m48.10s	0.016 ± 0.171	0.003 ± 0.305
111	—	363	—	—	5h35m10.65s	-5d23m03.40s	0.162 ± 0.133	-0.200 ± 0.193	0.030 ± 0.657	-0.081 ± 0.560	0.094 ± 0.393	-0.053 ± 0.301	-0.284 ± 0.218	-0.284 ± 0.218
112	—	260	—	—	5h35m10.69s	-5d23m32.80s	0.033 ± 0.165	0.084 ± 0.241	0.068 ± 0.673	0.121 ± 0.462	-0.020 ± 0.398	0.012 ± 0.170	-0.011 ± 0.216	-0.011 ± 0.216
113	—	489	—	—	5h35m10.71s	-5d22m20.30s	-0.029 ± 0.139	0.196 ± 0.212	0.148 ± 0.522	0.219 ± 0.456	0.070 ± 0.397	0.094 ± 0.472	0.095 ± 0.168	0.095 ± 0.168
114	—	392	—	—	5h35m10.73s	-5d22m54.50s	0.046 ± 0.146	0.161 ± 0.199	-0.127 ± 0.561	0.159 ± 0.526	-0.163 ± 0.437	-0.068 ± 0.354	0.049 ± 0.202	0.049 ± 0.202
115	—	224	—	4	5h35m10.73s	-5d23m44.67s	0.401 ± 0.077	0.374 ± 0.067	0.160 ± 0.038	0.004 ± 0.481	0.313 ± 0.066	0.543 ± 0.083	0.088 ± 0.202	0.088 ± 0.202
116	—	576	—	—	5h35m10.82s	-5d21m48.90s	-0.027 ± 0.149	0.279 ± 0.245	0.201 ± 0.608	0.042 ± 0.566	-0.085 ± 0.470	0.169 ± 0.525	0.090 ± 0.207	0.090 ± 0.207
117	—	426	—	—	5h35m10.85s	-5d22m40.80s	0.066 ± 0.160	-0.108 ± 0.196	0.062 ± 0.544	-0.066 ± 0.556	0.023 ± 0.335	0.170 ± 0.383	-0.018 ± 0.220	-0.018 ± 0.220
118	—	529	—	—	5h35m10.88s	-5d22m06.00s	-0.022 ± 0.167	0.060 ± 0.218	-0.080 ± 0.476	-0.022 ± 0.471	0.087 ± 0.399	0.025 ± 0.435	-0.058 ± 0.216	-0.058 ± 0.216
119	109-246	416	—	—	5h35m10.90s	-5d22m46.38s	0.088 ± 0.159	0.037 ± 0.234	0.077 ± 0.535	0.100 ± 0.558	0.032 ± 0.441	0.021 ± 0.449	0.070 ± 0.228	0.070 ± 0.228
120	109-327	286	—	—	5h35m10.95s	-5d23m26.58s	0.132 ± 0.172	-0.002 ± 0.207	0.310 ± 0.595	0.420 ± 0.573	0.225 ± 0.411	0.212 ± 0.202	0.052 ± 0.205	0.052 ± 0.205
121	—	93	—	—	5h35m10.95s	-5d24m48.80s	-0.047 ± 0.117	0.108 ± 0.223	-0.092 ± 0.998	0.089 ± 0.809	-0.113 ± 0.620	0.130 ± 0.212	0.065 ± 0.316	0.065 ± 0.316
122	—	582	—	—	5h35m10.97s	-5d21m46.40s	-0.122 ± 0.175	0.055 ± 0.262	0.258 ± 0.667	0.074 ± 0.569	0.076 ± 0.483	-0.071 ± 0.492	0.059 ± 0.253	0.059 ± 0.253
123	—	473	—	—	5h35m10.99s	-5d22m24.80s	0.006 ± 0.152	0.015 ± 0.207	-0.061 ± 0.437	-0.180 ± 0.463	-0.055 ± 0.400	-0.104 ± 0.356	0.022 ± 0.222	0.022 ± 0.222
124	—	415	—	—	5h35m11.04s	-5d22m46.70s	-0.006 ± 0.159	-0.022 ± 0.210	-0.102 ± 0.568	-0.047 ± 0.505	-0.065 ± 0.368	0.217 ± 0.434	-0.079 ± 0.189	-0.079 ± 0.189
125	—	329	—	—	5h35m11.09s	-5d23m14.70s	0.026 ± 0.150	0.187 ± 0.197	-0.288 ± 0.612	0.034 ± 0.640	0.003 ± 0.402	-0.050 ± 0.285	-0.036 ± 0.226	-0.036 ± 0.226
126	—	111	—	—	5h35m11.15s	-5d24m36.50s	-0.034 ± 0.175	-0.079 ± 0.185	0.016 ± 0.740	-0.033 ± 0.722	-0.008 ± 0.517	0.034 ± 0.191	-0.063 ± 0.244	-0.063 ± 0.244
127	—	24	—	—	5h35m11.16s	-5d25m32.30s	-0.104 ± 0.134	0.171 ± 0.223	-1.142 ± 1.779	0.120 ± 0.654	0.044 ± 0.867	0.044 ± 0.867
128	—	434	—	—	5h35m11.20s	-5d22m37.80s	0.045 ± 0.159	0.012 ± 0.209	0.053 ± 0.461	0.026 ± 0.514	-0.061 ± 0.361	0.103 ± 0.417	0.010 ± 0.185	0.010 ± 0.185
129	—	515	—	—	5h35m11.21s	-5d22m10.80s	-0.023 ± 0.147	-0.160 ± 0.199	0.052 ± 0.534	0.202 ± 0.449	-0.024 ± 0.420	0.008 ± 0.440	0.007 ± 0.185	0.007 ± 0.185
130	—	148	—	—	5h35m11.27s	-5d24m16.50s	-0.031 ± 0.147	-0.013 ± 0.180	-0.125 ± 0.567	0.073 ± 0.557	-0.007 ± 0.409	-0.129 ± 0.166	-0.033 ± 0.184	-0.033 ± 0.184
131	—	666	—	—	5h35m11.29s	-5d21m03.10s	-0.057 ± 0.219	0.028 ± 0.282	-1.066 ± 1.890	-0.197 ± 1.818	-0.167 ± 1.384	0.264 ± 1.233	-0.041 ± 0.659	-0.041 ± 0.659
132	114-426	127	—	—	5h35m11.32s	-5d24m26.54s	0.056 ± 0.167	-0.017 ± 0.196	0.172 ± 0.647	0.045 ± 0.708	0.096 ± 0.432	-0.018 ± 0.200	0.064 ± 0.220	0.064 ± 0.220
133	—	643	—	—	5h35m11.32s	-5d21m15.60s								

TABLE 2 — *Continued*

ID	Proplyd Name	HC00 ID	GMR ID	Z04a ID	Other Names	R.A. [J2000]	Dec [J2000]	$F_{\nu, 6\text{cm}}$ [mJy]	$F_{\nu, 3.6\text{cm}}$ [mJy]	$F_{\nu, 1.3\text{cm}, 1^a}$ [mJy]	$F_{\nu, 1.3\text{cm}, 2^a}$ [mJy]	$F_{\nu, 1.3\text{cm}, 3^a}$ [mJy]	$F_{\nu, 1.3\text{cm}, 4^a}$ [mJy]	$F_{\nu, 1.3\text{cm}, \text{mean}^a}$ [mJy]
161	—	395	—	—	5h35m11.98s	-5d22m54.13s	-0.044 ± 0.160	0.099 ± 0.177	0.185 ± 0.604	0.094 ± 0.626	0.132 ± 0.420	-0.046 ± 0.394	0.153 ± 0.157	
162	—	772	—	—	5h35m11.98s	-5d22m08.00s	-0.072 ± 0.157	0.123 ± 0.206	-0.166 ± 0.495	0.098 ± 0.488	0.053 ± 0.351	-0.063 ± 0.439	-0.092 ± 0.209	
163	121-1925	—	—	—	5h35m12.09s	-5d19m24.80s	0.022 ± 0.283	-0.052 ± 0.903	
164	—	95	—	—	5h35m12.12s	-5d24m48.00s	-0.024 ± 0.125	-0.029 ± 0.183	-0.174 ± 0.984	-0.324 ± 1.005	-0.120 ± 0.549	0.100 ± 0.242	0.017 ± 0.324	
165	121-434	117	—	—	5h35m12.12s	-5d24m33.85s	0.060 ± 0.122	0.162 ± 0.170	-0.083 ± 0.828	0.108 ± 0.696	0.080 ± 0.485	-0.012 ± 0.229	-0.017 ± 0.245	
166	—	746	—	—	5h35m12.14s	-5d21m48.50s	-0.089 ± 0.165	0.060 ± 0.221	-0.067 ± 0.620	0.020 ± 0.578	-0.092 ± 0.452	-0.222 ± 0.479	0.051 ± 0.255	
167	—	263	—	—	5h35m12.15s	-5d23m32.00s	-0.149 ± 0.150	0.047 ± 0.182	-0.255 ± 0.725	0.146 ± 0.715	0.082 ± 0.470	-0.129 ± 0.264	-0.112 ± 0.209	
168	—	747	—	—	5h35m12.16s	-5d21m53.80s	-0.050 ± 0.154	0.136 ± 0.219	0.015 ± 0.544	-0.218 ± 0.572	-0.157 ± 0.438	0.291 ± 0.428	0.060 ± 0.208	
169	—	88	—	—	5h35m12.17s	-5d24m52.20s	-0.034 ± 0.147	-0.033 ± 0.175	0.181 ± 1.181	-0.053 ± 0.952	-0.264 ± 0.645	-0.025 ± 0.279	-0.218 ± 0.329	
170	—	751	—	—	5h35m12.20s	-5d22m30.80s	-0.036 ± 0.160	-0.006 ± 0.187	0.144 ± 0.422	-0.224 ± 0.496	-0.077 ± 0.403	0.111 ± 0.502	-0.181 ± 0.187	
171	—	77	—	—	5h35m12.21s	-5d24m56.50s	-0.111 ± 0.140	-0.024 ± 0.176	-0.383 ± 1.199	0.260 ± 1.255	0.125 ± 0.581	0.040 ± 0.280	0.041 ± 0.320	
172	—	72	—	—	5h35m12.25s	-5d24m58.80s	-0.078 ± 0.160	-0.021 ± 0.208	-0.090 ± 0.131	-0.418 ± 1.124	0.157 ± 0.797	-0.001 ± 0.281	-0.122 ± 0.347	
173	—	752	—	—	5h35m12.27s	-5d22m26.96s	-0.031 ± 0.169	0.060 ± 0.168	-0.041 ± 0.524	0.135 ± 0.042	-0.163 ± 0.391	-0.245 ± 0.390	-0.103 ± 0.187	
174	—	698	—	—	5h35m12.28s	-5d20m45.20s	0.061 ± 0.216	-0.028 ± 0.337	-0.019 ± 2.334	-0.013 ± 1.811	-0.118 ± 1.203	
175	—	215	—	—	5h35m12.28s	-5d23m48.10s	-0.083 ± 0.177	-0.026 ± 0.232	-0.446 ± 0.668	-0.009 ± 0.654	0.250 ± 0.400	-0.026 ± 0.236	-0.156 ± 0.227	
176	—	762	—	—	5h35m12.37s	-5d21m54.80s	0.073 ± 0.167	-0.076 ± 0.211	0.191 ± 0.501	0.001 ± 0.566	0.185 ± 0.387	0.329 ± 0.373	0.154 ± 0.204	
177	124-132	616	—	—	5h35m12.38s	-5d21m31.49s	0.076 ± 0.169	-0.005 ± 0.223	0.056 ± 0.840	0.134 ± 0.871	-0.113 ± 0.556	0.283 ± 0.532	0.082 ± 0.316	
178	—	206	—	—	5h35m12.39s	-5d23m51.70s	-0.017 ± 0.175	0.023 ± 0.222	0.193 ± 0.645	-0.129 ± 0.613	0.222 ± 0.451	0.052 ± 0.257	0.107 ± 0.245	
179	—	692	—	—	5h35m12.40s	-5d20m47.90s	0.046 ± 0.196	0.045 ± 0.304	0.262 ± 2.116	-0.690 ± 1.990	-0.695 ± 0.992	
180	—	753	—	—	5h35m12.43s	-5d22m08.70s	0.071 ± 0.175	0.085 ± 0.193	0.096 ± 0.520	-0.218 ± 0.537	0.115 ± 0.384	-0.293 ± 0.443	-0.144 ± 0.193	
181	—	761	—	—	5h35m12.46s	-5d21m37.80s	0.038 ± 0.162	-0.066 ± 0.202	0.069 ± 0.651	-0.126 ± 0.644	0.063 ± 0.529	0.030 ± 0.501	0.025 ± 0.246	
182	—	169	—	—	5h35m12.47s	-5d24m03.70s	0.036 ± 0.207	0.050 ± 0.174	-0.064 ± 0.685	-0.168 ± 0.644	-0.232 ± 0.497	0.008 ± 0.255	0.144 ± 0.201	
183	—	106	—	—	5h35m12.49s	-5d24m38.10s	-0.019 ± 0.156	-0.061 ± 0.171	0.052 ± 0.825	0.191 ± 0.855	0.055 ± 0.456	-0.052 ± 0.233	-0.046 ± 0.279	
184	—	368	33	—	5h35m12.56s	-5d23m02.04s	0.165 ± 0.156	0.106 ± 0.210	0.119 ± 0.693	0.140 ± 0.621	-0.025 ± 0.456	-0.068 ± 0.362	-0.222 ± 0.233	
185	—	228	—	—	5h35m12.60s	-5d23m44.20s	0.057 ± 0.187	-0.009 ± 0.192	-0.156 ± 0.703	0.034 ± 0.723	0.024 ± 0.415	-0.062 ± 0.283	-0.241 ± 0.242	
186	—	696	—	—	5h35m12.65s	-5d20m47.30s	0.084 ± 0.181	-0.087 ± 0.311	1.223 ± 2.178	0.688 ± 1.982	-0.459 ± 0.107	
187	—	609	—	—	5h35m12.67s	-5d21m33.40s	0.039 ± 0.186	-0.029 ± 0.270	-0.160 ± 0.687	0.310 ± 0.865	0.158 ± 0.597	0.007 ± 0.606	0.200 ± 0.286	
188	—	770	—	—	5h35m12.68s	-5d21m47.60s	-0.070 ± 0.164	0.065 ± 0.192	0.152 ± 0.591	0.403 ± 0.656	0.042 ± 0.509	0.131 ± 0.448	0.236 ± 0.192	
189	—	128	—	—	5h35m12.70s	-5d24m26.50s	-0.034 ± 0.140	-0.028 ± 0.179	-0.239 ± 0.747	-0.008 ± 0.712	-0.008 ± 0.470	-0.122 ± 0.232	-0.111 ± 0.214	
190	—	—	—	—	5h35m12.72s	-5d23m53.09s	0.336 ± 0.090	0.064 ± 0.201	0.529 ± 0.680	0.376 ± 0.630	0.237 ± 0.415	-0.074 ± 0.285	-0.018 ± 0.255	
191	—	712	—	—	5h35m12.77s	-5d21m58.90s	-0.064 ± 0.142	0.112 ± 0.225	-0.199 ± 0.592	-0.059 ± 0.604	-0.052 ± 0.417	0.195 ± 0.409	0.066 ± 0.232	
192	—	706	—	—	5h35m12.79s	-5d21m57.90s	0.008 ± 0.176	-0.028 ± 0.202	-0.025 ± 0.505	0.075 ± 0.570	-0.181 ± 0.453	0.090 ± 0.439	-0.022 ± 0.215	
193	—	699	—	—	5h35m12.83s	-5d20m43.60s	0.098 ± 0.209	-0.000 ± 0.396	0.291 ± 2.280	...	0.494 ± 1.260	
194	—	606	—	—	5h35m12.85s	-5d21m33.90s	-0.064 ± 0.196	0.086 ± 0.245	0.030 ± 0.875	-0.141 ± 0.789	0.038 ± 0.603	0.062 ± 0.630	0.142 ± 0.293	
195	—	659	—	—	5h35m12.86s	-5d21m05.00s	0.134 ± 0.193	-0.045 ± 0.286	0.059 ± 0.972	-0.013 ± 1.500	0.280 ± 1.156	0.541 ± 0.939	0.447 ± 0.519	
196	—	608	—	—	5h35m12.89s	-5d21m33.70s	-0.002 ± 0.185	-0.266 ± 0.244	-0.029 ± 0.712	-0.300 ± 0.652	0.102 ± 0.567	-0.032 ± 0.227	...	
197	—	84	—	—	5h35m12.90s	-5d24m54.40s	-0.025 ± 0.144	-0.004 ± 0.201	0.301 ± 0.925	0.249 ± 0.874	-0.150 ± 0.644	0.091 ± 0.247	0.004 ± 0.308	
198	—	74	—	—	5h35m12.95s	-5d24m58.00s	0.120 ± 0.151	0.042 ± 0.167	-0.028 ± 0.892	-0.161 ± 1.021	0.216 ± 0.642	-0.142 ± 0.290	0.039 ± 0.272	
199	—	—	—	—	5h35m12.97s	-5d23m30.01s	0.129 ± 0.173	0.060 ± 0.177	0.142 ± 0.820	-0.417 ± 0.827	0.267 ± 0.607	0.535 ± 0.146	0.026 ± 0.216	
200	—	—	7	—	5h35m12.99s	-5d23m55.01s	-0.039 ± 0.195	0.117 ± 0.304	0.261 ± 3.633	-0.120 ± 0.677	0.188 ± 0.667	0.492 ± 0.105	0.660 ± 0.228	
201	—	683	—	—	5h35m13.02s	-5d20m25.90s	0.032 ± 0.201	0.060 ± 0.268	1.492 ± 3.327	0.930 ± 3.637	0.261 ± 1.773	-0.809 ± 1.569	0.201 ± 0.866	
202	—	544	—	—	5h35m13.03s	-5d22m01.00s	0.070 ± 0.163	0.013 ± 0.196	0.120 ± 0.546	-0.064 ± 0.536	0.180 ± 0.460	-0.118 ± 0.432	0.091 ± 0.201	
203	—	505	—	—	5h35m13.05s	-5d22m15.20s	0.058 ± 0.152	-0.044 ± 0.184	0.028 ± 0.498	0.231 ± 0.472	-0.120 ± 0.376	-0.016 ± 0.449	0.025 ± 0.213	
204	131-046	—	—	—	5h35m13.05s	-5d20m45.79s	-0.060 ± 0.219	-0.028 ± 0.354	-0.638 ± 2.384	0.979 ± 1.666	0.459 ± 1.348	
205	—	562	—	—	5h35m13.06s	-5d21m53.20s	-0.013 ± 0.150	0.051 ± 0.233	0.181 ± 0.517	-0.087 ± 0.627	0.092 ± 0.382	-0.054 ± 0.436	0.006 ± 0.222	
206	—	599	—	—	5h35m13.07s	-5d21m39.00s	0.015 ± 0.166	-0.048 ± 0.257	0.175 ± 0.764	-0.077 ± 0.689	0.189 ± 0.453	-0.141 ± 0.439	-0.035 ± 0.263	
207	—	402	—	—	5h35m13.09s	-5d22m53.20s	0.001 ± 0.161	0.005 ± 0.183	0.097 ± 0.658	0.258 ± 0.616	-0.046 ± 0.436	-0.055 ± 0.400	-0.099 ± 0.220	
208	—	648	—	—	5h35m13.11s	-5d21m13.40s	-0.085 ± 0.163	-0.005 ± 0.230	0.198 ± 1.430	-0.242 ± 1.300	0.048 ± 0.898	0.137 ± 0.796	-0.012 ± 0.441	
209	131-247	707	—	8	5h35m13.11s	-5d22m47.23s	0.364 ± 0.124	0.196 ± 0.058	0.417 ± 0.562	-0.188 ± 0.618	0.420 ± 0.400	0.136 ± 0.368	0.498 ± 0.995	
210	—	87	—	—	5h35m13.12s	-5d24m53.00s	-0.004 ± 0.126	-0.120 ± 0.191	-0.123 ± 0.791	0.199 ± 0.907	0.505 ± 0.614	-0.043 ± 0.264	0.054 ± 0.323	
211	—	487	—	—	5h35m13.18s	-5d22m21.20s	0.014 ± 0.169	-0.115 ± 0.198	-0.137 ± 0.505	-0.044 ± 0.587	-0.078 ± 0.406	0.096 ± 0.522	0.050 ± 0.190	
212	—	721	—	—	5h35m13.18s	-5d24m24.90s	0.057 ± 0.160	-0.008 ± 0.190	0.006 ± 0.750	-0.160 ± 0.591	0.154 ± 0.434	-0.181 ± 0.228	-0.000 ± 0.196	
213	—	Q	9	—	5h35m13.21s	-5d22m54.82s	0.108 ± 0.148	0.005 ± 0.193	-0.023 ± 0.674	-0.307 ± 0.601	1.769 ± 0.187	0.574 ± 0.388	0.399 ± 0.048	
214	—	80	—	—	5h35m13.21s	-5d24m55.50s	-0.030 ± 0.130	-0.018 ± 0.179	0.325 ± 0.957	-0.274 ± 1.043	0.048 ± 0.599	0.075 ± 0.271	0.115 ± 0.285	
215	—	682	—	—	5h35m13.22s	-5d20m52.80s	-0.025 ± 0.169	0.002 ± 0.279	-0.260 ± 2.713	-0.709 ± 3.659	-0.218 ± 1.781	-0.001 ± 0.1761	0.457 ± 0.894	
216	—	190	—	—	5h35m13.23s	-5d23m55.50s	-0.113 ± 0.179	-0.095 ± 0.184	-0.395 ± 0.701	0.027 ± 0.587	-0.227 ± 0.437	-0.233 ± 0.343	-0.182 ± 0.231	
217	132-1832	—	—	—										

TABLE 2 — *Continued*

ID	Proplyd Name	HC00 ID	GMR ID	Z04a ID	Other Names	R.A. [J2000]	Dec [J2000]	$F_{\nu, 6\text{cm}}$ [mJy]	$F_{\nu, 3.6\text{cm}}$ [mJy]	$F_{\nu, 1.3\text{cm}, 1}$ ^a [mJy]	$F_{\nu, 1.3\text{cm}, 2}$ ^a [mJy]	$F_{\nu, 1.3\text{cm}, 3}$ ^a [mJy]	$F_{\nu, 1.3\text{cm}, 4}$ ^a [mJy]	$F_{\nu, 1.3\text{cm}, \text{mean}}$ ^a [mJy]
241	136-1955	—	—	—	—	5h35m13.62s	-5d19m55.04s	-0.081 ± 0.258	0.007 ± 0.570
242	—	—	—	—	—	5h35m13.63s	-5d24m09.19s	-0.043 ± 0.171	0.082 ± 0.173	-0.138 ± 0.633	0.374 ± 0.665	0.133 ± 0.452	-0.210 ± 0.279	0.187 ± 0.041
243	—	—	—	—	MM22	5h35m13.65s	-5d23m54.94s	-0.071 ± 0.235	0.045 ± 0.218	0.288 ± 0.780	0.236 ± 0.555	0.297 ± 0.434	-0.210 ± 0.443	-0.085 ± 0.336
244	—	222	—	—	—	5h35m13.68s	-5d23m45.40s	-0.097 ± 0.220	-0.404 ± 0.168	-0.413 ± 0.607	-0.633 ± 0.710	-0.224 ± 0.442	0.028 ± 0.381	0.151 ± 0.242
245	—	719	—	—	—	5h35m13.70s	-5d25m31.90s	0.070 ± 0.140	0.025 ± 0.180	-0.003 ± 0.277	-0.060 ± 1.185	0.503 ± 0.723	-0.014 ± 0.257	0.192 ± 0.403
246	—	—	—	—	MM8	5h35m13.71s	-5d23m46.89s	0.173 ± 0.242	-0.094 ± 0.176	0.240 ± 0.063	0.379 ± 0.118	0.259 ± 0.078	0.480 ± 0.189	0.657 ± 0.184
247	—	602	—	—	—	5h35m13.73s	-5d21m35.83s	-0.032 ± 0.148	-0.140 ± 0.239	0.073 ± 0.738	-0.074 ± 0.887	-0.032 ± 0.521	0.022 ± 0.546	0.204 ± 0.077
248	—	483	—	—	—	5h35m13.75s	-5d22m22.00s	-0.079 ± 0.145	0.061 ± 0.183	-0.161 ± 0.745	0.248 ± 0.637	0.207 ± 0.450	-0.051 ± 0.467	0.115 ± 0.230
249	—	—	—	—	MM13	5h35m13.75s	-5d24m07.74s	-0.007 ± 0.133	0.123 ± 0.188	0.275 ± 0.705	-0.234 ± 0.588	-0.012 ± 0.406	0.201 ± 0.337	0.468 ± 0.220
250	—	499	—	—	—	5h35m13.78s	-5d22m17.40s	-0.074 ± 0.166	0.103 ± 0.223	-0.112 ± 0.504	0.469 ± 0.585	-0.177 ± 0.424	-0.243 ± 0.396	-0.221 ± 0.251
251	138-207	703	—	—	—	5h35m13.80s	-5d22m07.02s	-0.069 ± 0.161	-0.056 ± 0.187	-0.001 ± 0.541	0.116 ± 0.531	-0.031 ± 0.440	-0.048 ± 0.390	0.060 ± 0.022
252	—	548	—	—	—	5h35m13.80s	-5d21m59.67s	0.006 ± 0.168	0.192 ± 0.218	-0.370 ± 0.654	0.440 ± 0.570	0.109 ± 0.495	-0.028 ± 0.441	0.186 ± 0.074
253	—	242	—	—	—	5h35m13.80s	-5d23m40.12s	0.094 ± 0.193	-0.271 ± 0.177	-0.387 ± 0.749	0.198 ± 0.070	0.143 ± 0.050	-0.107 ± 0.386	0.185 ± 0.051
254	—	541	—	—	—	5h35m13.81s	-5d22m02.80s	0.137 ± 0.164	-0.073 ± 0.232	0.019 ± 0.617	0.342 ± 0.509	0.021 ± 0.455	-0.052 ± 0.398	-0.029 ± 0.232
255	—	525	—	—	—	5h35m13.83s	-5d22m09.10s	0.009 ± 0.159	-0.048 ± 0.194	-0.382 ± 0.522	-0.081 ± 0.536	0.136 ± 0.358	-0.112 ± 0.418	-0.009 ± 0.253
256	—	254	—	—	—	5h35m13.86s	-5d23m35.00s	0.051 ± 0.196	-0.004 ± 0.194	-0.138 ± 0.631	-0.240 ± 0.734	0.352 ± 0.488	0.103 ± 0.368	0.335 ± 0.225
257	—	—	—	—	—	5h35m13.88s	-5d23m57.21s	0.138 ± 0.224	0.180 ± 0.205	0.364 ± 0.090	0.157 ± 0.466	0.198 ± 0.055	-0.211 ± 0.406	0.230 ± 0.050
258	—	130	—	—	—	5h35m13.88s	-5d24m26.20s	-0.004 ± 0.154	0.105 ± 0.172	-0.057 ± 0.512	0.347 ± 0.533	-0.116 ± 0.397	-0.146 ± 0.225	-0.297 ± 0.224
259	—	—	—	—	—	5h35m13.93s	-5d24m09.41s	-0.128 ± 0.188	-0.267 ± 0.198	-0.212 ± 0.616	0.355 ± 0.076	0.367 ± 0.085	0.099 ± 0.270	0.010 ± 0.244
260	—	134	—	—	—	5h35m13.93s	-5d24m25.50s	0.085 ± 0.140	-0.030 ± 0.191	-0.052 ± 0.524	0.035 ± 0.590	-0.116 ± 0.388	0.067 ± 0.287	-0.080 ± 0.204
261	139-320	314	—	—	—	5h35m13.93s	-5d23m20.16s	0.309 ± 0.097	0.295 ± 0.086	-0.104 ± 0.698	0.413 ± 0.920	0.140 ± 0.454	0.232 ± 0.403	0.377 ± 0.288
262	—	—	—	—	—	5h35m13.93s	-5d24m09.49s	0.344 ± 0.130	0.168 ± 0.055	0.476 ± 0.179	0.225 ± 0.078	0.236 ± 0.092	0.518 ± 0.139	0.684 ± 0.135
263	—	451	—	—	—	5h35m13.97s	-5d22m31.90s	0.012 ± 0.142	0.117 ± 0.195	0.183 ± 0.507	0.274 ± 0.610	-0.031 ± 0.475	0.192 ± 0.364	0.242 ± 0.189
264	—	—	—	—	—	5h35m13.97s	-5d22m36.79s	-0.157 ± 0.151	-0.025 ± 0.212	0.163 ± 0.683	0.180 ± 0.561	0.143 ± 0.432	0.265 ± 0.392	0.337 ± 0.043
265	—	—	—	—	—	5h35m13.97s	-5d24m09.84s	-0.049 ± 0.188	0.172 ± 0.043	0.205 ± 0.062	0.166 ± 0.053	0.188 ± 0.051	0.093 ± 0.312	0.240 ± 0.032
266	—	552	—	—	—	5h35m13.98s	-5d21m58.00s	0.051 ± 0.171	-0.122 ± 0.218	0.090 ± 0.558	-0.088 ± 0.566	-0.013 ± 0.440	0.078 ± 0.426	0.042 ± 0.215
267	—	629	—	—	—	5h35m13.98s	-5d21m23.30s	-0.021 ± 0.141	-0.005 ± 0.241	-0.286 ± 1.289	-0.137 ± 1.012	0.167 ± 0.772	-0.024 ± 0.702	-0.022 ± 0.438
268	—	—	—	—	MM23	5h35m14.00s	-5d22m45.04s	0.114 ± 0.158	-0.075 ± 0.185	0.143 ± 0.696	0.334 ± 0.644	0.053 ± 0.460	0.142 ± 0.366	0.389 ± 0.242
269	—	760	—	—	—	5h35m14.01s	-5d21m51.90s	-0.024 ± 0.164	-0.130 ± 0.219	-0.017 ± 0.722	-0.132 ± 0.650	-0.004 ± 0.456	-0.101 ± 0.382	-0.058 ± 0.240
270	—	—	—	11	—	5h35m14.01s	-5d22m23.29s	0.416 ± 0.170	0.341 ± 0.107	-0.393 ± 0.923	0.146 ± 0.740	0.570 ± 0.616	0.012 ± 0.473	0.089 ± 0.346
271	—	—	—	—	—	5h35m14.03s	-5d23m29.91s	-0.053 ± 0.180	-0.028 ± 0.178	-0.101 ± 0.644	0.514 ± 0.098	-0.129 ± 0.466	0.086 ± 0.399	0.020 ± 0.236
272	—	247	—	—	—	5h35m14.05s	-5d23m38.50s	0.058 ± 0.181	-0.087 ± 0.207	0.231 ± 0.718	0.548 ± 0.642	0.222 ± 0.461	-0.236 ± 0.370	0.025 ± 0.222
273	140-1952	—	—	—	—	5h35m14.05s	-5d19m51.90s	0.100 ± 0.268	0.143 ± 0.600
274	—	704	—	—	—	5h35m14.06s	-5d22m05.70s	0.046 ± 0.152	-0.112 ± 0.199	0.046 ± 0.560	0.332 ± 0.568	-0.033 ± 0.407	-0.131 ± 0.409	-0.022 ± 0.220
275	—	—	31	—	—	5h35m14.06s	-5d23m51.30s	0.052 ± 0.362	0.012 ± 0.244	-0.317 ± 0.549	0.452 ± 0.632	0.123 ± 0.467	-0.068 ± 0.396	-0.064 ± 0.300
276	141-520	36	—	—	—	5h35m14.06s	-5d25m20.50s	0.153 ± 0.121	0.146 ± 0.215	0.016 ± 0.799	0.058 ± 0.840	-0.172 ± 0.635	0.152 ± 0.216	0.233 ± 0.290
277	—	438	R	—	—	5h35m14.07s	-5d22m36.63s	0.105 ± 0.166	-0.086 ± 0.193	0.356 ± 0.594	0.252 ± 0.542	-0.508 ± 0.368	-0.001 ± 0.321	0.245 ± 0.216
278	—	705	B	—	—	5h35m14.09s	-5d22m23.08s	-0.045 ± 0.166	-0.036 ± 0.250	-0.692 ± 0.933	-0.170 ± 0.913	-0.206 ± 0.642	0.008 ± 0.481	-0.294 ± 0.582
279	—	779	—	12	—	5h35m14.11s	-5d22m22.67s	2.611 ± 0.285	4.593 ± 0.469	15.747 ± 1.596	14.092 ± 1.425	11.914 ± 1.200	20.249 ± 2.038	13.098 ± 1.370
280	—	—	13	—	—	5h35m14.14s	-5d23m56.75s	0.499 ± 0.167	0.732 ± 0.150	0.660 ± 0.124	0.637 ± 0.113	0.579 ± 0.094	0.846 ± 0.175	0.344 ± 0.133
281	142-301	371	C	14	—	5h35m14.16s	-5d23m01.29s	8.857 ± 0.954	7.024 ± 0.846	1.292 ± 4.658	1.124 ± 5.151	1.629 ± 5.030	6.611 ± 5.958	3.366 ± 5.840
282	—	67	—	—	—	5h35m14.18s	-5d25m00.70s	0.025 ± 0.127	-0.051 ± 0.209	-0.164 ± 0.695	0.174 ± 0.586	-0.153 ± 0.485	-0.129 ± 0.195	-0.096 ± 0.209
283	—	—	—	—	—	5h35m14.18s	-5d26m20.96s	0.614 ± 0.094	0.565 ± 0.099	0.590 ± 0.232	0.219 ± 0.855	0.091 ± 1.141
284	—	—	—	—	—	5h35m14.22s	-5d22m25.91s	0.055 ± 0.144	-0.078 ± 0.227	-0.043 ± 0.625	0.341 ± 0.176	0.182 ± 0.047	0.085 ± 0.336	0.323 ± 0.044
285	—	690	—	—	—	5h35m14.22s	-5d20m45.05s	-0.034 ± 0.187	-0.173 ± 0.283	0.525 ± 1.674	...	-0.057 ± 1.385
286	143-425	135	—	—	15	5h35m14.28s	-5d24m24.72s	0.293 ± 0.088	0.088 ± 0.193	-0.088 ± 0.586	-0.042 ± 0.611	0.016 ± 0.356	0.518 ± 0.240	0.329 ± 0.107
287	—	—	—	—	—	5h35m14.28s	-5d23m53.01s	0.910 ± 0.345	0.522 ± 0.282	0.610 ± 0.593	0.452 ± 0.601	0.393 ± 0.365	0.736 ± 0.445	0.348 ± 0.224
288	—	361	—	—	—	5h35m14.29s	-5d23m04.30s	0.147 ± 0.228	0.097 ± 0.228	0.451 ± 0.747	0.451 ± 0.871	-0.087 ± 0.542	-0.096 ± 0.389	0.287 ± 0.297
289	—	—	—	—	—	5h35m14.30s	-5d22m36.73s	-0.049 ± 0.168	-0.006 ± 0.201	-0.292 ± 0.675	0.253 ± 0.500	0.129 ± 0.430	-0.100 ± 0.390	0.165 ± 0.031
290	—	458	—	—	—	5h35m14.31s	-5d22m30.70s	0.120 ± 0.144	0.111 ± 0.172	0.104 ± 0.555	-0.147 ± 0.700	-0.059 ± 0.350	0.118 ± 0.386	0.049 ± 0.247
291	—	537	—	—	—	5h35m14.31s	-5d22m04.40s	-0.005 ± 0.148	0.055 ± 0.159	-0.115 ± 0.541	-0.051 ± 0.638	-0.028 ± 0.409	-0.045 ± 0.360	0.285 ± 0.193
292	—	—	—	—	—	5h35m14.31s	-5d22m42.03s	-0.006 ± 0.149	0.077 ± 0.187	-0.166 ± 0.517	0.259 ± 0.608	0.067 ± 0.425	0.159 ± 0.358	0.252 ± 0.331
293	—	345	—	—	16	5h35m14.32s	-5d23m08.30s	-0.025 ± 0.190	0.017 ± 0.219	-0.189 ± 0.747	0.168 ± 0.760	-0.019 ± 0.504	0.008 ± 0.429	0.131 ± 0.260
294	—	—	—	—	—	5h35m14.34s	-5d23m17.42s	0.114 ± 0.204	0.181 ± 0.048	-0.261 ± 0.760	0.039 ± 0.785	-0.124 ± 0.597	0.476 ± 0.134	0.613 ± 0.250
295	144-522	33	—	—	—	5h35m14.34s	-5d25m22.40s	0.205 ± 0.144	0.023 ± 0.201	0.378 ± 0.918				

TABLE 2 — *Continued*

ID	Proplyd Name	HC00 ID	GMR ID	Z04a ID	Other Names	R.A. [J2000]	Dec [J2000]	$F_{\nu, 6\text{cm}}$ [mJy]	$F_{\nu, 3.6\text{cm}}$ [mJy]	$F_{\nu, 1.3\text{cm}, 1^a}$ [mJy]	$F_{\nu, 1.3\text{cm}, 2^a}$ [mJy]	$F_{\nu, 1.3\text{cm}, 3^a}$ [mJy]	$F_{\nu, 1.3\text{cm}, 4^a}$ [mJy]	$F_{\nu, 1.3\text{cm}, \text{mean}^a}$ [mJy]
321	—	756	—	—	5h35m14.67s	-5d22m38.60s	0.046 ± 0.164	-0.035 ± 0.202	-0.022 ± 0.624	0.346 ± 0.731	-0.266 ± 0.378	-0.039 ± 0.359	—	-0.050 ± 0.251
322	—	369	—	—	5h35m14.67s	-5d23m01.90s	0.101 ± 0.196	0.157 ± 0.186	0.187 ± 0.684	-0.055 ± 0.828	-0.410 ± 0.452	0.146 ± 0.369	0.153 ± 0.293	—
323	—	575	—	—	5h35m14.69s	-5d21m49.50s	0.060 ± 0.149	-0.009 ± 0.243	0.164 ± 0.701	0.290 ± 0.772	-0.050 ± 0.535	0.085 ± 0.391	0.097 ± 0.261	—
324	—	757	—	—	5h35m14.69s	-5d22m38.20s	-0.012 ± 0.156	0.140 ± 0.192	0.706 ± 0.732	0.370 ± 0.612	0.022 ± 0.440	0.126 ± 0.349	0.407 ± 0.262	—
325	—	—	—	—	5h35m14.69s	-5d22m11.00s	-0.114 ± 0.160	-0.075 ± 0.181	-0.092 ± 0.717	0.197 ± 0.649	0.215 ± 0.048	0.139 ± 0.361	0.189 ± 0.042	—
326	—	411	—	—	5h35m14.70s	-5d22m49.40s	-0.180 ± 0.176	0.061 ± 0.191	-0.199 ± 0.661	-0.142 ± 0.723	0.497 ± 0.466	0.083 ± 0.365	-0.029 ± 0.234	—
327	—	755	—	—	5h35m14.71s	-5d22m35.50s	-0.127 ± 0.158	-0.022 ± 0.187	-0.057 ± 0.569	0.303 ± 0.603	0.019 ± 0.387	0.042 ± 0.361	0.074 ± 0.255	—
328	—	657	—	—	5h35m14.72s	-5d21m06.30s	-0.035 ± 0.188	0.112 ± 0.285	0.441 ± 2.975	0.822 ± 2.707	0.177 ± 1.414	0.201 ± 1.010	0.617 ± 0.622	—
329	—	465	—	—	5h35m14.73s	-5d22m29.80s	-0.013 ± 0.162	-0.094 ± 0.210	-0.493 ± 0.698	-0.546 ± 0.562	0.276 ± 0.418	0.187 ± 0.384	-0.167 ± 0.268	—
330	—	464	—	—	5h35m14.73s	-5d22m29.82s	-0.008 ± 0.157	-0.094 ± 0.239	0.225 ± 0.055	0.259 ± 0.057	0.344 ± 0.451	0.184 ± 0.411	0.153 ± 0.036	—
331	147-323	302	—	20	5h35m14.73s	-5d23m22.95s	0.733 ± 0.260	-0.129 ± 0.214	0.236 ± 0.750	0.029 ± 0.890	0.520 ± 0.499	0.237 ± 0.440	0.730 ± 0.301	—
332	—	—	—	—	5h35m14.80s	-5d22m30.68s	0.058 ± 0.175	0.024 ± 0.199	0.099 ± 0.652	0.366 ± 0.111	0.260 ± 0.057	0.139 ± 0.413	0.384 ± 0.080	—
333	148-305	—	—	22	5h35m14.81s	-5d23m04.80s	0.349 ± 0.092	0.350 ± 0.110	-0.153 ± 0.705	0.380 ± 0.843	-0.012 ± 0.431	0.284 ± 0.353	-0.130 ± 0.266	—
334	—	220	—	—	5h35m14.82s	-5d23m46.50s	0.293 ± 0.261	0.427 ± 0.213	0.191 ± 0.484	0.295 ± 0.583	-0.354 ± 0.414	-0.021 ± 0.362	-0.001 ± 0.219	—
335	—	773	—	—	5h35m14.82s	-5d22m23.20s	0.017 ± 0.151	0.051 ± 0.182	0.186 ± 0.572	0.135 ± 0.662	0.183 ± 0.420	-0.225 ± 0.398	0.018 ± 0.225	—
336	—	324	—	—	5h35m14.84s	-5d23m16.00s	-0.009 ± 0.232	0.009 ± 0.206	-0.565 ± 0.702	0.360 ± 0.898	0.229 ± 0.488	-0.071 ± 0.429	-0.058 ± 0.333	—
337	—	771	—	—	5h35m14.86s	-5d22m44.10s	-0.104 ± 0.166	-0.100 ± 0.158	0.442 ± 0.627	-0.182 ± 0.612	0.021 ± 0.451	0.034 ± 0.385	0.066 ± 0.233	—
338	—	453	—	—	5h35m14.87s	-5d22m31.70s	0.049 ± 0.169	0.029 ± 0.199	0.432 ± 0.629	0.263 ± 0.651	-0.043 ± 0.470	0.022 ± 0.364	0.382 ± 0.265	—
339	—	714	—	—	5h35m14.88s	-5d23m05.10s	-0.133 ± 0.220	-0.276 ± 0.204	0.417 ± 0.684	-0.569 ± 0.898	-0.304 ± 0.430	0.019 ± 0.399	-0.137 ± 0.282	—
340	—	157	—	—	5h35m14.90s	-5d24m11.80s	0.129 ± 0.181	0.132 ± 0.170	-0.260 ± 0.437	-0.220 ± 0.455	-0.376 ± 0.397	-0.023 ± 0.265	0.039 ± 0.191	—
341	—	D	21	—	5h35m14.90s	-5d22m25.41s	0.812 ± 0.113	0.768 ± 0.097	0.687 ± 0.106	0.516 ± 0.087	1.772 ± 0.190	1.856 ± 0.241	1.320 ± 0.150	—
342	—	431	—	—	5h35m14.92s	-5d22m39.10s	-0.089 ± 0.149	-0.088 ± 0.180	0.031 ± 0.629	-0.101 ± 0.731	-0.229 ± 0.441	0.141 ± 0.310	0.133 ± 0.248	—
343	—	154	—	—	5h35m14.93s	-5d24m12.90s	-0.067 ± 0.210	-0.129 ± 0.156	-0.237 ± 0.453	-0.105 ± 0.488	-0.109 ± 0.395	-0.026 ± 0.262	-0.301 ± 0.193	—
344	149-329	275	—	23	5h35m14.93s	-5d23m29.02s	-0.162 ± 0.272	0.346 ± 0.079	-1.197 ± 0.686	0.781 ± 0.806	-0.129 ± 0.396	0.057 ± 0.417	0.244 ± 0.148	—
345	—	245	—	—	5h35m14.95s	-5d23m39.30s	0.209 ± 0.248	0.260 ± 0.219	-0.304 ± 0.656	-0.697 ± 0.650	-0.514 ± 0.427	-0.075 ± 0.423	-0.120 ± 0.270	—
346	—	673	—	—	5h35m14.96s	-5d21m00.80s	0.053 ± 0.192	-0.132 ± 0.296	—	—	-0.112 ± 1.785	0.557 ± 1.430	0.361 ± 0.898	—
347	—	147	—	—	5h35m14.97s	-5d24m17.20s	-0.194 ± 0.192	-0.101 ± 0.172	0.160 ± 0.501	-0.241 ± 0.521	-0.122 ± 0.377	-0.066 ± 0.216	-0.264 ± 0.185	—
348	—	546	—	—	5h35m15.00s	-5d22m00.00s	-0.073 ± 0.159	0.113 ± 0.210	-0.089 ± 0.695	-0.088 ± 0.696	-0.064 ± 0.433	-0.119 ± 0.316	-0.034 ± 0.255	—
349	—	334	—	—	5h35m15.00s	-5d23m14.30s	-0.011 ± 0.235	-0.059 ± 0.190	-0.401 ± 0.636	-0.194 ± 0.916	-0.240 ± 0.497	0.215 ± 0.442	-0.235 ± 0.293	—
350	150-147	581	—	—	5h35m15.01s	-5d21m47.37s	-0.031 ± 0.177	0.014 ± 0.247	-0.301 ± 0.930	-0.138 ± 0.817	-0.079 ± 0.563	-0.018 ± 0.353	-0.250 ± 0.266	—
351	—	684	—	—	5h35m15.02s	-5d20m52.60s	0.015 ± 0.194	0.047 ± 0.269	—	—	-0.453 ± 1.750	—	-0.070 ± 0.188	—
352	150-231	456	—	—	5h35m15.03s	-5d22m31.15s	0.192 ± 0.176	0.050 ± 0.167	0.220 ± 0.609	0.028 ± 0.619	0.293 ± 0.378	0.259 ± 0.406	0.362 ± 0.233	—
353	—	373	—	—	5h35m15.04s	-5d23m01.10s	-0.061 ± 0.160	0.186 ± 0.203	-0.470 ± 0.704	-0.180 ± 0.837	-0.086 ± 0.497	-0.145 ± 0.356	-0.370 ± 0.255	—
354	—	195	—	—	5h35m15.04s	-5d23m54.50s	0.112 ± 0.481	-0.218 ± 0.402	-0.222 ± 0.600	-0.273 ± 0.478	0.124 ± 0.357	-0.177 ± 0.546	-0.184 ± 0.277	—
355	—	298	—	—	5h35m15.07s	-5d23m23.40s	0.095 ± 0.240	-0.040 ± 0.219	-0.136 ± 0.617	-0.482 ± 0.812	-0.010 ± 0.550	-0.356 ± 0.419	-0.577 ± 0.330	—
356	—	744	—	—	5h35m15.07s	-5d24m22.10s	0.132 ± 0.161	-0.066 ± 0.171	0.134 ± 0.531	0.337 ± 0.390	0.222 ± 0.335	-0.103 ± 0.235	0.007 ± 0.162	—
357	—	—	24	—	5h35m15.07s	-5d23m52.96s	0.420 ± 0.515	0.648 ± 0.408	0.231 ± 0.569	0.290 ± 0.517	-0.181 ± 0.363	0.219 ± 0.395	0.052 ± 0.329	—
358	—	—	25	—	5h35m15.15s	-5d23m53.63s	0.649 ± 0.495	0.457 ± 0.405	0.159 ± 0.644	0.053 ± 0.602	0.623 ± 0.424	-0.074 ± 0.408	-0.161 ± 0.276	—
359	—	149	—	—	5h35m15.16s	-5d24m17.10s	0.258 ± 0.174	-0.031 ± 0.189	-0.424 ± 0.479	0.223 ± 0.540	0.143 ± 0.338	-0.013 ± 0.198	0.012 ± 0.176	—
360	—	219	—	—	5h35m15.16s	-5d23m46.70s	0.225 ± 0.309	0.591 ± 0.328	-0.275 ± 0.525	0.672 ± 0.540	0.252 ± 0.402	0.154 ± 0.391	0.503 ± 0.296	—
361	—	—	—	—	5h35m15.16s	-5d22m17.37s	0.132 ± 0.154	0.018 ± 0.184	-0.703 ± 0.670	0.109 ± 0.638	0.199 ± 0.518	0.040 ± 0.343	0.029 ± 0.096	—
362	—	694	—	—	5h35m15.17s	-5d20m48.20s	0.021 ± 0.189	0.090 ± 0.313	—	—	—	—	—	—
363	—	359	—	—	5h35m15.18s	-5d23m05.00s	-0.030 ± 0.183	-0.107 ± 0.208	0.036 ± 0.713	-0.640 ± 0.822	0.148 ± 0.508	0.174 ± 0.401	0.022 ± 0.292	—
364	—	—	26	—	5h35m15.18s	-5d24m03.61s	0.098 ± 0.245	-0.002 ± 0.238	0.085 ± 0.529	0.479 ± 0.475	0.213 ± 0.344	0.069 ± 0.374	0.062 ± 0.245	—
365	—	—	27	—	5h35m15.19s	-5d23m32.55s	0.609 ± 0.355	0.480 ± 0.284	-0.187 ± 0.588	0.638 ± 0.715	0.002 ± 0.427	0.653 ± 0.418	1.366 ± 0.327	—
366	—	687	—	—	5h35m15.20s	-5d20m51.40s	-0.007 ± 0.192	0.071 ± 0.318	—	—	—	—	—	—
367	—	398	—	—	5h35m15.20s	-5d22m54.40s	-0.103 ± 0.178	-0.050 ± 0.187	-0.138 ± 0.738	-0.554 ± 0.639	-0.049 ± 0.462	0.105 ± 0.386	0.053 ± 0.275	—
368	152-738	—	—	—	5h35m15.21s	-5d27m37.85s	-0.042 ± 0.209	0.110 ± 0.406	—	—	—	—	—	—
369	—	478	—	—	5h35m15.21s	-5d22m24.10s	0.085 ± 0.173	0.083 ± 0.197	0.184 ± 0.678	-0.093 ± 0.580	0.005 ± 0.440	0.088 ± 0.402	0.134 ± 0.192	—
370	—	437	—	—	5h35m15.21s	-5d22m36.70s	-0.006 ± 0.158	0.082 ± 0.177	-0.474 ± 0.586	0.085 ± 0.556	0.208 ± 0.324	-0.044 ± 0.350	-0.111 ± 0.213	—
371	152-319	318	—	28	5h35m15.21s	-5d23m18.80s	1.412 ± 0.257	0.895 ± 0.176	0.006 ± 0.658	0.815 ± 1.146	0.346 ± 0.519	0.272 ± 0.473	0.551 ± 0.337	—
372	—	211	—	—	5h35m15.25s	-5d23m49.80s	0.183 ± 0.396	0.045 ± 0.242	0.655 ± 0.513	1.095 ± 0.601	-0.092 ± 0.328	0.295 ± 0.379	0.862 ± 0.232	—
373	—	—	28	—	5h35m15.26s	-5d23m47.26s	0.527 ± 0.364	0.378 ± 0.283	-0.252 ± 0.566	-0.327 ± 0.534	0.749 ± 0.388	0.375 ± 0.393	0.493 ± 0.283	—
374	—	386	—	29	5h35m15.26s	-5d22m56.88s	-0.117 ± 0.148	0.131 ± 0.042	0.446 ± 0.617	0.078 ± 0.820	0.267 ± 0.077	0.195 ± 0.343	0.215 ± 0.089	—
375	—	558	—	—	5h35m15.27s	-5d21m55.70s	-0.066 ± 0.159	0.108 ± 0.187	0.098 ± 0.702	0.051 ± 0.714	0.064 ± 0.447</td			

TABLE 2 — *Continued*

ID	Proplyd Name	HC00 ID	GMR ID	Z04a ID	Other Names	R.A. [J2000]	Dec [J2000]	$F_{\nu, 6\text{cm}}$ [mJy]	$F_{\nu, 3.6\text{cm}}$ [mJy]	$F_{\nu, 1.3\text{cm}, 1^a}$ [mJy]	$F_{\nu, 1.3\text{cm}, 2^a}$ [mJy]	$F_{\nu, 1.3\text{cm}, 3^a}$ [mJy]	$F_{\nu, 1.3\text{cm}, 4^a}$ [mJy]	$F_{\nu, 1.3\text{cm}, \text{mean}^a}$ [mJy]
401	—	389	—	—	5h35m15.64s	-5d22m56.45s	-0.019 ± 0.208	0.192 ± 0.044	0.209 ± 0.070	-0.502 ± 0.806	0.024 ± 0.477	-0.027 ± 0.338	0.123 ± 0.048	
402	—	46	—	—	5h35m15.67s	-5d25m10.50s	0.050 ± 0.141	0.038 ± 0.151	-0.185 ± 0.466	0.050 ± 0.411	0.083 ± 0.341	0.024 ± 0.147	0.027 ± 0.210	
403	—	246	—	—	5h35m15.68s	-5d23m39.10s	-0.147 ± 0.219	-0.156 ± 0.200	-0.321 ± 0.616	-0.494 ± 0.617	-0.183 ± 0.407	0.108 ± 0.385	-0.080 ± 0.224	
404	—	23	—	—	5h35m15.68s	-5d25m33.30s	0.001 ± 0.145	0.083 ± 0.158	-0.026 ± 0.688	-0.052 ± 0.556	0.143 ± 0.455	-0.030 ± 0.201	-0.119 ± 0.234	
405	—	236	—	—	5h35m15.70s	-5d23m41.90s	0.162 ± 0.228	-0.153 ± 0.207	-0.391 ± 0.549	-0.258 ± 0.728	-0.194 ± 0.379	0.181 ± 0.401	0.656 ± 0.263	
406	—	—	29	—	5h35m15.72s	-5d23m12.54s	-0.018 ± 0.310	0.046 ± 0.232	0.515 ± 0.632	0.927 ± 1.004	0.570 ± 0.685	0.249 ± 0.449	0.526 ± 0.639	
407	—	—	32	—	5h35m15.73s	-5d23m02.33s	-0.005 ± 0.243	-0.061 ± 0.199	-0.466 ± 0.802	0.532 ± 0.727	0.008 ± 0.497	0.033 ± 0.301	-0.090 ± 0.308	
408	157-323	307	26	37	5h35m15.73s	-5d23m22.51s	2.421 ± 0.295	2.774 ± 0.316	1.940 ± 0.364	1.360 ± 0.350	1.673 ± 0.230	2.958 ± 0.438	2.310 ± 0.364	
409	—	248	—	—	5h35m15.76s	-5d23m38.38s	0.024 ± 0.252	0.017 ± 0.219	0.138 ± 0.460	0.163 ± 0.634	0.127 ± 0.043	-0.067 ± 0.349	0.072 ± 0.025	
410	—	158	—	—	5h35m15.77s	-5d24m11.50s	0.057 ± 0.230	0.115 ± 0.199	0.023 ± 0.471	0.345 ± 0.399	0.076 ± 0.277	-0.054 ± 0.272	-0.100 ± 0.186	
411	—	—	11	—	5h35m15.77s	-5d23m22.80s	-0.142 ± 0.256	-0.326 ± 0.283	0.401 ± 1.009	0.444 ± 0.876	-0.465 ± 0.552	1.272 ± 0.467	0.102 ± 0.489	
412	—	598	—	—	5h35m15.77s	-5d21m39.80s	0.020 ± 0.166	0.027 ± 0.239	-0.024 ± 0.904	-0.019 ± 0.819	-0.101 ± 0.628	0.011 ± 0.436	-0.027 ± 0.316	
413	—	344	25	38	5h35m15.77s	-5d23m09.89s	2.490 ± 0.308	2.610 ± 0.278	2.344 ± 0.254	2.404 ± 0.271	3.608 ± 0.371	0.922 ± 0.203	1.427 ± 0.152	
414	—	—	39	—	5h35m15.79s	-5d23m23.96s	0.346 ± 0.277	0.567 ± 0.283	-0.033 ± 0.800	0.281 ± 0.983	1.202 ± 0.471	0.075 ± 0.426	1.197 ± 0.379	
415	—	137	—	—	5h35m15.79s	-5d24m24.70s	0.003 ± 0.139	-0.095 ± 0.158	-0.567 ± 0.418	-0.154 ± 0.397	0.082 ± 0.326	-0.154 ± 0.210	-0.451 ± 0.185	
416	158-327	287	13	40	5h35m15.80s	-5d23m26.55s	9.918 ± 1.052	9.568 ± 1.005	2.948 ± 1.240	5.809 ± 1.462	4.426 ± 0.813	8.033 ± 0.899	7.292 ± 1.116	
417	—	340	—	—	5h35m15.81s	-5d23m12.00s	0.111 ± 0.305	0.275 ± 0.202	0.168 ± 0.836	0.452 ± 0.994	0.201 ± 0.581	0.041 ± 0.454	0.641 ± 0.808	
418	—	336	12	41	5h35m15.83s	-5d23m14.17s	6.089 ± 0.621	5.018 ± 0.507	2.665 ± 0.282	40.855 ± 4.090	20.738 ± 2.081	5.124 ± 0.538	9.655 ± 0.972	
419	—	635	—	—	5h35m15.84s	-5d21m21.20s	0.022 ± 0.158	-0.010 ± 0.269	-0.377 ± 1.637	0.586 ± 1.790	0.130 ± 1.002	-0.002 ± 0.554	0.206 ± 0.428	
420	—	420	—	—	5h35m15.84s	-5d22m45.90s	-0.092 ± 0.167	-0.205 ± 0.177	0.226 ± 0.644	0.185 ± 0.588	0.016 ± 0.425	0.049 ± 0.257	0.006 ± 0.262	
421	158-323	306	—	42	5h35m15.84s	-5d23m22.49s	8.726 ± 0.896	10.344 ± 1.049	7.469 ± 0.846	8.504 ± 0.937	9.550 ± 0.998	10.725 ± 1.100	8.700 ± 0.918	
422	—	342	—	—	5h35m15.85s	-5d23m11.00s	-0.163 ± 0.326	0.027 ± 0.218	-0.256 ± 0.583	-0.487 ± 1.072	-0.118 ± 0.706	0.085 ± 0.349	-0.052 ± 0.553	
423	158-326	291	10	43	5h35m15.85s	-5d23m25.57s	5.929 ± 0.668	5.325 ± 0.612	0.785 ± 0.910	0.754 ± 0.991	1.799 ± 0.582	4.762 ± 0.670	4.416 ± 0.802	
424	—	370	—	—	5h35m15.88s	-5d23m01.99s	0.523 ± 0.151	0.336 ± 0.098	0.315 ± 0.612	0.425 ± 0.756	-0.388 ± 0.448	-0.202 ± 0.355	-0.091 ± 0.300	
425	—	447	—	—	5h35m15.89s	-5d22m33.20s	0.080 ± 0.165	0.048 ± 0.202	0.098 ± 0.647	-0.237 ± 0.596	0.065 ± 0.418	0.012 ± 0.304	0.076 ± 0.211	
426	—	122	—	—	5h35m15.90s	-5d24m31.20s	0.118 ± 0.177	0.078 ± 0.167	-0.129 ± 0.474	-0.153 ± 0.370	-0.018 ± 0.307	0.014 ± 0.192	-0.163 ± 0.150	
427	159-338	250	24	44	5h35m15.91s	-5d23m37.98s	1.779 ± 0.225	2.118 ± 0.241	1.240 ± 0.202	1.335 ± 0.239	1.725 ± 0.238	2.010 ± 0.238	1.602 ± 0.226	
428	159-418	145	—	—	5h35m15.91s	-5d24m17.78s	0.716 ± 0.172	0.431 ± 0.101	0.253 ± 0.476	0.195 ± 0.072	0.216 ± 0.379	0.435 ± 0.093	0.079 ± 0.183	
429	159-221	490	—	—	5h35m15.94s	-5d22m21.07s	0.092 ± 0.159	0.202 ± 0.207	0.480 ± 0.665	0.318 ± 0.610	0.133 ± 0.383	-0.097 ± 0.311	0.036 ± 0.274	
430	159-350	213	9	45	5h35m15.95s	-5d23m49.81s	11.575 ± 1.237	8.040 ± 0.917	3.238 ± 0.821	3.416 ± 0.727	3.754 ± 0.669	10.868 ± 1.229	7.629 ± 1.488	
431	—	769	—	—	5h35m15.96s	-5d22m41.10s	0.042 ± 0.177	-0.012 ± 0.211	-0.213 ± 0.557	-0.220 ± 0.617	0.056 ± 0.404	-0.000 ± 0.357	0.033 ± 0.272	
432	—	304	—	—	5h35m15.97s	-5d23m22.70s	-0.040 ± 0.213	0.023 ± 0.227	0.302 ± 0.768	-0.379 ± 0.731	0.824 ± 0.472	-0.285 ± 0.428	-0.026 ± 0.391	
433	160-353	202	—	46	5h35m16.00s	-5d23m52.97s	3.910 ± 0.509	2.561 ± 0.445	0.194 ± 0.094	0.754 ± 0.438	0.624 ± 0.862	2.313 ± 0.325	2.394 ± 0.732	
434	—	651	—	—	5h35m16.00s	-5d21m09.87s	0.294 ± 0.074	0.319 ± 0.131	-0.636 ± 0.339	-0.154 ± 2.808	0.056 ± 1.481	0.234 ± 0.797	0.039 ± 0.628	
435	—	584	—	—	5h35m16.01s	-5d21m47.00s	0.109 ± 0.161	-0.136 ± 0.238	-0.138 ± 0.865	-0.065 ± 0.927	-0.025 ± 0.610	-0.031 ± 0.348	-0.027 ± 0.325	
436	—	565	—	—	5h35m16.01s	-5d21m53.10s	-0.023 ± 0.171	0.043 ± 0.179	-0.186 ± 0.761	0.010 ± 0.673	0.291 ± 0.529	0.031 ± 0.289	0.023 ± 0.275	
437	—	23	47	—	5h35m16.04s	-5d23m53.09s	-0.274 ± 0.273	-0.571 ± 0.271	-0.522 ± 0.629	-0.253 ± 0.568	-0.403 ± 0.373	3.644 ± 0.383	3.314 ± 0.438	
438	161-324	296	8	48	5h35m16.07s	-5d23m24.38s	4.004 ± 0.427	5.095 ± 0.522	4.510 ± 0.496	5.194 ± 0.567	5.619 ± 0.579	5.881 ± 0.618	4.814 ± 0.500	
439	—	350	15	49	5h35m16.07s	-5d23m07.07s	4.956 ± 0.538	5.031 ± 0.534	2.076 ± 0.460	3.217 ± 0.624	3.026 ± 0.445	4.159 ± 0.503	3.328 ± 0.499	
440	—	—	—	—	5h35m16.08s	-5d23m53.44s	0.427 ± 0.095	1.050 ± 0.129	1.533 ± 0.167	0.088 ± 0.470	-0.253 ± 0.509	-0.356 ± 0.318	0.033 ± 0.044	
441	—	401	—	—	5h35m16.08s	-5d22m54.10s	-0.021 ± 0.188	0.098 ± 0.252	0.432 ± 0.572	0.140 ± 0.685	-0.357 ± 0.471	0.124 ± 0.261	0.016 ± 0.256	
442	161-328	285	22	50	5h35m16.08s	-5d23m27.84s	2.290 ± 0.301	2.202 ± 0.285	0.686 ± 37.210	-0.111 ± 0.752	1.132 ± 0.291	1.783 ± 0.321	1.691 ± 0.364	
443	—	159	—	—	5h35m16.10s	-5d24m11.50s	0.503 ± 0.237	0.430 ± 0.205	-0.195 ± 0.421	-0.125 ± 0.429	-0.263 ± 0.357	0.101 ± 0.278	0.077 ± 0.197	
444	—	303	—	51	5h35m16.10s	-5d23m23.11s	0.347 ± 0.118	0.244 ± 0.068	-0.187 ± 0.744	0.045 ± 0.835	0.163 ± 0.051	0.322 ± 0.374	0.331 ± 0.376	
445	—	354	—	—	5h35m16.11s	-5d23m06.80s	-0.197 ± 0.240	-0.070 ± 0.262	0.008 ± 0.809	-0.396 ± 0.799	-0.685 ± 0.532	0.044 ± 0.383	-0.033 ± 0.419	
446	161-314	335	—	—	5h35m16.11s	-5d23m16.41s	1.035 ± 0.225	0.776 ± 0.153	0.191 ± 0.741	0.409 ± 0.922	-0.20 ± 0.517	0.116 ± 0.417	0.463 ± 0.383	
447	—	511	—	—	5h35m16.12s	-5d22m12.50s	-0.094 ± 0.160	-0.024 ± 0.166	-0.143 ± 0.664	-0.449 ± 0.562	0.210 ± 0.431	0.100 ± 0.251	-0.022 ± 0.210	
448	—	393	—	—	5h35m16.14s	-5d22m55.20s	0.377 ± 0.192	-0.014 ± 0.239	0.078 ± 0.622	-0.311 ± 0.599	-0.163 ± 0.436	0.246 ± 0.265	0.026 ± 0.257	
449	—	768	—	—	5h35m16.14s	-5d22m45.10s	0.065 ± 0.198	0.025 ± 0.201	-0.112 ± 0.536	-0.029 ± 0.624	-0.062 ± 0.472	-0.045 ± 0.282	-0.302 ± 0.232	
450	—	520	—	—	5h35m16.18s	-5d22m11.30s	0.177 ± 0.150	0.234 ± 0.201	-0.136 ± 0.619	0.304 ± 0.588	0.041 ± 0.484	0.171 ± 0.320	0.022 ± 0.209	
451	—	650	—	—	5h35m16.19s	-5d21m10.90s	-0.075 ± 0.146	0.136 ± 0.257	0.614 ± 3.111	-0.917 ± 2.366	0.101 ± 1.310	0.104 ± 0.767	0.214 ± 0.632	
452	162-133	615	—	—	5h35m16.20s	-5d21m32.39s	0.120 ± 0.150	-0.142 ± 0.249	-0.172 ± 1.205	-0.170 ± 1.170	0.284 ± 0.764	-0.173 ± 0.382	0.340 ± 0.438	
453	—	78	—	—	5h35m16.20s	-5d24m45.40s	0.114 ± 0.131	0.030 ± 0.144	0.004 ± 0.472	-0.127 ± 0.437	0.061 ± 0.345	0.081 ± 0.157	0.040 ± 0.179	
454	—	435	—	—	5h35m16.20s	-5d22m37.50s	-0.198 ± 0.215	-0.203 ± 0.187	-0.366 ± 0.556	0.328 ± 0.608	-0.032 ± 0.423	-0.096 ± 0.284	-0.223 ± 0.249	
455	—	710	—	—	5h35m16.22s	-5d24m56.00s	0.087 ± 0.155	0.027 ± 0.155	-0.004 ± 0.370	0.116 ± 0.354	0.005 ± 0.377	-0.065 ± 0.159	-0.135 ± 0.149	
456	—	758	—											

TABLE 2 — *Continued*

ID	Proplyd	Name	HC00 ID	GMR ID	Z04a ID	Other Names	R.A. [J2000]	Dec [J2000]	$F_{\nu, 6\text{cm}}$ [mJy]	$F_{\nu, 3.6\text{cm}}$ [mJy]	$F_{\nu, 1.3\text{cm}, 1^a}$ [mJy]	$F_{\nu, 1.3\text{cm}, 2^a}$ [mJy]	$F_{\nu, 1.3\text{cm}, 3^a}$ [mJy]	$F_{\nu, 1.3\text{cm}, 4^a}$ [mJy]	$F_{\nu, 1.3\text{cm}, \text{mean}^a}$ [mJy]
481	166-406	165	—	—	—	—	5h35m16.58s	-5d24m06.05s	0.158 ± 0.211	-0.041 ± 0.192	0.134 ± 0.047	-0.219 ± 0.431	0.249 ± 0.302	0.441 ± 0.256	0.598 ± 0.185
482	—	644	—	—	—	—	5h35m16.59s	-5d21m15.60s	0.053 ± 0.157	-0.024 ± 0.277	-0.276 ± 2.337	0.185 ± 2.200	-0.718 ± 1.243	-0.126 ± 0.513	-0.310 ± 0.544
483	166-250	—	—	57	—	—	5h35m16.60s	-5d22m50.37s	0.427 ± 0.108	0.506 ± 0.120	0.351 ± 0.568	0.143 ± 0.619	0.272 ± 0.097	0.242 ± 0.073	0.445 ± 0.137
484	166-316	325	21	58	—	—	5h35m16.62s	-5d23m16.15s	1.758 ± 0.232	2.227 ± 0.250	1.954 ± 0.229	2.177 ± 0.307	2.330 ± 0.257	2.407 ± 0.284	2.081 ± 0.230
485	—	126	—	—	—	—	5h35m16.63s	-5d24m28.10s	0.113 ± 0.168	-0.040 ± 0.176	-0.070 ± 0.381	0.212 ± 0.398	-0.018 ± 0.309	-0.017 ± 0.194	0.105 ± 0.172
486	—	620	—	—	—	—	5h35m16.64s	-5d21m30.90s	-0.064 ± 0.160	-0.022 ± 0.227	-0.129 ± 1.205	-0.116 ± 1.195	0.198 ± 0.693	-0.090 ± 0.394	0.161 ± 0.386
487	—	567	—	—	—	—	5h35m16.65s	-5d21m52.70s	-0.076 ± 0.156	-0.000 ± 0.194	0.034 ± 0.701	-0.137 ± 0.697	0.145 ± 0.507	-0.068 ± 0.252	-0.090 ± 0.252
488	—	280	—	—	—	—	5h35m16.66s	-5d23m28.90s	0.009 ± 0.240	0.024 ± 0.224	-0.463 ± 0.654	-0.080 ± 0.670	1.012 ± 0.400	-0.107 ± 0.375	-0.315 ± 0.276
489	—	293	—	—	—	—	5h35m16.73s	-5d23m25.20s	0.075 ± 0.193	-0.175 ± 0.300	-0.218 ± 0.650	-0.135 ± 0.788	-0.658 ± 0.435	-0.215 ± 0.429	-0.411 ± 0.372
490	167-231	457	—	—	—	—	5h35m16.74s	-5d22m31.30s	-0.132 ± 0.190	0.034 ± 0.217	0.078 ± 0.591	-0.007 ± 0.605	0.183 ± 0.402	0.049 ± 0.252	0.093 ± 0.242
491	167-317	323	6	59	—	—	5h35m16.76s	-5d23m16.49s	16.563 ± 1.673	22.058 ± 2.218	17.198 ± 1.812	20.801 ± 2.164	21.385 ± 2.174	22.660 ± 2.280	18.481 ± 1.888
492	—	170	—	—	—	—	5h35m16.77s	-5d24m04.28s	0.421 ± 0.105	0.410 ± 0.090	0.193 ± 0.050	0.139 ± 0.040	0.593 ± 0.081	0.620 ± 0.102	0.611 ± 0.097
493	—	5	—	—	—	—	5h35m16.77s	-5d23m26.51s	0.070 ± 0.205	-0.181 ± 0.271	0.762 ± 0.806	0.548 ± 0.730	-0.151 ± 0.468	0.299 ± 0.389	0.361 ± 0.533
494	168-328	284	17	60	—	—	5h35m16.77s	-5d23m28.09s	2.894 ± 0.324	3.554 ± 0.373	2.876 ± 0.328	3.124 ± 0.343	3.687 ± 0.387	3.921 ± 0.426	3.363 ± 0.354
495	—	518	—	—	—	—	5h35m16.78s	-5d22m11.70s	0.108 ± 0.140	0.085 ± 0.227	-0.047 ± 0.622	-0.194 ± 0.575	-0.002 ± 0.383	0.058 ± 0.239	0.088 ± 0.247
496	168-235	—	—	—	—	—	5h35m16.81s	-5d22m34.71s	0.142 ± 0.168	-0.123 ± 0.189	-0.058 ± 0.540	-0.113 ± 0.655	-0.068 ± 0.431	-0.003 ± 0.237	0.230 ± 0.251
497	—	120	—	—	—	—	5h35m16.82s	-5d24m32.20s	-0.083 ± 0.164	-0.068 ± 0.166	0.240 ± 0.345	-0.194 ± 0.352	-0.128 ± 0.318	0.057 ± 0.168	0.197 ± 0.141
498	—	235	—	—	—	—	5h35m16.84s	-5d23m42.30s	0.058 ± 0.176	0.220 ± 0.209	1.224 ± 0.565	0.343 ± 0.470	0.054 ± 0.392	-0.075 ± 0.306	0.489 ± 0.246
499	168-326	289	20	61	—	—	5h35m16.85s	-5d23m26.28s	13.503 ± 1.372	16.537 ± 1.675	9.008 ± 0.950	10.444 ± 1.091	10.821 ± 1.102	17.633 ± 1.797	9.694 ± 0.997
500	—	349	—	—	—	—	5h35m16.87s	-5d23m07.10s	0.084 ± 0.161	0.036 ± 0.216	0.824 ± 0.572	0.118 ± 0.656	-0.373 ± 0.442	-0.010 ± 0.260	0.127 ± 0.237
501	169-338	—	—	62	—	—	5h35m16.89s	-5d23m38.09s	0.320 ± 0.079	0.360 ± 0.072	0.499 ± 0.144	0.352 ± 0.197	0.338 ± 0.082	0.190 ± 0.329	0.494 ± 0.138
502	—	484	—	—	—	—	5h35m16.90s	-5d22m22.50s	0.085 ± 0.171	0.093 ± 0.180	0.031 ± 0.544	0.004 ± 0.537	0.011 ± 0.396	-0.103 ± 0.224	-0.019 ± 0.256
503	—	441	—	—	—	—	5h35m16.91s	-5d22m35.20s	-0.011 ± 0.193	0.034 ± 0.208	0.151 ± 0.457	0.082 ± 0.670	-0.043 ± 0.430	0.055 ± 0.209	0.212 ± 0.217
504	—	397	—	—	—	—	5h35m16.91s	-5d22m55.10s	0.123 ± 0.189	0.008 ± 0.167	0.225 ± 0.529	0.337 ± 0.615	-0.026 ± 0.407	0.032 ± 0.230	0.343 ± 0.232
505	—	—	M	—	—	—	5h35m16.92s	-5d23m58.27s	-0.173 ± 0.299	-0.056 ± 0.275	-0.105 ± 0.461	0.067 ± 0.431	-0.734 ± 0.380	-0.093 ± 0.306	0.016 ± 0.223
506	—	494	—	—	—	—	5h35m16.94s	-5d22m20.70s	-0.043 ± 0.179	-0.088 ± 0.185	-0.230 ± 0.552	0.224 ± 0.621	0.026 ± 0.371	0.057 ± 0.250	-0.161 ± 0.236
507	—	—	27	—	—	—	5h35m16.94s	-5d23m16.01s	0.023 ± 0.187	-0.029 ± 0.190	-1.409 ± 0.702	-0.199 ± 0.835	-0.958 ± 0.407	0.173 ± 0.364	0.171 ± 0.311
508	—	524	—	—	—	—	5h35m16.94s	-5d22m09.90s	-0.062 ± 0.183	0.139 ± 0.221	0.319 ± 0.576	0.128 ± 0.600	0.223 ± 0.375	-0.081 ± 0.277	-0.022 ± 0.224
509	—	675	—	—	—	—	5h35m16.95s	-5d20m59.90s	0.057 ± 0.198	-0.039 ± 0.285	-0.185 ± 0.932	0.174 ± 0.916	0.784 ± 0.926
510	—	3	—	—	—	—	5h35m16.95s	-5d25m47.10s	0.005 ± 0.138	-0.071 ± 0.162	0.154 ± 0.731	0.085 ± 0.716	-0.089 ± 0.535	0.055 ± 0.202	0.018 ± 0.256
511	—	182	—	—	—	—	5h35m16.97s	-5d23m59.67s	0.517 ± 0.245	0.263 ± 0.262	0.676 ± 0.465	0.563 ± 0.405	0.219 ± 0.278	0.661 ± 0.319	1.142 ± 0.247
512	170-249	414	E	63	—	—	5h35m16.97s	-5d22m48.72s	3.607 ± 0.421	3.355 ± 0.420	1.031 ± 0.581	1.721 ± 3.648	1.351 ± 69.472	2.820 ± 0.382	3.231 ± 0.661
513	—	587	—	—	—	—	5h35m16.98s	-5d21m45.40s	-0.005 ± 0.174	0.028 ± 0.213	0.095 ± 0.801	0.132 ± 0.825	-0.070 ± 0.541	-0.209 ± 0.282	-0.121 ± 0.276
514	—	623	—	—	—	—	5h35m16.98s	-5d21m29.40s	-0.022 ± 0.147	-0.009 ± 0.257	0.071 ± 1.320	-0.052 ± 1.270	0.072 ± 0.672	-0.116 ± 0.391	-0.046 ± 0.392
515	170-301	375	—	—	—	—	5h35m16.98s	-5d23m00.99s	0.381 ± 0.118	0.328 ± 0.099	-0.171 ± 0.682	0.004 ± 0.669	0.297 ± 0.430	0.083 ± 0.248	0.022 ± 0.158
516	170-337	252	4	64	—	—	5h35m16.98s	-5d23m36.98s	10.244 ± 1.059	8.989 ± 0.939	3.676 ± 0.974	3.863 ± 0.774	5.147 ± 0.709	8.758 ± 0.958	7.099 ± 0.926
517	—	450	—	—	—	—	5h35m17.01s	-5d22m33.10s	-0.093 ± 0.186	-0.032 ± 0.203	-0.106 ± 0.601	-0.150 ± 0.561	-0.037 ± 0.421	-0.171 ± 0.256	-0.020 ± 0.215
518	171-334	259	3	65	—	—	5h35m17.07s	-5d23m34.03s	3.369 ± 0.356	3.874 ± 0.407	2.884 ± 0.416	3.201 ± 0.444	3.733 ± 0.426	3.865 ± 0.429	3.560 ± 0.407
519	171-340	244	—	66	—	—	5h35m17.07s	-5d23m39.78s	2.574 ± 0.419	0.780 ± 0.370	0.141 ± 0.524	0.647 ± 0.579	0.705 ± 0.389	0.898 ± 0.382	1.237 ± 1.354
520	—	631	—	—	—	—	5h35m17.07s	-5d21m23.70s	0.030 ± 0.163	0.052 ± 0.245	0.060 ± 1.562	-0.509 ± 1.466	-0.380 ± 0.940	0.031 ± 0.365	-0.005 ± 0.398
521	—	410	—	—	—	—	5h35m17.12s	-5d22m50.10s	-0.139 ± 0.223	-0.265 ± 0.206	-0.159 ± 0.546	0.032 ± 0.616	-0.266 ± 0.444	0.039 ± 0.225	-0.016 ± 0.284
522	—	75	—	—	—	—	5h35m17.12s	-5d24m48.70s	0.057 ± 0.121	-0.012 ± 0.143	0.002 ± 0.411	-0.057 ± 0.387	0.017 ± 0.323	0.041 ± 0.143	-0.078 ± 0.162
523	—	517	—	—	—	—	5h35m17.13s	-5d22m11.90s	-0.130 ± 0.165	-0.085 ± 0.230	0.114 ± 0.607	-0.033 ± 0.581	0.147 ± 0.473	0.205 ± 0.228	0.250 ± 0.220
524	171-434	118	—	—	—	—	5h35m17.13s	-5d24m34.53s	-0.095 ± 0.151	0.130 ± 0.045	-0.020 ± 0.405	0.212 ± 0.336	-0.011 ± 0.287	0.070 ± 0.144	0.039 ± 0.141
525	—	107	—	—	—	—	5h35m17.15s	-5d24m39.00s	0.111 ± 0.140	-0.028 ± 0.191	-0.167 ± 0.426	0.034 ± 0.365	-0.127 ± 0.275	0.071 ± 0.168	0.094 ± 0.150
526	—	315	—	—	—	—	5h35m17.16s	-5d23m20.40s	-0.145 ± 0.221	-0.161 ± 0.196	0.336 ± 0.636	0.125 ± 0.642	-0.387 ± 0.398	0.095 ± 0.352	0.386 ± 0.242
527	—	661	—	—	—	—	5h35m17.22s	-5d21m05.40s	0.071 ± 0.144	0.129 ± 0.295	0.785 ± 3.297	0.287 ± 3.344	0.122 ± 1.848	-0.217 ± 0.658	-0.255 ± 0.797
528	172-028	—	—	—	—	—	5h35m17.22s	-5d20m27.84s	-0.159 ± 0.210	0.098 ± 0.382
529	—	618	—	—	—	—	5h35m17.22s	-5d21m31.70s	1.598 ± 0.179	3.208 ± 0.329	6.968 ± 0.719	4.538 ± 0.480	0.470 ± 0.583	-0.131 ± 0.334	1.254 ± 0.132
530	—	—	67	—	—	—	5h35m17.23s	-5d23m26.55s	1.181 ± 0.374	0.414 ± 0.236	1.425 ± 0.643	0.804 ± 0.695	0.356 ± 0.417	0.727 ± 0.383	1.345 ± 0.297
531	—	330	—	—	—	—	5h35m17.24s	-5d23m16.60s	0.019 ± 0.184	0.000 ± 0.220	0.404 ± 0.620	0.369 ± 0.672	-0.006 ± 0.501	-0.048 ± 0.289	0.144 ± 0.242
532	—	138	—	—	—	—	5h35m17.27s	-5d24m24.20s	-0.128 ± 0.154	0.066 ± 0.159	0.075 ± 0.427	0.113 ± 0.372	-0.064 ± 0.287	0.111 ± 0.149	0.090 ± 0.184
533	—	9	—	—	—	—	5h35m17.29s	-5d25m45.20s	-0.015 ± 0.141	0.047 ± 0.156	0.093 ± 0.750	0.067 ± 0.626	0.021 ± 0.485	-0.011 ± 0.184	0.073 ± 0.232
534	—	—	—	—	—	—	5h35m17.32s	-5d22m34.90s	-0.166 ± 0.203	-0.252 ± 0.214	-0.238 ± 0.567	0.254 ± 0.519	-0.002 ± 0.454	0.036 ± 0.228	0.085 ± 0.303
535	173-341	239	—	68	—	—	5h35m17.33s	-5d23m41.42s	1.201 ± 0.168	0.860 ± 0.130	0.589 ± 2.773	0.606 ± 1.633	0.513 ± 1.106	0.785 ± 1.633	0.760 ± 0.159
536	—	493	—	—	—	—	5h35m17.34s	-5d22m21.20s	-0.026 ± 0.151	0.069 ± 0.219	0.241 ± 0.536	-0.155 ± 0.556	-0.102 ± 0.419	0.054 ± 0.222	0.142 ± 0.233
537	173-236	440	L	69	—	—	5h35m17.35s	-5d22m23.59s	3.073 ± 0.376	2.332 ± 0.311	1.436 ± 3.520	0.985 ± 0.559	1.094 ± 1.498	2.269 ± 0.308	2.741 ± 0.524
538	—	640	—</td												

TABLE 2 — *Continued*

ID	Proplyd Name	HC00 ID	GMR ID	Z04a ID	Other Names	R.A. [J2000]	Dec [J2000]	$F_{\nu, 6\text{cm}}$ [mJy]	$F_{\nu, 3.6\text{cm}}$ [mJy]	$F_{\nu, 1.3\text{cm}, 1}$ ^a [mJy]	$F_{\nu, 1.3\text{cm}, 2}$ ^a [mJy]	$F_{\nu, 1.3\text{cm}, 3}$ ^a [mJy]	$F_{\nu, 1.3\text{cm}, 4}$ ^a [mJy]	$F_{\nu, 1.3\text{cm}, \text{mean}}$ ^a [mJy]
561	176-252	405	—	—	5h35m17.65s	-5d22m51.68s	-0.002 ± 0.183	0.029 ± 0.205	-0.147 ± 0.541	-0.059 ± 0.542	0.164 ± 0.382	0.099 ± 0.236	0.081 ± 0.230	
562	—	527	—	—	5h35m17.66s	-5d22m07.90s	0.100 ± 0.170	-0.053 ± 0.219	0.149 ± 0.546	0.043 ± 0.580	0.008 ± 0.461	-0.001 ± 0.194	-0.067 ± 0.227	
563	—	47	—	—	5h35m17.66s	-5d25m10.70s	0.018 ± 0.142	0.014 ± 0.168	-0.011 ± 0.525	0.090 ± 0.395	0.018 ± 0.320	0.076 ± 0.139	0.090 ± 0.170	
564	177-341W	241	1	72	—	5h35m17.68s	-5d23m40.89s	13.538 ± 1.400	10.992 ± 1.159	2.802 ± 0.989	4.251 ± 1.347	4.883 ± 0.985	10.267 ± 1.178	8.002 ± 1.133
565	177-454	86	—	—	5h35m17.69s	-5d24m54.10s	0.014 ± 0.158	0.089 ± 0.169	0.223 ± 0.392	0.141 ± 0.392	0.017 ± 0.273	0.077 ± 0.159	0.204 ± 0.150	
566	177-541	14	—	—	5h35m17.71s	-5d25m40.83s	0.067 ± 0.133	0.040 ± 0.183	0.117 ± 0.683	-0.008 ± 0.641	0.084 ± 0.459	-0.014 ± 0.180	0.105 ± 0.227	
567	177-341E	—	—	—	5h35m17.73s	-5d23m41.10s	0.243 ± 0.206	-0.062 ± 0.269	-0.461 ± 0.803	-0.185 ± 0.639	-0.897 ± 0.526	0.285 ± 0.363	-0.354 ± 0.510	
568	177-444	98	—	—	5h35m17.74s	-5d24m43.78s	0.077 ± 0.128	-0.067 ± 0.150	0.131 ± 0.371	0.150 ± 0.378	-0.027 ± 0.303	0.023 ± 0.124	0.009 ± 0.143	
569	—	333	—	—	5h35m17.74s	-5d23m14.90s	-0.102 ± 0.141	-0.026 ± 0.175	-0.109 ± 0.586	0.375 ± 0.567	0.107 ± 0.374	-0.106 ± 0.290	-0.105 ± 0.220	
570	—	462	—	—	5h35m17.76s	-5d22m31.00s	0.101 ± 0.176	0.179 ± 0.220	0.054 ± 0.598	0.291 ± 0.572	0.052 ± 0.383	0.071 ± 0.206	0.160 ± 0.210	
571	—	234	—	—	5h35m17.77s	-5d23m42.60s	0.407 ± 0.208	-0.029 ± 0.225	-0.232 ± 0.512	0.219 ± 0.534	1.216 ± 0.419	0.344 ± 0.360	0.863 ± 0.297	
572	—	230	—	—	5h35m17.79s	-5d23m44.20s	0.176 ± 0.224	-0.324 ± 0.185	0.232 ± 0.600	0.020 ± 0.536	-0.361 ± 0.350	0.276 ± 0.305	0.353 ± 0.244	
573	178-441	104	—	—	5h35m17.82s	-5d24m41.08s	0.034 ± 0.146	-0.040 ± 0.136	-0.008 ± 0.406	-0.241 ± 0.407	-0.034 ± 0.297	0.108 ± 0.134	0.170 ± 0.151	
574	—	124	—	—	5h35m17.82s	-5d24m30.60s	-0.016 ± 0.127	0.046 ± 0.155	0.146 ± 0.419	-0.164 ± 0.404	0.101 ± 0.322	-0.053 ± 0.163	-0.124 ± 0.143	
575	—	332	—	—	5h35m17.82s	-5d23m15.60s	0.074 ± 0.149	-0.107 ± 0.211	-0.086 ± 0.575	-0.078 ± 0.647	0.323 ± 0.393	-0.210 ± 0.250	-0.402 ± 0.252	
576	—	496	—	—	5h35m17.83s	-5d22m19.60s	0.066 ± 0.173	-0.017 ± 0.207	-0.258 ± 0.523	0.029 ± 0.430	-0.016 ± 0.369	-0.118 ± 0.205	-0.110 ± 0.238	
577	178-258	383	—	—	5h35m17.84s	-5d22m58.18s	0.002 ± 0.178	0.013 ± 0.188	0.087 ± 0.552	-0.106 ± 0.577	0.363 ± 0.324	0.114 ± 0.178	0.442 ± 0.225	
578	—	681	—	—	5h35m17.86s	-5d20m54.10s	-0.046 ± 0.204	0.096 ± 0.345	0.192 ± 0.293	-0.180 ± 0.120	-0.328 ± 0.1401	
579	—	367	—	—	5h35m17.87s	-5d23m03.10s	0.015 ± 0.143	-0.109 ± 0.176	-0.552 ± 0.537	-0.375 ± 0.557	-0.032 ± 0.386	-0.118 ± 0.228	0.403 ± 0.250	
580	—	542	—	—	5h35m17.88s	-5d22m03.00s	-0.112 ± 0.161	0.059 ± 0.198	0.019 ± 0.616	-0.206 ± 0.556	-0.370 ± 0.461	-0.032 ± 0.224	-0.058 ± 0.251	
581	—	—	—	—	5h35m17.89s	-5d18m35.10s	0.120 ± 0.418	
582	—	566	—	—	5h35m17.90s	-5d21m53.40s	0.042 ± 0.146	-0.097 ± 0.207	0.153 ± 0.618	-0.251 ± 0.692	-0.061 ± 0.428	-0.047 ± 0.204	-0.027 ± 0.220	
583	179-056	679	—	—	5h35m17.92s	-5d20m55.47s	-0.103 ± 0.157	0.088 ± 0.322	0.477 ± 0.2630	-0.131 ± 0.989	0.081 ± 0.377	0.081 ± 0.165	
584	—	56	—	—	5h35m17.94s	-5d25m06.50s	0.051 ± 0.185	-0.018 ± 0.172	0.326 ± 0.442	-0.031 ± 0.404	0.065 ± 0.316	0.141 ± 0.152	0.081 ± 0.165	
585	—	689	—	—	5h35m17.95s	-5d20m49.30s	-0.069 ± 0.189	0.049 ± 0.350	
586	—	35	—	—	5h35m17.95s	-5d25m21.30s	0.011 ± 0.134	0.050 ± 0.179	0.137 ± 0.430	0.003 ± 0.476	-0.045 ± 0.378	0.042 ± 0.164	0.059 ± 0.173	
587	—	425	G	73	—	5h35m17.95s	-5d22m45.45s	1.839 ± 0.209	1.971 ± 0.207	1.731 ± 0.183	22.228 ± 2.225	1.552 ± 0.164	1.022 ± 0.134	3.034 ± 0.344
588	—	21	—	—	5h35m17.96s	-5d25m34.10s	0.004 ± 0.161	0.044 ± 0.163	0.328 ± 0.650	-0.002 ± 0.610	-0.033 ± 0.373	0.047 ± 0.173	0.061 ± 0.226	
589	179-354	764	—	—	5h35m17.96s	-5d23m52.55s	0.158 ± 0.179	-0.036 ± 0.192	0.388 ± 0.488	-0.139 ± 0.549	0.081 ± 0.371	0.200 ± 0.225	0.066 ± 0.197	
590	—	256	—	—	5h35m17.97s	-5d23m35.50s	0.073 ± 0.178	0.154 ± 0.186	-0.652 ± 0.602	-0.096 ± 0.594	0.222 ± 0.405	-0.054 ± 0.327	-0.099 ± 0.232	
591	—	676	—	—	5h35m17.98s	-5d20m59.60s	-0.047 ± 0.175	0.251 ± 0.294	-0.204 ± 0.2343	0.144 ± 0.738	0.084 ± 0.109	0.084 ± 0.109	
592	—	501	—	—	5h35m18.03s	-5d22m18.20s	0.075 ± 0.151	0.151 ± 0.212	-0.089 ± 0.459	-0.003 ± 0.526	0.170 ± 0.424	-0.005 ± 0.214	0.082 ± 0.200	
593	—	535	—	—	5h35m18.03s	-5d22m05.50s	0.066 ± 0.163	0.058 ± 0.219	0.207 ± 0.631	0.326 ± 0.553	0.083 ± 0.397	-0.067 ± 0.208	0.056 ± 0.253	
594	—	174	—	—	5h35m18.04s	-5d24m03.10s	0.012 ± 0.179	-0.191 ± 0.178	0.105 ± 0.388	0.324 ± 0.416	-0.042 ± 0.313	0.095 ± 0.253	0.011 ± 0.221	
595	180-331	271	19	74	—	5h35m18.05s	-5d23m30.74s	5.230 ± 0.562	4.608 ± 0.497	1.291 ± 0.385	1.772 ± 0.446	2.446 ± 0.425	4.319 ± 0.757	3.048 ± 0.585
596	—	594	—	—	5h35m18.05s	-5d21m41.20s	0.045 ± 0.152	-0.119 ± 0.244	0.002 ± 0.932	-0.300 ± 0.803	0.055 ± 0.517	-0.096 ± 0.234	-0.022 ± 0.284	
597	—	177	—	—	5h35m18.08s	-5d24m01.20s	0.138 ± 0.179	0.128 ± 0.149	0.064 ± 0.479	-0.047 ± 0.475	0.155 ± 0.328	-0.020 ± 0.251	0.039 ± 0.173	
598	—	372	—	—	5h35m18.08s	-5d22m01.80s	-0.007 ± 0.148	0.036 ± 0.196	0.230 ± 0.602	-0.097 ± 0.592	-0.080 ± 0.391	-0.045 ± 0.223	-0.175 ± 0.232	
599	181-247	418	—	—	5h35m18.09s	-5d22m47.16s	0.248 ± 0.194	0.130 ± 0.211	0.371 ± 0.488	0.150 ± 0.519	-0.023 ± 0.430	0.275 ± 0.156	0.029 ± 0.362	
600	181-825	—	—	—	5h35m18.10s	-5d28m25.04s	0.085 ± 0.271	0.250 ± 0.633	
601	—	253	N	—	5h35m18.10s	-5d23m36.08s	0.099 ± 0.194	-0.091 ± 0.179	0.636 ± 0.558	-0.182 ± 0.624	0.121 ± 0.363	-0.222 ± 0.364	-0.044 ± 0.253	
602	182-316	269	—	—	5h35m18.10s	-5d23m31.53s	0.027 ± 0.201	0.059 ± 0.262	-0.217 ± 0.575	0.198 ± 0.542	-0.058 ± 0.416	0.048 ± 0.357	0.004 ± 0.247	
603	—	221	—	—	5h35m18.21s	-5d24m36.40s	0.013 ± 0.194	-0.274 ± 0.158	0.203 ± 0.503	-0.058 ± 0.484	-0.093 ± 0.376	-0.246 ± 0.270	-0.006 ± 0.208	
604	—	125	—	—	5h35m18.22s	-5d24m30.30s	-0.081 ± 0.143	-0.009 ± 0.152	0.146 ± 0.426	0.043 ± 0.418	-0.003 ± 0.270	0.010 ± 0.157	-0.113 ± 0.151	
605	182-413	774	O	—	5h35m18.23s	-5d24m12.83s	1.379 ± 0.283	0.990 ± 0.405	0.592 ± 0.449	0.040 ± 0.458	0.615 ± 0.320	0.684 ± 0.358	1.032 ± 0.286	
606	—	19	—	—	5h35m18.23s	-5d25m35.20s	0.028 ± 0.155	-0.093 ± 0.177	-0.221 ± 0.506	0.179 ± 0.567	-0.170 ± 0.435	-0.088 ± 0.167	-0.236 ± 0.213	
607	—	533	—	—	5h35m18.24s	-5d22m06.30s	0.027 ± 0.143	-0.046 ± 0.194	0.163 ± 0.505	0.161 ± 0.514	-0.188 ± 0.399	-0.011 ± 0.176	0.082 ± 0.213	
608	—	331	—	75	—	5h35m18.25s	-5d23m15.63s	0.827 ± 0.132	0.676 ± 0.109	0.374 ± 0.159	0.379 ± 0.250	0.488 ± 0.161	0.683 ± 0.158	0.045 ± 0.223
609	—	348	—	—	5h35m18.28s	-5d23m07.50s	-0.032 ± 0.157	-0.043 ± 0.181	0.102 ± 0.574	0.296 ± 0.651	0.169 ± 0.375	0.048 ± 0.231	-0.117 ± 0.214	
610	183-439	109	—	—	5h35m18.28s	-5d24m38.88s	0.111 ± 0.145	0.043 ± 0.147	0.084 ± 0.417	0.198 ± 0.407	0.022 ± 0.282	0.001 ± 0.145	0.038 ± 0.152	
611	—	735	—	—	5h35m18.30s	-5d21m49.50s	0.024 ± 0.167	-0.014 ± 0.230	-0.037 ± 0.681	0.247 ± 0.652	-0.160 ± 0.524	0.077 ± 0.219	0.247 ± 0.262	
612	183-419	143	—	—	5h35m18.32s	-5d24m19.19s	0.361 ± 0.125	0.078 ± 0.149	0.292 ± 0.457	0.298 ± 0.411	0.171 ± 0.272	0.334 ± 0.208	0.036 ± 0.153	
613	—	108	—	—	5h35m18.33s	-5d24m38.90s	-0.109 ± 0.152	-0.075 ± 0.124	0.084 ± 0.414	-0.161 ± 0.370	0.063 ± 0.308	0.043 ± 0.146	0.062 ± 0.168	
614	—	66	—	—	5h35m18.33s	-5d25m02.70s	0.059 ± 0.163	-0.003 ± 0.166	0.006 ± 0.387	0.043 ± 0.398	0.088 ± 0.307	-0.002 ± 0.143	0.118 ± 0.172	
615	183-405	168	—	—	5h35m18.34s	-5d24m04.88s	0.085 ± 0.175	-0.080 ± 0.176	0.036 ± 0.498	0.048 ± 0.467	0.055 ± 0.315	-0.044 ± 0.234	-0.039 ± 0.164	
616	184-427	423	—	—	5h35m18.36s	-5d24m26.87s	0.314 ± 0.081	0.256 ± 0.078	0.167 ± 0.466	0.141 ± 0.415				

TABLE 2 — *Continued*

ID	Proplyd Name	HC00 ID	GMR ID	Z04a ID	Other Names	R.A. [J2000]	Dec [J2000]	$F_{\nu, 6\text{cm}}$ [mJy]	$F_{\nu, 3.6\text{cm}}$ [mJy]	$F_{\nu, 1.3\text{cm}, 1^a}$ [mJy]	$F_{\nu, 1.3\text{cm}, 2^a}$ [mJy]	$F_{\nu, 1.3\text{cm}, 3^a}$ [mJy]	$F_{\nu, 1.3\text{cm}, 4^a}$ [mJy]	$F_{\nu, 1.3\text{cm}, \text{mean}^a}$ [mJy]
641	—	695	—	—	5h35m18.93s	-5d20m48.60s	-0.016 ± 0.184	-0.203 ± 0.291	0.038 ± 2.346	0.397 ± 1.014	0.774 ± 1.110
642	—	686	—	—	5h35m18.96s	-5d20m52.20s	-0.025 ± 0.171	0.145 ± 0.310	-0.040 ± 0.374	-0.038 ± 0.177	-0.159 ± 0.192
643	—	498	—	—	5h35m18.96s	-5d22m18.80s	0.233 ± 0.144	-0.018 ± 0.224	-0.170 ± 0.457	0.183 ± 0.536	-0.040 ± 0.374	-0.038 ± 0.177	-0.159 ± 0.192	-0.159 ± 0.192
644	—	655	—	—	5h35m18.97s	-5d21m07.80s	0.005 ± 0.191	-0.118 ± 0.309	0.429 ± 2.538	0.154 ± 2.416	0.413 ± 1.510	0.068 ± 0.519	-0.259 ± 0.755	-0.259 ± 0.755
645	—	311	—	—	5h35m18.97s	-5d23m22.00s	-0.096 ± 0.140	-0.078 ± 0.208	-0.526 ± 0.589	0.163 ± 0.612	-0.144 ± 0.429	-0.082 ± 0.216	-0.216 ± 0.206	-0.216 ± 0.206
646	190-251	409	—	—	5h35m19.04s	-5d22m50.67s	0.130 ± 0.158	-0.008 ± 0.259	0.092 ± 0.494	0.085 ± 0.562	0.267 ± 0.421	-0.073 ± 0.197	0.144 ± 0.246	0.144 ± 0.246
647	—	65	—	—	5h35m19.04s	-5d25m03.00s	-0.032 ± 0.159	-0.154 ± 0.167	0.305 ± 0.485	0.051 ± 0.480	0.117 ± 0.344	-0.087 ± 0.158	-0.026 ± 0.173	-0.026 ± 0.173
648	—	351	—	—	5h35m19.07s	-5d23m07.50s	-0.134 ± 0.149	0.207 ± 0.210	0.118 ± 0.569	-0.159 ± 0.606	0.064 ± 0.414	0.017 ± 0.216	-0.140 ± 0.229	-0.140 ± 0.229
649	191-350	214	—	—	5h35m19.07s	-5d23m49.67s	1.325 ± 0.255	0.417 ± 0.170	0.277 ± 0.470	0.309 ± 0.484	0.185 ± 0.069	0.428 ± 0.190	0.803 ± 2.760	0.803 ± 2.760
650	—	357	—	—	5h35m19.11s	-5d23m06.30s	0.084 ± 0.165	0.142 ± 0.195	-0.068 ± 0.502	0.374 ± 0.612	-0.200 ± 0.328	0.013 ± 0.179	0.058 ± 0.200	0.058 ± 0.200
651	—	288	—	—	5h35m19.12s	-5d22m27.10s	0.036 ± 0.158	0.088 ± 0.177	-0.343 ± 0.667	0.112 ± 0.575	-0.031 ± 0.357	-0.014 ± 0.283	-0.211 ± 0.223	-0.211 ± 0.223
652	191-232	—	—	—	5h35m19.13s	-5d22m31.20s	-0.066 ± 0.183	-0.081 ± 0.221	0.151 ± 0.442	-0.078 ± 0.491	-0.017 ± 0.382	0.089 ± 0.195	0.174 ± 0.229	0.174 ± 0.229
653	—	444	—	—	5h35m19.14s	-5d22m34.60s	-0.045 ± 0.147	-0.027 ± 0.183	-0.034 ± 0.456	0.005 ± 0.543	-0.083 ± 0.403	0.000 ± 0.168	-0.028 ± 0.211	-0.028 ± 0.211
654	—	591	—	—	5h35m19.16s	-5d21m43.70s	-0.144 ± 0.159	0.103 ± 0.218	0.242 ± 0.816	-0.014 ± 0.719	0.112 ± 0.513	0.034 ± 0.230	0.010 ± 0.262	0.010 ± 0.262
655	—	408	—	—	5h35m19.22s	-5d22m50.70s	0.016 ± 0.180	-0.138 ± 0.219	-0.075 ± 0.502	0.020 ± 0.538	-0.073 ± 0.403	-0.030 ± 0.183	-0.193 ± 0.233	-0.193 ± 0.233
656	—	776	—	—	5h35m19.27s	-5d20m49.90s	-0.031 ± 0.209	0.056 ± 0.352	0.390 ± 0.781
657	—	691	—	—	5h35m19.27s	-5d20m49.50s	-0.061 ± 0.176	-0.266 ± 0.371
658	—	356	—	—	5h35m19.39s	-5d23m06.49s	0.220 ± 0.165	0.214 ± 0.174	0.188 ± 0.638	0.095 ± 0.632	-0.031 ± 0.430	0.248 ± 0.073	0.238 ± 0.225	0.238 ± 0.225
659	—	13	—	—	5h35m19.40s	-5d25m42.40s	0.052 ± 0.155	-0.002 ± 0.195	0.020 ± 0.803	0.004 ± 0.711	-0.040 ± 0.495	0.101 ± 0.200	0.068 ± 0.308	0.068 ± 0.308
660	—	491	—	—	5h35m19.47s	-5d22m21.80s	0.068 ± 0.176	0.134 ± 0.230	-0.052 ± 0.537	-0.108 ± 0.478	-0.050 ± 0.351	0.038 ± 0.187	-0.028 ± 0.207	-0.028 ± 0.207
661	—	665	—	—	5h35m19.51s	-5d21m04.50s	-0.116 ± 0.174	-0.186 ± 0.284	-0.099 ± 0.642	-0.668 ± 3.141	-0.188 ± 1.562	0.005 ± 0.512	-0.112 ± 0.843	-0.112 ± 0.843
662	—	728	—	—	5h35m19.51s	-5d23m39.70s	0.040 ± 0.163	-0.102 ± 0.168	-0.703 ± 0.665	0.112 ± 0.626	0.150 ± 0.395	-0.166 ± 0.226	-0.389 ± 0.228	-0.389 ± 0.228
663	—	580	—	—	5h35m19.55s	-5d21m49.20s	-0.008 ± 0.164	-0.012 ± 0.230	0.060 ± 0.754	-0.081 ± 0.688	-0.107 ± 0.489	0.005 ± 0.195	-0.167 ± 0.252	-0.167 ± 0.252
664	—	188	—	—	5h35m19.62s	-5d23m57.30s	-0.022 ± 0.151	-0.035 ± 0.147	-0.144 ± 0.496	0.019 ± 0.538	-0.014 ± 0.349	0.048 ± 0.203	0.031 ± 0.167	0.031 ± 0.167
665	—	54	—	—	5h35m19.62s	-5d25m07.78s	-0.062 ± 0.160	-0.033 ± 0.144	0.121 ± 0.481	0.325 ± 0.601	-0.178 ± 0.291	0.080 ± 0.172	0.056 ± 0.193	0.056 ± 0.193
666	—	366	—	—	5h35m19.63s	-5d23m03.60s	0.060 ± 0.148	-0.056 ± 0.200	-0.099 ± 0.548	0.013 ± 0.584	0.010 ± 0.395	0.101 ± 0.169	0.110 ± 0.209	0.110 ± 0.209
667	—	123	—	—	5h35m19.64s	-5d24m31.60s	0.040 ± 0.157	0.077 ± 0.156	0.018 ± 0.504	-0.099 ± 0.461	0.054 ± 0.345	0.084 ± 0.203	0.086 ± 0.162	0.086 ± 0.162
668	197-427	133	P	—	5h35m19.65s	-5d24m26.47s	0.521 ± 0.196	0.105 ± 0.157	0.240 ± 0.431	0.338 ± 0.497	0.247 ± 0.353	0.413 ± 0.152	0.563 ± 1034.349	0.563 ± 1034.349
669	—	103	—	—	5h35m19.66s	-5d24m42.20s	0.177 ± 0.136	0.069 ± 0.168	-0.094 ± 0.458	0.157 ± 0.416	-0.150 ± 0.379	-0.007 ± 0.173	-0.017 ± 0.187	-0.017 ± 0.187
670	—	59	—	—	5h35m19.68s	-5d25m05.20s	0.097 ± 0.156	0.022 ± 0.159	0.088 ± 0.594	-0.057 ± 0.566	-0.010 ± 0.349	-0.007 ± 0.154	-0.084 ± 0.207	-0.084 ± 0.207
671	—	446	—	—	5h35m19.68s	-5d22m34.20s	0.032 ± 0.139	0.000 ± 0.226	0.005 ± 0.456	0.090 ± 0.602	-0.050 ± 0.350	0.091 ± 0.162	0.145 ± 0.241	0.145 ± 0.241
672	198-222	492	—	—	5h35m19.82s	-5d22m21.62s	0.403 ± 0.106	0.248 ± 0.234	0.098 ± 0.467	0.079 ± 0.493	0.300 ± 0.370	0.227 ± 0.187	0.243 ± 0.223	0.243 ± 0.223
673	—	654	—	—	5h35m19.84s	-5d21m08.00s	0.023 ± 0.207	0.120 ± 0.297	-0.627 ± 2.969	-0.456 ± 2.546	0.078 ± 1.457	-0.260 ± 0.580	-0.465 ± 0.625	-0.465 ± 0.625
674	198-448	96	—	—	5h35m19.84s	-5d24m47.86s	0.310 ± 0.144	0.031 ± 0.174	0.357 ± 0.455	0.011 ± 0.492	-0.175 ± 0.345	0.122 ± 0.168	0.164 ± 0.172	0.164 ± 0.172
675	—	210	—	—	5h35m19.86s	-5d22m51.60s	0.145 ± 0.155	0.120 ± 0.148	0.231 ± 0.561	0.229 ± 0.537	0.033 ± 0.373	-0.096 ± 0.210	-0.048 ± 0.176	-0.048 ± 0.176
676	—	531	—	—	5h35m19.90s	-5d22m07.30s	-0.003 ± 0.153	-0.010 ± 0.224	0.189 ± 0.518	0.119 ± 0.595	0.060 ± 0.471	0.103 ± 0.192	0.092 ± 0.191	0.092 ± 0.191
677	—	176	—	—	5h35m19.93s	-5d24m02.60s	0.132 ± 0.171	-0.278 ± 0.155	0.185 ± 0.446	0.137 ± 0.481	0.236 ± 0.354	0.106 ± 0.182	0.089 ± 0.183	0.089 ± 0.183
678	—	564	—	—	5h35m19.97s	-5d21m54.00s	0.020 ± 0.156	-0.023 ± 0.253	0.006 ± 0.618	-0.087 ± 0.665	0.136 ± 0.439	-0.044 ± 0.174	-0.075 ± 0.221	-0.075 ± 0.221
679	—	452	—	—	5h35m19.98s	-5d22m32.80s	0.058 ± 0.177	-0.026 ± 0.202	-0.276 ± 0.563	0.169 ± 0.558	0.196 ± 0.415	0.019 ± 0.198	-0.020 ± 0.212	-0.020 ± 0.212
680	—	766	—	—	5h35m20.00s	-5d23m28.80s	0.050 ± 0.163	-0.054 ± 0.177	0.092 ± 0.598	0.224 ± 0.550	0.034 ± 0.349	-0.008 ± 0.207	0.051 ± 0.211	0.051 ± 0.211
681	—	34	—	—	5h35m20.03s	-5d25m22.40s	0.083 ± 0.158	0.023 ± 0.147	-0.009 ± 0.730	-0.017 ± 0.615	0.125 ± 0.400	-0.060 ± 0.162	0.009 ± 0.227	0.009 ± 0.227
682	—	474	—	—	5h35m20.03s	-5d22m26.50s	0.049 ± 0.189	0.150 ± 0.241	0.161 ± 0.494	-0.130 ± 0.538	0.085 ± 0.470	-0.039 ± 0.149	-0.032 ± 0.233	-0.032 ± 0.233
683	—	17	—	—	5h35m20.05s	-5d25m37.70s	0.103 ± 0.132	-0.110 ± 0.160	-0.155 ± 0.737	0.266 ± 0.712	-0.128 ± 0.461	0.052 ± 0.190	0.082 ± 0.222	0.082 ± 0.222
684	200-106	660	—	—	5h35m20.06s	-5d21m05.88s	0.119 ± 0.152	-0.107 ± 0.323	-0.979 ± 2.983	-0.498 ± 2.854	-0.331 ± 1.585	0.087 ± 0.652	0.451 ± 2.704	0.451 ± 2.704
685	—	45	—	—	5h35m20.06s	-5d25m14.30s	0.059 ± 0.163	0.046 ± 0.155	0.210 ± 0.580	-0.072 ± 0.487	0.021 ± 0.436	-0.039 ± 0.158	-0.029 ± 0.196	-0.029 ± 0.196
686	—	700	—	—	5h35m20.09s	-5d20m43.90s	0.049 ± 0.186	0.000 ± 0.387
687	—	365	—	—	5h35m20.13s	-5d23m04.50s	-0.058 ± 0.141	-0.168 ± 0.175	-0.125 ± 0.590	0.114 ± 0.570	-0.035 ± 0.437	0.122 ± 0.182	0.251 ± 0.227	0.251 ± 0.227
688	—	613	—	—	5h35m20.14s	-5d21m33.70s	0.028 ± 0.161	-0.063 ± 0.255	0.206 ± 1.176	-0.013 ± 1.155	0.037 ± 0.774	0.059 ± 0.230	0.226 ± 0.329	0.226 ± 0.329
689	201-534	25	—	—	5h35m20.15s	-5d22m33.87s	0.049 ± 0.139	-0.013 ± 0.178	-0.009 ± 0.669	0.161 ± 0.741	-0.155 ± 0.442	0.051 ± 0.167	0.036 ± 0.230	0.036 ± 0.230
690	202-228	468	—	—	5h35m20.16s	-5d22m28.31s	0.045 ± 0.153	-0.011 ± 0.238	0.163 ± 0.571	0.203 ± 0.426	-0.179 ± 0.409	0.170 ± 0.060	0.043 ± 0.214	0.043 ± 0.214
691	—	—	—	—	5h35m20.17s	-5d26m39.13s	0.093 ± 0.198	0.244 ± 0.056	...	0.384 ± 2.994	0.274 ± 1.505	0.091 ± 0.610	0.169 ± 0.829	0.169 ± 0.829
692	—	346	—	—	5h35m20.18s	-5d23m08.50s	-0.172 ± 0.139	0.141 ± 0.189	0.043 ± 0.611	0.094 ± 0.625	-0.066 ± 0.466	-0.047 ± 0.176	0.027 ± 0.199	0.027 ± 0.199
693	—	678												

TABLE 2 — *Continued*

ID	Proplyd Name	HC00 ID	GMR ID	Z04a ID	Other Names	R.A. [J2000]	Dec [J2000]	$F_{\nu, 6\text{cm}}$ [mJy]	$F_{\nu, 3.6\text{cm}}$ [mJy]	$F_{\nu, 1.3\text{cm}, 1^a}$ [mJy]	$F_{\nu, 1.3\text{cm}, 2^a}$ [mJy]	$F_{\nu, 1.3\text{cm}, 3^a}$ [mJy]	$F_{\nu, 1.3\text{cm}, 4^a}$ [mJy]	$F_{\nu, 1.3\text{cm}, \text{mean}^a}$ [mJy]
721	—	649	—	—	5h35m20.80s	-5d21m13.70s	-0.188 ± 0.198	-0.022 ± 0.321	0.698 ± 2.589	0.025 ± 2.781	-0.382 ± 1.476	0.087 ± 0.499	0.375 ± 0.690	
722	—	22	—	—	5h35m20.90s	-5d25m34.50s	-0.047 ± 0.150	-0.036 ± 0.166	0.024 ± 0.852	-0.057 ± 0.778	0.238 ± 0.503	-0.015 ± 0.172	0.025 ± 0.219	
723	—	312	—	—	5h35m20.92s	-5d23m21.80s	0.049 ± 0.137	0.193 ± 0.157	-0.084 ± 0.644	0.123 ± 0.627	-0.270 ± 0.382	-0.135 ± 0.206	-0.258 ± 0.173	
724	—	574	—	—	5h35m20.93s	-5d21m50.90s	0.106 ± 0.141	0.143 ± 0.247	-0.030 ± 0.908	-0.076 ± 0.720	-0.090 ± 0.575	0.132 ± 0.232	0.083 ± 0.279	
725	209-151	—	—	—	5h35m21.00s	-5d21m52.30s	0.130 ± 0.142	0.272 ± 0.262	-0.034 ± 0.788	-0.103 ± 0.797	-0.149 ± 0.580	-0.018 ± 0.237	-0.001 ± 0.315	
726	—	196	—	—	5h35m21.02s	-5d22m22.90s	0.083 ± 0.179	0.043 ± 0.210	-0.219 ± 0.720	0.082 ± 0.549	0.118 ± 0.429	0.104 ± 0.198	-0.023 ± 0.238	
727	—	486	—	—	5h35m21.03s	-5d22m25.25s	0.087 ± 0.163	0.073 ± 0.243	0.483 ± 0.648	0.170 ± 0.581	0.091 ± 0.449	-0.012 ± 0.184	0.059 ± 0.211	
728	—	403	—	—	5h35m21.05s	-5d23m49.03s	2.031 ± 0.217	2.282 ± 0.237	2.712 ± 0.280	0.683 ± 0.098	2.420 ± 0.248	0.996 ± 0.117	1.373 ± 0.140	
730	—	217	30	77	5h35m21.11s	-5d20m55.50s	0.164 ± 0.205	0.161 ± 0.428	
731	—	680	—	—	5h35m21.12s	-5d22m50.20s	0.035 ± 0.141	-0.172 ± 0.202	-0.259 ± 0.625	-0.327 ± 0.627	0.155 ± 0.483	-0.074 ± 0.167	0.013 ± 0.215	
732	—	729	—	—	5h35m21.15s	-5d25m57.04s	-0.022 ± 0.157	0.008 ± 0.181	-0.159 ± 0.806	0.143 ± 0.807	0.124 ± 0.540	0.068 ± 0.189	0.051 ± 0.286	
733	212-557	—	—	—	5h35m21.18s	-5d23m33.10s	0.025 ± 0.158	0.030 ± 0.190	0.148 ± 0.601	-0.001 ± 0.586	-0.129 ± 0.379	-0.022 ± 0.177	-0.023 ± 0.190	
734	—	264	—	—	5h35m21.19s	-5d24m00.15s	-0.032 ± 0.161	0.002 ± 0.158	0.153 ± 0.423	0.053 ± 0.432	-0.023 ± 0.382	-0.033 ± 0.131	-0.016 ± 0.178	
735	212-400	184	—	—	5h35m21.19s	-5d22m20.30s	0.072 ± 0.157	-0.046 ± 0.219	-0.049 ± 0.612	0.198 ± 0.821	0.184 ± 0.538	0.044 ± 0.202	0.086 ± 0.273	
736	—	551	—	—	5h35m21.23s	-5d22m20.30s	0.079 ± 0.133	0.057 ± 0.237	-0.497 ± 0.593	-0.200 ± 0.643	0.588 ± 0.083	-0.066 ± 0.171	0.114 ± 0.029	
737	212-260	381	—	—	5h35m21.25s	-5d22m59.49s	0.048 ± 0.151	0.018 ± 0.184	-0.026 ± 0.623	0.079 ± 0.562	0.076 ± 0.472	-0.022 ± 0.160	-0.186 ± 0.188	
738	—	326	—	—	5h35m21.25s	-5d23m16.80s	0.008 ± 0.161	-0.018 ± 0.184	-0.101 ± 0.620	-0.135 ± 0.731	-0.016 ± 0.620	-0.149 ± 0.181	-0.131 ± 0.251	
739	—	734	—	—	5h35m21.28s	-5d22m09.10s	-0.089 ± 0.180	-0.005 ± 0.264	-0.322 ± 0.686	-0.125 ± 0.731	-0.016 ± 0.620	-0.041 ± 0.158	0.047 ± 0.254	
740	213-533	27	—	—	5h35m21.29s	-5d25m33.11s	0.057 ± 0.156	-0.037 ± 0.186	-0.101 ± 0.798	-0.118 ± 0.594	0.025 ± 0.475	0.041 ± 0.158	0.047 ± 0.254	
741	—	79	—	—	5h35m21.30s	-5d24m57.35s	0.073 ± 0.137	0.067 ± 0.182	0.087 ± 0.641	0.261 ± 0.598	0.100 ± 0.439	-0.086 ± 0.170	-0.072 ± 0.225	
742	—	507	—	—	5h35m21.30s	-5d22m15.70s	-0.012 ± 0.174	0.051 ± 0.245	-0.097 ± 0.727	-0.164 ± 0.630	0.083 ± 0.489	-0.062 ± 0.185	-0.058 ± 0.256	
743	213-346	225	—	—	5h35m21.31s	-5d23m46.05s	0.085 ± 0.162	-0.169 ± 0.149	0.161 ± 0.488	-0.148 ± 0.486	0.261 ± 0.338	-0.013 ± 0.157	-0.020 ± 0.179	
744	—	160	—	—	5h35m21.33s	-5d24m11.40s	0.018 ± 0.173	0.147 ± 0.190	0.143 ± 0.500	0.019 ± 0.425	0.168 ± 0.373	0.046 ± 0.136	0.049 ± 0.149	
745	—	20	—	—	5h35m21.35s	-5d25m35.00s	0.038 ± 0.137	-0.010 ± 0.167	-0.153 ± 0.692	-0.017 ± 0.682	-0.094 ± 0.499	-0.090 ± 0.151	-0.045 ± 0.222	
746	—	229	—	—	5h35m21.37s	-5d23m45.40s	0.048 ± 0.151	-0.014 ± 0.175	0.087 ± 0.534	0.073 ± 0.435	0.065 ± 0.363	0.008 ± 0.164	0.118 ± 0.177	
747	—	532	—	—	5h35m21.39s	-5d22m07.40s	-0.021 ± 0.168	-0.007 ± 0.239	0.300 ± 0.743	-0.071 ± 0.734	0.065 ± 0.489	-0.003 ± 0.241	-0.038 ± 0.256	
748	215-652	—	—	—	5h35m21.45s	-5d26m52.40s	-0.074 ± 0.167	-0.069 ± 0.226	-0.002 ± 3.102	1.402 ± 2.474	-0.450 ± 1.551	0.389 ± 0.510	0.090 ± 0.730	
749	215-317	328	—	—	5h35m21.50s	-5d23m16.71s	0.100 ± 0.135	0.013 ± 0.160	-0.402 ± 0.620	-0.119 ± 0.592	0.310 ± 0.388	0.129 ± 0.173	0.038 ± 0.227	
750	215-106	663	—	—	5h35m21.56s	-5d21m05.60s	0.111 ± 0.167	-0.020 ± 0.361	1.089 ± 2.160	0.156 ± 0.816	0.080 ± 1.207	
751	216-541	15	—	—	5h35m21.60s	-5d25m40.65s	0.009 ± 0.135	0.058 ± 0.158	0.014 ± 0.750	0.112 ± 0.704	-0.021 ± 0.408	-0.069 ± 0.163	-0.053 ± 0.219	
752	216-715	—	—	—	5h35m21.62s	-5d27m14.65s	0.014 ± 0.177	0.069 ± 0.297	
753	—	294	—	—	5h35m21.63s	-5d23m25.80s	-0.042 ± 0.145	0.031 ± 0.180	-0.126 ± 0.674	0.399 ± 0.573	0.016 ± 0.401	-0.038 ± 0.139	-0.168 ± 0.205	
754	—	516	—	—	5h35m21.64s	-5d22m12.70s	-0.061 ± 0.168	0.014 ± 0.261	0.164 ± 0.693	-0.044 ± 0.583	0.076 ± 0.550	-0.091 ± 0.194	-0.022 ± 0.269	
755	—	31	—	—	5h35m21.66s	-5d25m26.50s	-0.016 ± 0.156	0.015 ± 0.176	0.146 ± 0.689	-0.111 ± 0.653	-0.243 ± 0.445	0.034 ± 0.175	0.047 ± 0.241	
756	—	255	—	—	5h35m21.67s	-5d21m47.40s	0.044 ± 0.148	-0.074 ± 0.268	0.251 ± 1.117	0.144 ± 0.812	0.071 ± 0.702	0.034 ± 0.258	0.048 ± 0.364	
757	—	585	—	—	5h35m21.68s	-5d21m47.20s	0.076 ± 0.159	-0.060 ± 0.255	0.507 ± 0.967	0.066 ± 1.175	0.066 ± 0.654	-0.157 ± 0.282	-0.053 ± 0.351	
758	—	730	—	—	5h35m21.71s	-5d22m38.30s	0.149 ± 0.165	0.037 ± 0.242	0.014 ± 0.699	-0.175 ± 0.614	0.171 ± 0.477	-0.021 ± 0.188	-0.246 ± 0.264	
759	—	218	—	—	5h35m21.73s	-5d23m48.40s	-0.016 ± 0.130	-0.079 ± 0.162	0.194 ± 0.454	-0.016 ± 0.420	0.076 ± 0.377	0.003 ± 0.119	0.087 ± 0.183	
760	218-339	249	—	—	5h35m21.77s	-5d23m39.40s	0.174 ± 0.057	0.186 ± 0.202	0.056 ± 0.553	0.220 ± 0.551	0.016 ± 0.354	0.176 ± 0.151	0.082 ± 0.201	
761	218-354	204	—	—	5h35m21.80s	-5d23m53.90s	0.107 ± 0.152	0.166 ± 0.192	0.033 ± 0.509	0.041 ± 0.521	-0.036 ± 0.337	0.142 ± 0.129	0.002 ± 0.183	
762	—	343	—	—	5h35m21.81s	-5d23m10.70s	-0.015 ± 0.167	0.062 ± 0.166	-0.019 ± 0.685	-0.026 ± 0.627	0.028 ± 0.471	-0.017 ± 0.165	-0.046 ± 0.245	
763	218-529	30	—	—	5h35m21.83s	-5d25m28.43s	-0.002 ± 0.141	-0.071 ± 0.194	-0.194 ± 0.692	0.045 ± 0.580	0.036 ± 0.418	0.002 ± 0.159	-0.049 ± 0.248	
764	—	432	—	—	5h35m21.83s	-5d22m40.30s	0.070 ± 0.135	-0.032 ± 0.218	-0.291 ± 0.686	-0.033 ± 0.745	0.242 ± 0.526	0.105 ± 0.180	0.285 ± 0.235	
765	218-306	358	—	—	5h35m21.84s	-5d23m06.48s	0.262 ± 0.147	0.124 ± 0.224	-0.030 ± 0.632	-0.015 ± 0.697	0.147 ± 0.457	0.082 ± 0.190	-0.025 ± 0.234	
766	—	528	—	—	5h35m21.86s	-5d22m08.40s	0.021 ± 0.161	-0.029 ± 0.274	0.224 ± 0.749	-0.211 ± 0.697	-0.135 ± 0.608	-0.179 ± 0.228	0.040 ± 0.261	
767	—	197	—	—	5h35m21.89s	-5d23m26.50s	0.044 ± 0.150	-0.204 ± 0.201	0.068 ± 0.421	0.146 ± 0.497	-0.177 ± 0.357	0.108 ± 0.116	0.045 ± 0.175	
768	—	355	—	—	5h35m21.89s	-5d23m07.20s	-0.144 ± 0.155	-0.036 ± 0.190	-0.344 ± 0.617	-0.077 ± 0.722	0.016 ± 0.476	0.107 ± 0.177	0.045 ± 0.219	
769	—	136	—	—	5h35m21.98s	-5d24m26.10s	-0.068 ± 0.119	-0.129 ± 0.160	0.155 ± 0.409	0.041 ± 0.486	0.186 ± 0.384	-0.013 ± 0.130	0.173 ± 0.188	
770	—	91	—	—	5h35m21.99s	-5d24m30.50s	0.142 ± 0.177	0.009 ± 0.166	0.252 ± 0.679	0.064 ± 0.613	0.134 ± 0.410	0.013 ± 0.172	0.038 ± 0.233	
771	221-433	121	—	—	5h35m22.09s	-5d24m32.88s	0.349 ± 0.151	0.378 ± 0.204	-0.030 ± 0.512	0.407 ± 0.488	0.218 ± 0.379	0.134 ± 0.158	0.240 ± 0.189	
772	—	142	—	—	5h35m22.12s	-5d24m20.20s	0.010 ± 0.137	-0.058 ± 0.153	-0.212 ± 0.477	-0.143 ± 0.501	0.010 ± 0.346	-0.023 ± 0.115	-0.035 ± 0.198	
773	—	55	—	—	5h35m22.12s	-5d25m07.60s	0.047 ± 0.148	0.179 ± 0.156	-0.012 ± 0.766	-0.140 ± 0.592	-0.054 ± 0.443	-0.079 ± 0.165	-0.130 ± 0.230	
774	—	449	—	—	5h35m22.13s	-5d22m34.10s	0.076 ± 0.164	0.021 ± 0.213	0.041 ± 0.815	-0.404 ± 0.877	0.224 ± 0.543	-0.035 ± 0.182	-0.107 ± 0.293	
775	—	512	—	—	5h35m22.16s	-5d22m33.10s	-0.021 ± 0.147	-0.019 ± 0.263	0.036 ± 0.891	0.155 ± 0.895	0.005 ± 0.573	-0.131 ± 0.190	-0.000 ± 0.294	
776	—	139	—	—	5h35m22.19s	-5d24m24.90s	-0.030 ± 0.125	0.021 ± 0.174	-0.024 ± 0.471	-0.014 ± 0.514	-0.056 ± 0.353	-0.010 ± 0.146	0.027 ± 0.194	
777	—	503	—	—	5h35m22.25s	-5d22m17.40s	0.083 ± 0.121	0.034 ± 0.253	-0.084 ± 0.845	-0.087 ± 0.897	-0.002 ± 0.711	-0.084 ± 0.232	-0.112 ± 0.284	

TABLE 2 — *Continued*

ID	Proplyd Name	HC00 ID	GMR ID	Z04a ID	Other Names	R.A. [J2000]	Dec [J2000]	$F_{\nu, 6\text{cm}}$ [mJy]	$F_{\nu, 3.6\text{cm}}$ [mJy]	$F_{\nu, 1.3\text{cm}, 1^a}$ [mJy]	$F_{\nu, 1.3\text{cm}, 2^a}$ [mJy]	$F_{\nu, 1.3\text{cm}, 3^a}$ [mJy]	$F_{\nu, 1.3\text{cm}, 4^a}$ [mJy]	$F_{\nu, 1.3\text{cm}, \text{mean}^a}$ [mJy]
801	231-838	—	—	—	5h35m23.10s	-5d28m37.34s	-0.053 ± 0.341	0.139 ± 0.982
802	—	216	—	—	5h35m23.15s	-5d23m49.30s	0.003 ± 0.134	-0.004 ± 0.174	0.051 ± 0.488	0.136 ± 0.432	-0.010 ± 0.375	0.022 ± 0.134	0.082 ± 0.180	0.082 ± 0.180
803	231-502	68	—	—	5h35m23.16s	-5d25m02.25s	-0.046 ± 0.139	0.042 ± 0.165	-0.081 ± 0.552	0.005 ± 0.619	-0.031 ± 0.439	0.023 ± 0.155	0.149 ± 0.215	0.149 ± 0.215
804	—	470	—	—	5h35m23.19s	-5d22m28.40s	-0.017 ± 0.141	-0.021 ± 0.269	0.892 ± 1.267	-0.394 ± 1.281	0.050 ± 0.761	-0.191 ± 0.310	-0.488 ± 0.390	-0.488 ± 0.390
805	—	778	—	—	5h35m23.19s	-5d23m58.30s	0.019 ± 0.114	-0.090 ± 0.178	-0.066 ± 0.432	0.109 ± 0.449	-0.087 ± 0.322	0.058 ± 0.117	-0.004 ± 0.180	-0.004 ± 0.180
806	—	607	—	—	5h35m23.22s	-5d21m35.90s	-0.061 ± 0.163	0.008 ± 0.328	-0.316 ± 2.821	0.124 ± 2.807	0.102 ± 1.579	-0.031 ± 0.569	-0.186 ± 0.753	-0.186 ± 0.753
807	232-453	92	—	—	5h35m23.23s	-5d24m52.85s	-0.026 ± 0.142	-0.031 ± 0.173	-0.227 ± 0.593	-0.001 ± 0.613	0.058 ± 0.439	-0.062 ± 0.158	-0.104 ± 0.237	-0.104 ± 0.237
808	—	164	—	—	5h35m23.26s	-5d24m07.40s	-0.098 ± 0.143	0.042 ± 0.185	0.111 ± 0.543	-0.120 ± 0.400	-0.002 ± 0.341	0.028 ± 0.113	0.025 ± 0.187	0.025 ± 0.187
809	—	763	—	—	5h35m23.31s	-5d25m05.80s	0.041 ± 0.157	0.053 ± 0.179	-0.078 ± 0.664	0.020 ± 0.564	0.041 ± 0.428	0.024 ± 0.140	-0.002 ± 0.242	-0.002 ± 0.242
810	—	316	—	—	5h35m23.34s	-5d23m20.80s	0.108 ± 0.156	0.037 ± 0.202	0.096 ± 0.692	-0.156 ± 0.592	0.032 ± 0.410	0.004 ± 0.161	-0.039 ± 0.218	-0.039 ± 0.218
811	—	628	—	—	5h35m23.34s	-5d21m25.50s	0.020 ± 0.165	0.209 ± 0.407	0.777 ± 2.332	-0.210 ± 0.844
812	—	736	—	—	5h35m23.34s	-5d20m48.10s	-0.005 ± 0.187	0.187 ± 0.494
813	—	669	—	—	5h35m23.36s	-5d21m03.70s	-0.039 ± 0.201	0.114 ± 0.473
814	234-853	—	—	—	5h35m23.40s	-5d28m53.19s	0.133 ± 0.395	-0.093 ± 1.075
815	—	677	—	—	5h35m23.44s	-5d21m00.00s	-0.018 ± 0.185	0.004 ± 0.413
816	—	—	—	—	5h35m23.49s	-5d20m01.60s	0.184 ± 0.271	-0.413 ± 0.970
817	—	89	—	—	5h35m23.54s	-5d24m54.30s	0.049 ± 0.155	-0.177 ± 0.158	-0.053 ± 0.629	0.089 ± 0.575	0.080 ± 0.387	-0.021 ± 0.156	-0.038 ± 0.207	-0.038 ± 0.207
818	—	212	—	—	5h35m23.54s	-5d23m51.00s	0.087 ± 0.143	-0.088 ± 0.181	-0.098 ± 0.477	0.061 ± 0.388	0.056 ± 0.317	0.077 ± 0.135	0.071 ± 0.189	0.071 ± 0.189
819	236-527	32	—	—	5h35m23.60s	-5d25m26.52s	-0.019 ± 0.149	0.025 ± 0.152	-0.012 ± 0.462	0.012 ± 0.455	0.064 ± 0.368	0.045 ± 0.132	0.073 ± 0.208	0.073 ± 0.208
820	—	281	—	—	5h35m23.64s	-5d23m29.90s	-0.002 ± 0.152	0.021 ± 0.199	0.006 ± 0.599	0.070 ± 0.498	-0.028 ± 0.367	-0.053 ± 0.136	-0.149 ± 0.190	-0.149 ± 0.190
821	—	270	—	—	5h35m23.66s	-5d23m31.96s	-0.015 ± 0.136	-0.072 ± 0.222	-0.001 ± 0.534	-0.226 ± 0.512	-0.178 ± 0.461	0.917 ± 0.107	1.326 ± 0.270	1.326 ± 0.270
822	237-627	—	—	—	5h35m23.66s	-5d26m27.15s	0.069 ± 0.178	0.053 ± 0.224	-0.553 ± 0.725	0.127 ± 0.688	-0.112 ± 0.489	0.107 ± 0.180	0.070 ± 0.246	0.070 ± 0.246
823	—	227	—	—	5h35m23.66s	-5d23m46.40s	-0.053 ± 0.142	-0.104 ± 0.177	0.152 ± 0.434	-0.076 ± 0.433	-0.108 ± 0.380	-0.008 ± 0.138	0.035 ± 0.160	0.035 ± 0.160
824	—	645	—	—	5h35m23.67s	-5d21m16.40s	0.052 ± 0.175	-0.144 ± 0.426
825	—	81	—	—	5h35m23.68s	-5d24m57.40s	0.035 ± 0.143	-0.091 ± 0.183	0.372 ± 0.566	0.033 ± 0.594	-0.086 ± 0.394	-0.036 ± 0.154	0.035 ± 0.201	0.035 ± 0.201
826	—	519	—	—	5h35m23.69s	-5d22m12.80s	0.037 ± 0.185	-0.063 ± 0.244	0.047 ± 1.978	-0.140 ± 1.685	-0.052 ± 1.129	0.137 ± 0.438	0.440 ± 0.553	0.440 ± 0.553
827	—	319	—	—	5h35m23.72s	-5d23m19.90s	0.108 ± 0.130	-0.191 ± 0.244	-0.118 ± 0.667	-0.117 ± 0.621	-0.023 ± 0.459	-0.023 ± 0.162	-0.141 ± 0.233	-0.141 ± 0.233
828	238-334	262	—	—	5h35m23.80s	-5d23m34.30s	-0.060 ± 0.132	0.066 ± 0.214	-0.026 ± 0.553	0.007 ± 0.521	0.114 ± 0.392	0.066 ± 0.147	0.126 ± 0.228	0.126 ± 0.228
829	—	152	—	—	5h35m23.81s	-5d24m16.80s	-0.065 ± 0.144	-0.157 ± 0.174	0.103 ± 0.467	-0.009 ± 0.476	0.031 ± 0.361	-0.010 ± 0.136	-0.024 ± 0.207	-0.024 ± 0.207
830	239-334	—	—	—	5h35m23.86s	-5d23m34.05s	-0.064 ± 0.165	-0.026 ± 0.169	0.069 ± 0.469	-0.167 ± 0.515	-0.151 ± 0.387	-0.027 ± 0.152	-0.041 ± 0.215	-0.041 ± 0.215
831	—	265	—	—	5h35m23.89s	-5d23m33.30s	-0.004 ± 0.168	0.017 ± 0.212	0.024 ± 0.545	0.224 ± 0.572	-0.072 ± 0.437	0.078 ± 0.153	0.079 ± 0.206	0.079 ± 0.206
832	—	641	—	—	5h35m23.89s	-5d21m18.70s	0.011 ± 0.153	-0.035 ± 0.367
833	—	379	—	—	5h35m23.92s	-5d23m00.50s	-0.020 ± 0.151	0.071 ± 0.219	0.088 ± 0.913	-0.122 ± 0.948	0.276 ± 0.572	-0.010 ± 0.206	0.039 ± 0.309	0.039 ± 0.309
834	—	662	—	—	5h35m23.93s	-5d21m06.40s	0.079 ± 0.171	0.049 ± 0.463
835	239-510	52	—	—	5h35m23.99s	-5d25m09.92s	0.245 ± 0.093	-0.002 ± 0.184	0.181 ± 0.615	0.001 ± 0.603	0.042 ± 0.406	0.140 ± 0.044	0.045 ± 0.168	0.045 ± 0.168
836	240-314	338	—	—	5h35m24.02s	-5d23m33.18s	0.209 ± 0.137	0.177 ± 0.201	0.036 ± 0.841	0.066 ± 0.676	-0.051 ± 0.545	0.197 ± 0.175	0.065 ± 0.238	0.065 ± 0.238
837	—	619	—	—	5h35m24.11s	-5d21m32.80s	-0.001 ± 0.165	0.023 ± 0.379	-0.360 ± 2.444	-0.201 ± 1.054	-0.009 ± 1.106	-0.009 ± 1.106
838	—	506	—	—	5h35m24.12s	-5d22m16.40s	-0.031 ± 0.181	-0.032 ± 0.296	0.147 ± 2.316	0.620 ± 2.176	0.246 ± 1.190	0.083 ± 0.459	0.057 ± 0.601	0.057 ± 0.601
839	—	561	—	—	5h35m24.13s	-5d21m55.70s	0.019 ± 0.147	0.097 ± 0.322	-1.026 ± 3.137	0.648 ± 3.005	0.406 ± 1.458	0.073 ± 0.640	-0.004 ± 0.815	-0.004 ± 0.815
840	242-519	41	—	—	5h35m24.24s	-5d25m18.75s	0.117 ± 0.167	0.131 ± 0.183	-0.101 ± 0.475	0.093 ± 0.439	0.046 ± 0.324	0.066 ± 0.141	0.161 ± 0.205	0.161 ± 0.205
841	—	460	—	—	5h35m24.35s	-5d22m32.40s	-0.085 ± 0.138	0.213 ± 0.258	-0.288 ± 2.114	0.648 ± 2.188	-0.195 ± 1.032	0.121 ± 0.353	0.023 ± 0.572	0.023 ± 0.572
842	244-440	110	—	—	5h35m24.44s	-5d24m39.86s	0.148 ± 0.208	0.093 ± 0.209	0.152 ± 0.678	0.115 ± 0.536	0.123 ± 0.038	0.024 ± 0.174	0.229 ± 1.142	0.229 ± 1.142
843	—	201	—	—	5h35m24.45s	-5d23m55.00s	-0.027 ± 0.152	0.022 ± 0.177	0.019 ± 0.544	-0.012 ± 0.442	0.062 ± 0.402	0.030 ± 0.129	0.021 ± 0.185	0.021 ± 0.185
844	245-632	—	—	—	5h35m24.45s	-5d26m31.55s	0.096 ± 0.206	-0.039 ± 0.244	-0.142 ± 0.710	-0.205 ± 0.680	0.196 ± 0.539	0.083 ± 0.149	0.033 ± 0.252	0.033 ± 0.252
845	—	183	—	—	5h35m24.47s	-5d24m01.10s	-0.032 ± 0.180	-0.087 ± 0.191	0.046 ± 0.481	0.151 ± 0.434	-0.112 ± 0.377	-0.076 ± 0.130	-0.071 ± 0.183	-0.071 ± 0.183
846	245-1910	—	—	—	5h35m24.48s	-5d19m09.84s	-0.004 ± 0.362
847	—	626	—	—	5h35m24.49s	-5d21m30.00s	0.124 ± 0.179	-0.167 ± 0.389
848	245-502	71	—	—	5h35m24.52s	-5d25m01.60s	0.356 ± 0.088	0.328 ± 0.101	0.063 ± 0.612	0.122 ± 0.531	0.157 ± 0.419	0.275 ± 0.070	0.531 ± 0.467	0.531 ± 0.467
849	—	407	—	—	5h35m24.60s	-5d22m52.00s	-0.014 ± 0.159	0.018 ± 0.215	0.099 ± 1.550	-0.522 ± 1.352	-0.297 ± 0.824	0.054 ± 0.319	-0.269 ± 0.427	-0.269 ± 0.427
850	—	668	—	—	5h35m24.63s	-5d21m04.40s	-0.091 ± 0.175	0.185 ± 0.486
851	—	427	—	—	5h35m24.66s	-5d22m42.60s	-0.093 ± 0.175	0.239 ± 0.268	-0.091 ± 1.848	0.628 ± 1.929	0.315 ± 1.027	0.207 ± 0.356	0.480 ± 0.515	0.480 ± 0.515
852	247-436	119	—	—	5h35m24.70s	-5d24m35.72s	0.107 ± 0.142	0.062 ± 0.203	-0.245 ± 0.653	0.266 ± 0.610	0.085 ± 0.461	-0.113 ± 0.142	-0.081 ± 0.200	-0.081 ± 0.200
853	—	101	—	—	5h35m24.70s	-5d24m44.20s	0.062 ± 0.145	-0.024 ± 0.179	-0.059 ± 0.722	-0.249 ± 0.639	0.184 ± 0.424	0.019 ± 0.146	0.043 ± 0.222	0.043 ± 0.222
854	—	113	—	—	5h35m24.73s	-5d24m38.50s	-0.106 ± 0.141	0.076 ± 0.203	0.106 ± 0.558	-0.016 ± 0.540	-0.169 ± 0.401	0.077 ± 0.147	0.054 ± 0.209	0.054 ± 0.209
855	—	617	—	—	5h35m24.74s	-5d21m34.00s	0.067 ± 0.191	0.215 ± 0.431
856	—	557	—	—	5h35m24.84s	-5d21m57.80s	-0.086 ± 0.168	-0.004 ± 0.336						

TABLE 2 — *Continued*

ID	Proplyd Name	HC00 ID	GMR ID	Z04a ID	Other Names	R.A. [J2000]	Dec [J2000]	$F_{\nu, 6\text{cm}}$ [mJy]	$F_{\nu, 3.6\text{cm}}$ [mJy]	$F_{\nu, 1.3\text{cm}, 1}$ ^a [mJy]	$F_{\nu, 1.3\text{cm}, 2}$ ^a [mJy]	$F_{\nu, 1.3\text{cm}, 3}$ ^a [mJy]	$F_{\nu, 1.3\text{cm}, 4}$ ^a [mJy]	$F_{\nu, 1.3\text{cm}, \text{mean}}$ ^a [mJy]
881	—	7	—	—	5h35m25.96s	-5d25m47.60s	-0.061 ± 0.136	-0.036 ± 0.203	0.020 ± 0.420	-0.004 ± 0.471	0.088 ± 0.358	0.012 ± 0.128	0.014 ± 0.169	
882	—	6	—	—	5h35m26.02s	-5d25m47.70s	0.066 ± 0.171	0.052 ± 0.218	-0.284 ± 0.422	0.031 ± 0.398	0.039 ± 0.372	-0.027 ± 0.109	-0.088 ± 0.184	
883	—	638	—	—	5h35m26.07s	-5d21m21.10s	-0.013 ± 0.165	-0.107 ± 0.545	
884	—	16	—	—	5h35m26.16s	-5d25m39.40s	0.110 ± 0.175	-0.027 ± 0.223	0.051 ± 0.507	0.148 ± 0.480	0.021 ± 0.341	-0.000 ± 0.128	0.042 ± 0.174	
885	—	394	—	—	5h35m26.16s	-5d22m57.10s	-0.048 ± 0.196	0.147 ± 0.293	0.383 ± 2.151	0.130 ± 1.980	0.020 ± 1.025	-0.166 ± 0.399	-0.028 ± 0.635	
886	262-521	39	—	—	5h35m26.18s	-5d25m20.44s	0.077 ± 0.190	-0.126 ± 0.179	0.212 ± 0.498	-0.093 ± 0.562	-0.017 ± 0.435	0.030 ± 0.120	0.018 ± 0.195	
887	—	502	—	—	5h35m26.24s	-5d22m19.50s	0.045 ± 0.141	0.057 ± 0.294	
888	—	642	—	—	5h35m26.26s	-5d21m18.90s	0.035 ± 0.211	0.056 ± 0.581	
889	—	737	—	—	5h35m26.29s	-5d20m59.70s	0.139 ± 0.182	0.005 ± 0.717	
890	—	702	—	—	5h35m26.36s	-5d25m40.10s	-0.070 ± 0.179	0.071 ± 0.221	0.019 ± 0.445	-0.021 ± 0.482	0.157 ± 0.344	0.033 ± 0.117	0.042 ± 0.173	
891	—	76	—	—	5h35m26.40s	-5d25m00.72s	0.297 ± 0.065	0.312 ± 0.074	0.277 ± 0.077	0.252 ± 0.077	0.171 ± 0.064	0.236 ± 0.055	0.372 ± 0.122	
892	—	377	—	—	5h35m26.41s	-5d23m02.40s	-0.041 ± 0.163	0.008 ± 0.286	0.584 ± 2.092	0.406 ± 1.932	0.273 ± 1.179	0.021 ± 0.442	0.395 ± 0.582	
893	264-532	28	—	—	5h35m26.42s	-5d25m31.60s	-0.124 ± 0.196	-0.039 ± 0.195	-0.074 ± 0.586	0.050 ± 0.424	0.131 ± 0.389	0.054 ± 0.134	0.132 ± 0.178	
894	—	480	—	—	5h35m26.46s	-5d22m25.80s	0.034 ± 0.167	0.094 ± 0.318	
895	—	232	—	—	5h35m26.50s	-5d23m45.00s	-0.058 ± 0.137	-0.037 ± 0.244	0.059 ± 0.936	0.046 ± 0.850	0.036 ± 0.557	0.071 ± 0.234	0.246 ± 0.308	
896	266-558	—	—	—	5h35m26.62s	-5d25m57.84s	-0.072 ± 0.165	0.049 ± 0.239	-0.027 ± 0.508	0.026 ± 0.465	0.006 ± 0.352	0.004 ± 0.150	0.001 ± 0.182	
897	—	—	—	—	5h35m27.44s	-5d26m28.14s	0.047 ± 0.194	-0.081 ± 0.304	0.093 ± 0.854	0.075 ± 0.818	0.087 ± 0.658	0.255 ± 0.061	0.003 ± 0.320	
898	281-306	—	—	—	5h35m28.13s	-5d23m06.45s	0.112 ± 0.157	0.150 ± 0.417	-0.242 ± 2.576	-0.020 ± 0.780	-0.486 ± 1.107	
899	282-614	—	—	—	5h35m28.20s	-5d26m14.20s	-0.069 ± 0.210	-0.053 ± 0.340	0.320 ± 0.964	0.215 ± 0.854	0.038 ± 0.586	0.067 ± 0.228	0.039 ± 0.351	
900	282-458	—	—	—	5h35m28.20s	-5d24m58.19s	0.304 ± 0.172	0.176 ± 0.259	0.415 ± 1.329	0.250 ± 1.098	-0.008 ± 0.763	0.124 ± 0.254	0.251 ± 0.390	
901	284-439	—	—	—	5h35m28.40s	-5d24m38.69s	0.011 ± 0.175	-0.050 ± 0.259	0.218 ± 2.121	0.005 ± 1.790	-0.300 ± 1.109	0.169 ± 0.384	0.173 ± 0.570	
902	—	—	—	—	5h35m28.55s	-5d20m56.59s	0.779 ± 0.143	0.626 ± 1.216	
903	294-606	—	—	—	5h35m29.48s	-5d26m06.63s	0.200 ± 0.233	-0.016 ± 0.333	0.114 ± 1.401	0.121 ± 1.302	-0.003 ± 0.892	-0.062 ± 0.256	-0.333 ± 0.426	
904	—	—	—	—	5h35m29.59s	-5d23m12.13s	1.579 ± 0.207	0.833 ± 0.161	
905	304-539	—	—	—	5h35m30.41s	-5d25m38.63s	0.045 ± 0.257	0.023 ± 0.361	0.123 ± 2.366	0.037 ± 2.095	0.054 ± 1.289	0.153 ± 0.427	0.349 ± 0.579	
906	314-816	—	—	—	5h35m31.40s	-5d28m16.48s	-0.211 ± 0.548	
907	321-602	—	—	—	5h35m32.10s	-5d26m01.94s	-0.088 ± 0.258	0.062 ± 0.527	
908	332-405	—	—	—	5h35m33.19s	-5d24m04.74s	0.039 ± 0.212	-0.342 ± 0.591	
909	353-130	—	—	—	5h35m35.32s	-5d21m29.59s	-0.047 ± 0.345	

^a Subscript 1 indicates the 1.3 cm data were taken on Nov 10, 2013, 2 on Mar. 3, 2014, 3 on Mar. 7, 2014, 4 on May 3, 2014, and mean indicates the image from the combined 1.3 cm tracks.

TABLE 3

ID	ν_{turn} [GHz]	$F_{\nu, \text{turn}}$ [mJy]	$F_{\nu, \text{dust, 230GHz}}$ [mJy]	$F_{\nu, \text{Band 1}}^{\text{a}}$ [mJy]	$F_{\nu, \text{Band 2}}^{\text{a}}$ [mJy]	$F_{\nu, \text{Band 3}}^{\text{a}}$ [mJy]	$F_{\nu, \text{Band 4}}^{\text{a}}$ [mJy]	$F_{\nu, \text{Band 5}}^{\text{a}}$ [mJy]	$F_{\nu, \text{Band 6}}^{\text{a}}$ [mJy]	$F_{\nu, \text{Band 7}}^{\text{a}}$ [mJy]	$F_{\nu, \text{Band 8}}^{\text{a}}$ [mJy]	$F_{\nu, \text{Band 9}}^{\text{a}}$ [mJy]	$F_{\nu, \text{Band 10}}^{\text{a}}$ [mJy]
11	< 5.5	3.188 ± 0.161	...	2.65	2.44	2.39	2.29	2.23	2.19	2.11	2.05	1.98	1.93
18	< 5.5	0.582 ± 0.078	...	0.48	0.45	0.44	0.42	0.41	0.40	0.38	0.37	0.36	0.35
69	> 22.0	0.265 ± 0.181	...	0.25	0.23	0.23	0.22	0.21	0.21	0.20	0.20	0.19	0.18
76	< 5.5	0.237 ± 0.021	...	0.20	0.18	0.18	0.17	0.17	0.16	0.16	0.15	0.15	0.14
77	11.477 ± 6.002	0.382 ± 0.055	...	0.34	0.31	0.31	0.30	0.29	0.28	0.27	0.26	0.25	0.25
97	16.116 ± 8.250	0.182 ± 0.040	...	0.17	0.16	0.15	0.15	0.14	0.14	0.13	0.13	0.13	0.12
103	> 22.0	0.165 ± 0.048	...	0.16	0.15	0.14	0.14	0.13	0.13	0.13	0.12	0.12	0.11
109	9.152 ± 8.250	0.057 ± 0.090	...	0.05	0.05	0.04	0.04	0.04	0.04	0.04	0.04	0.04	0.04
115	< 5.5	0.327 ± 0.028	...	0.27	0.25	0.24	0.24	0.23	0.23	0.22	0.21	0.20	0.20
134	300.000 ± 59.025	0.625 ± 0.191	31.179 ± 0.067	0.77	0.71	0.70	0.67	0.65	0.64	0.62	0.60	0.58	0.56
148	8.897 ± 6.799	0.151 ± 0.067	...	0.13	0.12	0.12	0.11	0.11	0.11	0.10	0.10	0.10	0.10
151	< 5.5	0.251 ± 0.049	...	0.21	0.19	0.19	0.18	0.18	0.17	0.17	0.16	0.16	0.15
154	< 5.5	2.878 ± 0.122	...	2.39	2.20	2.15	2.07	2.01	1.98	1.90	1.85	1.79	1.74
161	> 22.0	0.112 ± 0.108	...	0.11	0.10	0.09	0.09	0.09	0.09	0.09	0.08	0.08	0.08
173	> 22.0	0.113 ± 0.039	...	0.11	0.10	0.09	0.09	0.09	0.09	0.08	0.08	0.08	0.08
190	< 5.5	0.256 ± 0.072	...	0.21	0.20	0.19	0.18	0.18	0.18	0.17	0.16	0.16	0.15
199	> 22.0	0.317 ± 0.056	...	0.30	0.28	0.27	0.26	0.25	0.25	0.24	0.23	0.23	0.22
200	> 22.0	0.248 ± 0.039	...	0.24	0.22	0.21	0.20	0.20	0.20	0.19	0.18	0.18	0.17
209	< 5.5	0.239 ± 0.053	...	0.20	0.18	0.18	0.17	0.17	0.16	0.16	0.15	0.15	0.14
213	> 22.0	0.465 ± 0.044	...	0.44	0.41	0.40	0.38	0.37	0.37	0.35	0.34	0.33	0.32
219	< 5.5	0.177 ± 0.022	...	0.15	0.14	0.13	0.13	0.12	0.12	0.11	0.11	0.11	0.11
222	> 22.0	0.362 ± 0.080	...	0.35	0.32	0.31	0.30	0.29	0.28	0.27	0.26	0.25	0.25
229	13.758 ± 2.391	1.328 ± 0.094	...	1.21	1.11	1.09	1.05	1.02	1.00	0.96	0.94	0.90	0.88
232	5.899 ± 2.239	0.313 ± 0.069	21.865 ± 6.394	0.26	0.24	0.23	0.22	0.22	0.21	0.20	0.20	0.19	0.19
235	> 22.0	0.237 ± 0.061	...	0.23	0.21	0.20	0.19	0.19	0.18	0.18	0.17	0.17	0.16
236	89.990 ± 20.480	0.874 ± 0.128	157.197 ± 11.932	0.96	0.88	0.87	0.83	0.81	0.80	0.76	0.74	0.72	0.70
237	> 22.0	0.346 ± 0.038	...	0.33	0.30	0.30	0.29	0.28	0.27	0.26	0.25	0.24	0.24
238	< 5.5	0.973 ± 0.052	...	0.81	0.74	0.73	0.70	0.68	0.67	0.64	0.63	0.60	0.59
242	> 22.0	0.173 ± 0.039	...	0.17	0.15	0.15	0.14	0.14	0.14	0.13	0.12	0.12	0.12
246	300.000 ± 57.149	0.065 ± 0.011	273.937 ± 17.585	0.08	0.07	0.07	0.07	0.07	0.07	0.06	0.06	0.06	0.06
247	> 22.0	0.168 ± 0.071	...	0.16	0.15	0.14	0.13	0.13	0.13	0.12	0.12	0.12	0.12
251	> 22.0	0.058 ± 0.021	...	0.06	0.05	0.05	0.05	0.05	0.05	0.04	0.04	0.04	0.04
252	> 22.0	0.177 ± 0.067	...	0.17	0.16	0.15	0.14	0.14	0.13	0.13	0.13	0.12	0.12
253	> 22.0	0.161 ± 0.031	...	0.15	0.14	0.14	0.13	0.13	0.12	0.12	0.12	0.11	0.11
257	12.493 ± 8.250	0.219 ± 0.028	...	0.20	0.18	0.18	0.17	0.17	0.16	0.16	0.15	0.15	0.14
259	> 22.0	0.301 ± 0.052	...	0.29	0.26	0.26	0.25	0.24	0.23	0.22	0.21	0.21	0.21
261	< 5.5	0.309 ± 0.063	...	0.26	0.24	0.23	0.22	0.22	0.21	0.20	0.20	0.19	0.19
262	> 22.0	0.340 ± 0.042	...	0.32	0.30	0.29	0.28	0.27	0.26	0.25	0.24	0.24	0.24
264	> 22.0	0.130 ± 0.040	...	0.12	0.11	0.11	0.10	0.10	0.10	0.10	0.09	0.09	0.09
265	9.963 ± 4.865	0.175 ± 0.021	...	0.15	0.14	0.14	0.13	0.13	0.13	0.12	0.12	0.11	0.11
270	< 5.5	0.372 ± 0.087	...	0.31	0.28	0.28	0.27	0.26	0.26	0.25	0.24	0.23	0.22
271	> 22.0	0.343 ± 0.079	...	0.33	0.30	0.28	0.28	0.27	0.26	0.25	0.24	0.24	0.24
279	> 22.0	9.579 ± 0.397	...	9.14	8.42	8.23	7.91	7.68	7.58	7.27	7.08	6.83	6.65
280	9.415 ± 2.894	0.734 ± 0.052	...	0.64	0.59	0.58	0.56	0.54	0.53	0.51	0.50	0.48	0.47
281	< 5.5	6.976 ± 0.479	...	5.80	5.34	5.22	5.01	4.87	4.80	4.61	4.49	4.33	4.21
283	< 5.5	0.602 ± 0.068	...	0.50	0.46	0.45	0.43	0.42	0.41	0.40	0.39	0.37	0.36
284	> 22.0	0.203 ± 0.030	...	0.19	0.18	0.17	0.17	0.16	0.16	0.15	0.15	0.14	0.14
286	5.820 ± 3.860	0.304 ± 0.063	...	0.25	0.23	0.23	0.22	0.21	0.21	0.20	0.20	0.19	0.18
287	< 5.5	0.813 ± 0.138	...	0.68	0.62	0.61	0.58	0.57	0.56	0.54	0.52	0.50	0.49
289	> 22.0	0.184 ± 0.026	...	0.18	0.16	0.16	0.15	0.15	0.14	0.14	0.13	0.13	0.13
292	> 22.0	0.111 ± 0.128	...	0.11	0.10	0.09	0.09	0.09	0.09	0.08	0.08	0.08	0.08
294	> 22.0	0.358 ± 0.064	...	0.34	0.31	0.31	0.30	0.29	0.28	0.27	0.26	0.26	0.25
297	< 5.5	0.588 ± 0.068	...	0.49	0.45	0.44	0.42	0.41	0.40	0.39	0.38	0.36	0.35
301	22.608 ± 6.489	0.379 ± 0.053	103.200 ± 6.964	0.36	0.33	0.33	0.31	0.30	0.30	0.29	0.28	0.27	0.26
304	> 22.0	0.337 ± 0.168	...	0.32	0.30	0.29	0.28	0.27	0.27	0.26	0.25	0.24	0.23
305	< 5.5	0.149 ± 0.058	...	0.12	0.11	0.11	0.11	0.10	0.10	0.10	0.10	0.09	0.09
307	< 5.5	1.678 ± 0.073	...	1.39	1.28	1.26	1.21	1.17	1.16	1.11	1.08	1.04	1.01
308	> 22.0	2.589 ± 0.129	...	2.47	2.28	2.23	2.14	2.08	2.05	1.97	1.91	1.85	1.80
313	> 22.0	0.308 ± 0.039	...	0.29	0.27	0.26	0.25	0.25	0.24	0.23	0.22	0.21	0.21
315	> 22.0	0.489 ± 0.039	...	0.47	0.43	0.42	0.40	0.39	0.39	0.37	0.36	0.35	0.34
316	< 5.5	0.495 ± 0.108	...	0.41	0.38	0.37	0.36	0.35	0.34	0.33	0.32	0.31	0.30
319	8.897 ± 4.245	0.195 ± 0.027	...	0.17	0.16	0.15	0.15	0.14	0.14	0.14	0.13	0.13	0.12
325	> 22.0	0.193 ± 0.030	...	0.18	0.17	0.17	0.16	0.15	0.15	0.15	0.14	0.14	0.13
330	> 22.0	0.191 ± 0.026	...	0.18	0.17	0.16	0.16	0.15	0.15	0.14	0.14	0.14	0.13
331	25.930 ± 26.573	0.481 ± 0.189	7.114 ± 2.139	0.47	0.43	0.42	0.40	0.39	0.39	0.37	0.36	0.35	0.34
332	> 22.0	0.303 ± 0.042	...	0.29	0.27	0.26	0.25	0.24	0.24	0.23	0.22	0.22	0.21
333	< 5.5	0.320 ± 0.068	...	0.27	0.25	0.24	0.23	0.22	0.22	0.21	0.21	0.20	0.19
341	6.705 ± 2.443	0.921 ± 0.049	...	0.78	0.72	0.70	0.68	0.66	0.65	0.62	0.60	0.58	0.57
344	8.897 ± 3.322	0.288 ± 0.072	...	0.25	0.23	0.23	0.22	0.21	0.21	0.20	0.19	0.19	0.18
361	> 22.0	0.237 ± 0.081	...	0.23	0.21	0.20	0.19	0.19	0.18	0.18	0.18	0.17	0.16
371	< 5.5	0.936 ± 0.126	...	0.78	0.72	0.70	0.67	0.65	0.64	0.62	0.60	0.58	0.57
374	> 22.0	0.228 ± 0.044	...	0.22	0.20	0.20	0.19	0.18	0.18	0.17	0.17	0.16	0.16
378	> 22.0	0.131 ± 0.035	...	0.13	0.12	0.11	0.11	0.11	0.10	0.10	0.10	0.09	0.09
380	< 5.5	0.226 ± 0.028	...	0.19	0.17	0.17	0.16	0.16	0.16	0.15	0.15	0.14	0.14
382	15.230 ± 6.019	0											

TABLE 3 — *Continued*

ID	ν_{turn} [GHz]	$F_{\nu, \text{turn}}$ [mJy]	$F_{\nu, \text{dust, 230GHz}}$ [mJy]	$F_{\nu, \text{Band 1}}^{\text{a}}$ [mJy]	$F_{\nu, \text{Band 2}}^{\text{a}}$ [mJy]	$F_{\nu, \text{Band 3}}^{\text{a}}$ [mJy]	$F_{\nu, \text{Band 4}}^{\text{a}}$ [mJy]	$F_{\nu, \text{Band 5}}^{\text{a}}$ [mJy]	$F_{\nu, \text{Band 6}}^{\text{a}}$ [mJy]	$F_{\nu, \text{Band 7}}^{\text{a}}$ [mJy]	$F_{\nu, \text{Band 8}}^{\text{a}}$ [mJy]	$F_{\nu, \text{Band 9}}^{\text{a}}$ [mJy]	$F_{\nu, \text{Band 10}}^{\text{a}}$ [mJy]
393	> 22.0	0.144 ± 0.034	...	0.14	0.13	0.12	0.12	0.12	0.11	0.11	0.11	0.10	0.10
394	< 5.5	1.507 ± 0.074	...	1.25	1.15	1.13	1.08	1.05	1.04	1.00	0.97	0.94	0.91
399	< 5.5	0.710 ± 0.201	...	0.59	0.54	0.53	0.51	0.50	0.49	0.47	0.46	0.44	0.43
401	8.897 ± 3.322	0.173 ± 0.030	...	0.15	0.14	0.14	0.13	0.13	0.12	0.12	0.11	0.11	0.11
408	< 5.5	2.352 ± 0.125	0.418 ± 0.099	1.95	1.80	1.76	1.69	1.64	1.62	1.56	1.51	1.46	1.42
409	> 22.0	0.085 ± 0.021	...	0.08	0.07	0.07	0.07	0.07	0.07	0.06	0.06	0.06	0.06
413	< 5.5	2.122 ± 0.097	...	1.76	1.62	1.59	1.52	1.48	1.46	1.40	1.37	1.32	1.28
416	< 5.5	9.716 ± 0.397	5.518 ± 0.130	8.07	7.43	7.27	6.98	6.78	6.69	6.42	6.25	6.03	5.87
418	< 5.5	4.931 ± 0.222	3.744 ± 1.957	4.10	3.77	3.69	3.54	3.44	3.40	3.26	3.17	3.06	2.98
421	6.910 ± 1.017	10.001 ± 0.292	2.955 ± 0.098	8.50	7.83	7.66	7.35	7.14	7.04	6.76	6.59	6.35	6.18
423	< 5.5	5.603 ± 0.279	2.307 ± 0.100	4.66	4.29	4.19	4.03	3.91	3.86	3.70	3.61	3.48	3.38
424	< 5.5	0.327 ± 0.077	...	0.27	0.25	0.24	0.23	0.23	0.22	0.22	0.21	0.20	0.20
427	6.114 ± 1.027	1.903 ± 0.093	...	1.60	1.47	1.44	1.38	1.34	1.32	1.27	1.24	1.19	1.16
428	< 5.5	0.422 ± 0.050	...	0.35	0.32	0.30	0.29	0.29	0.28	0.27	0.26	0.25	0.25
430	< 5.5	10.314 ± 0.598	23.822 ± 1.580	8.57	7.89	7.72	7.41	7.20	7.10	6.82	6.64	6.40	6.23
433	< 5.5	2.953 ± 0.237	...	2.45	2.26	2.21	2.12	2.06	2.03	1.95	1.90	1.83	1.78
434	6.518 ± 2.374	0.326 ± 0.067	...	0.28	0.25	0.24	0.23	0.23	0.22	0.21	0.21	0.20	0.20
437	> 22.0	0.940 ± 0.173	...	0.90	0.83	0.81	0.78	0.75	0.74	0.71	0.70	0.67	0.65
438	9.965 ± 1.275	5.543 ± 0.195	0.472 ± 0.099	4.89	4.50	4.40	4.23	4.11	4.05	3.89	3.79	3.65	3.55
439	< 5.5	4.060 ± 0.209	5.918 ± 2.089	3.37	3.11	3.04	2.92	2.83	2.80	2.68	2.61	2.52	2.45
440	6.114 ± 1.677	0.453 ± 0.041	...	0.38	0.34	0.33	0.32	0.32	0.30	0.29	0.28	0.28	0.28
442	< 5.5	2.245 ± 0.154	1.546 ± 0.099	1.87	1.72	1.68	1.61	1.57	1.55	1.48	1.44	1.39	1.36
444	< 5.5	0.233 ± 0.041	...	0.19	0.18	0.17	0.17	0.16	0.15	0.15	0.14	0.14	0.14
446	< 5.5	0.768 ± 0.114	0.867 ± 0.198	0.64	0.59	0.57	0.55	0.54	0.53	0.51	0.49	0.48	0.46
460	8.431 ± 1.331	9.970 ± 0.287	1.876 ± 0.098	8.65	7.96	7.79	7.48	7.26	7.16	6.88	6.70	6.46	6.29
465	15.529 ± 1.806	4.832 ± 0.172	0.956 ± 0.100	4.46	4.10	4.01	3.85	3.74	3.69	3.54	3.45	3.33	3.24
466	< 5.5	0.506 ± 0.049	11.191 ± 0.622	0.42	0.39	0.38	0.36	0.35	0.35	0.33	0.33	0.31	0.31
469	11.806 ± 5.083	0.439 ± 0.037	...	0.39	0.36	0.35	0.34	0.33	0.33	0.31	0.31	0.29	0.29
473	> 22.0	1.386 ± 0.071	...	1.32	1.22	1.19	1.14	1.11	1.10	1.05	1.02	0.99	0.96
477	< 5.5	0.431 ± 0.093	...	0.36	0.33	0.32	0.31	0.30	0.28	0.28	0.27	0.26	0.26
481	> 22.0	0.165 ± 0.043	...	0.16	0.15	0.14	0.14	0.13	0.13	0.12	0.12	0.11	0.11
483	< 5.5	0.375 ± 0.048	...	0.31	0.29	0.28	0.27	0.26	0.26	0.25	0.24	0.23	0.23
484	9.467 ± 1.636	2.352 ± 0.104	0.621 ± 0.131	2.06	1.90	1.86	1.78	1.73	1.71	1.64	1.60	1.54	1.50
491	8.464 ± 0.970	21.520 ± 0.450	3.717 ± 0.131	18.67	17.19	16.81	16.14	15.69	15.47	14.85	14.46	13.94	13.57
492	< 5.5	0.335 ± 0.028	...	0.28	0.26	0.24	0.23	0.23	0.22	0.22	0.21	0.20	0.20
494	8.041 ± 1.374	3.658 ± 0.141	1.536 ± 0.099	3.16	2.91	2.84	2.73	2.65	2.62	2.51	2.45	2.36	2.30
499	< 5.5	12.669 ± 0.414	5.062 ± 0.157	10.53	9.69	9.48	9.10	8.84	8.72	8.38	8.16	7.86	7.65
501	10.543 ± 3.632	0.421 ± 0.045	...	0.37	0.34	0.34	0.32	0.31	0.30	0.29	0.28	0.27	0.27
511	20.248 ± 5.492	0.699 ± 0.128	...	0.66	0.61	0.60	0.57	0.56	0.55	0.53	0.51	0.49	0.48
512	< 5.5	3.496 ± 0.231	4.317 ± 0.622	2.91	2.67	2.62	2.51	2.44	2.41	2.31	2.25	2.17	2.11
515	< 5.5	0.349 ± 0.068	...	0.29	0.27	0.26	0.25	0.24	0.24	0.23	0.22	0.21	0.21
516	< 5.5	9.614 ± 0.386	5.804 ± 0.124	7.99	7.36	7.19	6.91	6.71	6.62	6.36	6.19	5.97	5.81
518	6.979 ± 1.091	3.902 ± 0.163	2.128 ± 0.132	3.32	3.06	2.99	2.87	2.79	2.75	2.64	2.57	2.48	2.41
519	< 5.5	1.147 ± 0.178	10.800 ± 0.162	0.95	0.88	0.86	0.82	0.80	0.79	0.76	0.74	0.71	0.69
524	8.897 ± 5.539	0.109 ± 0.039	...	0.09	0.09	0.09	0.08	0.08	0.08	0.08	0.07	0.07	0.07
529	6.715 ± 1.156	1.796 ± 0.101	...	1.52	1.40	1.37	1.32	1.28	1.26	1.21	1.18	1.14	1.11
530	19.098 ± 5.097	0.981 ± 0.162	...	0.92	0.85	0.83	0.80	0.78	0.76	0.73	0.71	0.69	0.67
535	< 5.5	0.830 ± 0.063	0.787 ± 0.297	0.69	0.63	0.62	0.60	0.58	0.57	0.55	0.53	0.51	0.50
537	< 5.5	2.728 ± 0.187	8.006 ± 0.628	2.27	2.09	2.04	1.96	1.90	1.88	1.80	1.76	1.69	1.65
539	> 22.0	0.058 ± 0.018	...	0.06	0.05	0.05	0.05	0.05	0.05	0.04	0.04	0.04	0.04
544	< 5.5	0.374 ± 0.039	...	0.31	0.29	0.28	0.27	0.26	0.26	0.25	0.24	0.23	0.23
546	< 5.5	0.412 ± 0.038	...	0.34	0.32	0.31	0.30	0.29	0.28	0.27	0.27	0.26	0.25
548	< 5.5	0.316 ± 0.083	...	0.26	0.24	0.24	0.23	0.22	0.22	0.21	0.20	0.19	0.19
549	> 22.0	0.313 ± 0.118	...	0.30	0.28	0.27	0.26	0.25	0.25	0.24	0.23	0.22	0.22
555	< 5.5	4.579 ± 0.206	7.897 ± 2.061	3.81	3.50	3.43	3.29	3.20	3.15	3.03	2.95	2.84	2.77
560	< 5.5	0.337 ± 0.087	...	0.29	0.27	0.26	0.25	0.25	0.24	0.23	0.23	0.22	0.21
564	< 5.5	11.794 ± 0.484	6.237 ± 0.160	9.80	9.02	8.82	8.47	8.23	8.12	7.80	7.59	7.32	7.12
587	< 5.5	1.806 ± 0.083	...	1.50	1.38	1.35	1.30	1.26	1.24	1.19	1.16	1.12	1.09
595	< 5.5	4.907 ± 0.308	...	4.08	3.75	3.67	3.53	3.43	3.38	3.24	3.16	3.04	2.96
599	< 5.5	0.225 ± 0.100	7.456 ± 2.401	0.19	0.17	0.17	0.16	0.16	0.15	0.15	0.14	0.14	0.14
605	< 5.5	0.912 ± 0.159	4.238 ± 0.490	0.76	0.70	0.68	0.66	0.64	0.63	0.60	0.59	0.57	0.55
608	< 5.5	0.718 ± 0.063	...	0.60	0.55	0.54	0.52	0.50	0.49	0.47	0.46	0.45	0.43
612	18.297 ± 10.071	0.403 ± 0.088	1.965 ± 0.491	0.38	0.35	0.34	0.33	0.32	0.31	0.30	0.29	0.28	0.27
616	< 5.5	0.266 ± 0.043	...	0.22	0.20	0.20	0.19	0.19	0.18	0.18	0.17	0.17	0.16
617	< 5.5	24.441 ± 0.958	0.000 ± 0.230	20.31	18.70	18.29	17.56	17.06	16.83	16.16	15.73	15.17	14.76
621	> 22.0	0.167 ± 0.048	...	0.16	0.15	0.14	0.14	0.13	0.13	0.13	0.12	0.12	0.12
649	< 5.5	0.344 ± 0.064	...	0.29	0.26	0.25	0.24	0.24	0.23	0.22	0.21	0.21	0.21
658	7.298 ± 8.250	0.260 ± 0.065	...	0.22	0.20	0.20	0.19	0.19	0.18	0.18	0.17	0.17	0.16
665	> 22.0	0.067 ± 0.013	...	0.06	0.06	0.06	0.06	0.05	0.05	0.05	0.05	0.05	0.05
668	< 5.5	0.323 ± 0.093	19.229 ± 0.624	0.27	0.25	0.24	0.23	0.23	0.22	0.21	0.21	0.20	0.20
672	< 5.5	0.340 ± 0.079	...	0.28	0.26	0.25	0.24	0.24	0.23	0.22	0.22	0.21	0.21
674	< 5.5	0.173 ± 0.080	5.458 ± 0.662	0.14	0.13	0.13	0.12	0.12	0.12	0.11	0.11	0	

TABLE 3 — *Continued*

ID	ν_{turn} [GHz]	$F_{\nu, \text{turn}}$ [mJy]	$F_{\nu, \text{dust, 230GHz}}$ [mJy]	$F_{\nu, \text{Band 1}}^{\text{a}}$ [mJy]	$F_{\nu, \text{Band 2}}^{\text{a}}$ [mJy]	$F_{\nu, \text{Band 3}}^{\text{a}}$ [mJy]	$F_{\nu, \text{Band 4}}^{\text{a}}$ [mJy]	$F_{\nu, \text{Band 5}}^{\text{a}}$ [mJy]	$F_{\nu, \text{Band 6}}^{\text{a}}$ [mJy]	$F_{\nu, \text{Band 7}}^{\text{a}}$ [mJy]	$F_{\nu, \text{Band 8}}^{\text{a}}$ [mJy]	$F_{\nu, \text{Band 9}}^{\text{a}}$ [mJy]	$F_{\nu, \text{Band 10}}^{\text{a}}$ [mJy]
730	< 5.5	1.433 ± 0.064	...	1.19	1.10	1.07	1.03	1.00	0.99	0.95	0.92	0.89	0.87
737	> 22.0	0.158 ± 0.027	...	0.15	0.14	0.14	0.13	0.13	0.12	0.12	0.12	0.11	0.11
760	5.977 ± 2.824	0.182 ± 0.051	2.172 ± 0.231	0.15	0.14	0.14	0.13	0.13	0.12	0.12	0.12	0.11	0.11
779	< 5.5	0.206 ± 0.058	...	0.17	0.16	0.15	0.15	0.14	0.14	0.14	0.13	0.13	0.12
786	> 22.0	0.152 ± 0.048	...	0.15	0.13	0.13	0.13	0.12	0.12	0.12	0.11	0.11	0.11
821	> 22.0	0.733 ± 0.086	...	0.70	0.64	0.63	0.60	0.59	0.58	0.56	0.54	0.52	0.51
835	< 5.5	0.171 ± 0.040	...	0.14	0.13	0.13	0.12	0.12	0.12	0.11	0.11	0.11	0.10
842	< 5.5	0.134 ± 0.040	...	0.11	0.10	0.10	0.10	0.09	0.09	0.09	0.09	0.08	0.08
848	< 5.5	0.334 ± 0.050	...	0.28	0.26	0.25	0.24	0.23	0.23	0.22	0.22	0.21	0.20
859	20.210 ± 8.250	0.130 ± 0.036	...	0.12	0.11	0.11	0.11	0.10	0.10	0.10	0.10	0.09	0.09
862	< 5.5	0.136 ± 0.021	...	0.11	0.10	0.10	0.10	0.09	0.09	0.09	0.09	0.08	0.08
891	< 5.5	0.287 ± 0.029	...	0.24	0.22	0.21	0.21	0.20	0.20	0.19	0.18	0.18	0.17
897	> 22.0	0.237 ± 0.057	...	0.23	0.21	0.20	0.20	0.19	0.19	0.18	0.18	0.17	0.16
902	...	0.740 ± 0.135	...	0.65	0.59	0.58	0.56	0.54	0.53	0.51	0.50	0.48	0.47
904	...	1.102 ± 0.125	...	0.96	0.89	0.87	0.83	0.81	0.80	0.77	0.75	0.72	0.70

^a Band 1 = 35 GHz, Band 2 = 80 GHz, Band 3 = 100 GHz, Band 4 = 150 GHz, Band 5 = 200 GHz, Band 6 = 230 GHz, Band 7 = 345 GHz, Band 8 = 450 GHz, Band 9 = 650 GHz, Band 10 = 850 GHz

TABLE 4

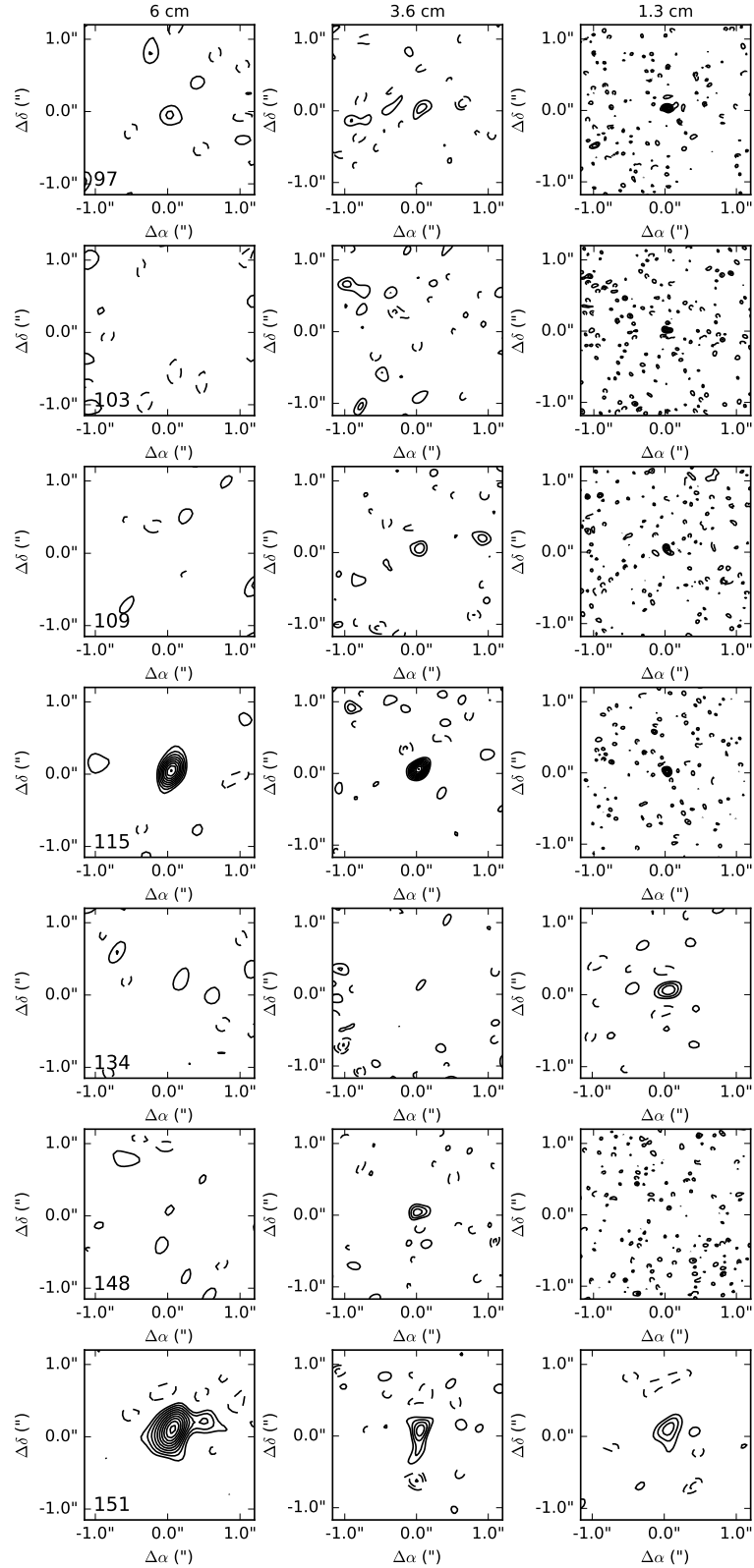
ID	1.3 cm Variable?	$(\Delta F/F)_{1.3cm}$	3.6 cm Variable?	$(\Delta F/F)_{3.6cm}$	6 cm Variable?	$(\Delta F/F)_{6cm}$
11	N	...	Y	20 ± 28	-	...
76	N	...	-	...	-	...
77	N	...	Y	144 ± 25	-	...
102	-	...	N	...	-	...
103	N	...	-	...	-	...
115	Y	78 ± 102	N	...	-	...
134	N	...	-	...	-	...
151	N	...	N	...	-	...
154	Y	37 ± 10	Y	152 ± 3	-	...
173	N	...	-	...	-	...
199	N	...	-	...	-	...
200	N	...	Y	71 ± 7	-	...
209	-	...	N	...	-	...
213	Y	158 ± 68	Y	77 ± 29	-	...
219	N	...	-	...	-	...
222	N	...	-	...	-	...
229	Y	29 ± 574	N	...	-	...
235	N	...	-	...	-	...
236	N	...	-	...	-	...
237	N	...	-	...	-	...
238	Y	64 ± 9	-	...	-	...
243	N	...	-	...	-	...
246	Y	45 ± 22	-	...	-	...
253	N	...	-	...	-	...
257	Y	122 ± 72	-	...	-	...
259	Y	125 ± 74	-	...	-	...
262	N	...	-	...	-	...
265	Y	129 ± 21	-	...	-	...
270	-	...	N	...	-	...
271	N	...	-	...	-	...
275	-	...	-	...	Y	100 ± 4
278	-	...	-	...	N	...
279	Y	20 ± 26	N	...	-	...
280	N	...	N	...	-	...
281	-	...	Y	28 ± 12	N	...
284	N	...	-	...	-	...
286	N	...	-	...	-	...
287	N	...	N	...	-	...
289	N	...	-	...	-	...
294	N	...	Y	52 ± 22	-	...
297	N	...	Y	25 ± 21	-	...
301	Y	29 ± 27	-	...	-	...
307	Y	38 ± 19	Y	67 ± 8	N	...
308	Y	19 ± 30	Y	38 ± 14	-	...
313	N	...	-	...	-	...
315	N	...	-	...	-	...
319	N	...	-	...	-	...
325	N	...	-	...	-	...
330	N	...	-	...	-	...
331	-	...	N	...	-	...
332	N	...	-	...	-	...
333	-	...	N	...	-	...
341	Y	51 ± 10	Y	55 ± 13	N	...
344	-	...	N	...	-	...
357	-	...	N	...	-	...
358	-	...	N	...	-	...
364	-	...	Y	73 ± 16	-	...
365	-	...	N	...	-	...
371	-	...	N	...	-	...
373	-	...	-	...	Y	91 ± 7
374	N	...	N	...	-	...
380	N	...	-	...	-	...
382	N	...	-	...	-	...
383	N	...	Y	39 ± 17	-	...
384	-	...	N	...	-	...
386	-	...	Y	36 ± 20	-	...

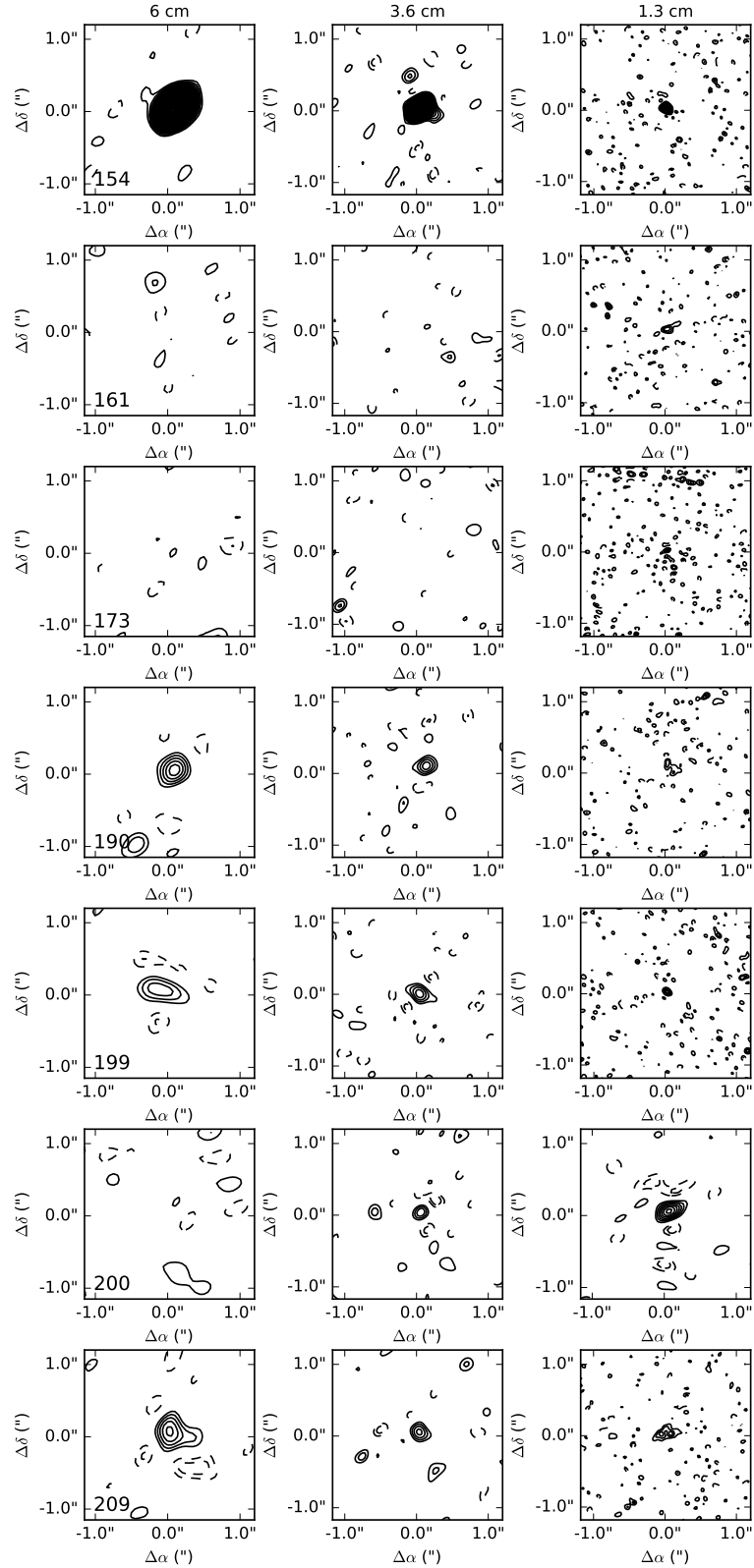
TABLE 4 — *Continued*

ID	1.3 cm Variable?	$(\Delta F/F)_{1.3cm}$	3.6 cm Variable?	$(\Delta F/F)_{3.6cm}$	6 cm Variable?	$(\Delta F/F)_{6cm}$
389	N	...	Y	70 ± 4	—	...
391	—	...	N	...	N	...
393	N	...	—	...	—	...
394	Y	72 ± 9	—	...	—	...
399	—	...	N	...	—	...
400	—	...	Y	60 ± 16	—	...
401	N	...	—	...	—	...
407	—	...	—	...	Y	101 ± 3
408	N	...	Y	31 ± 21	N	...
409	N	...	—	...	—	...
411	—	...	—	...	N	...
413	Y	41 ± 14	Y	23 ± 15	N	...
414	—	...	N	...	—	...
416	—	...	N	...	N	...
418	Y	88 ± 5	Y	63 ± 10	—	...
421	N	...	N	...	—	...
423	—	...	N	...	N	...
427	N	...	Y	33 ± 13	—	...
428	N	...	—	...	—	...
430	—	...	N	...	N	...
433	—	...	Y	39 ± 13	—	...
437	Y	284 ± 45	Y	215 ± 46	N	...
438	N	...	N	...	N	...
439	Y	24 ± 32	N	...	N	...
440	Y	299 ± 89	—	...	—	...
442	—	...	Y	29 ± 17	—	...
444	N	...	N	...	—	...
460	N	...	N	...	N	...
465	N	...	N	...	—	...
466	N	...	Y	51 ± 13	—	...
469	Y	108 ± 21	—	...	—	...
473	N	...	Y	55 ± 11	—	...
477	—	...	Y	60 ± 16	—	...
481	N	...	—	...	—	...
483	N	...	N	...	—	...
484	N	...	N	...	—	...
491	N	...	N	...	N	...
492	Y	57 ± 13	—	...	—	...
493	—	...	—	...	Y	102 ± 3
494	N	...	N	...	—	...
499	Y	28 ± 22	N	...	—	...
501	N	...	N	...	—	...
512	—	...	Y	27 ± 22	N	...
516	—	...	N	...	N	...
518	N	...	N	...	N	...
519	—	...	N	...	—	...
529	Y	99 ± 11	—	...	—	...
530	—	...	N	...	—	...
535	N	...	Y	31 ± 19	—	...
537	—	...	N	...	—	...
544	Y	102 ± 4	—	...	—	...
546	N	...	N	...	—	...
549	N	...	—	...	—	...
555	N	...	N	...	N	...
564	—	...	N	...	N	...
587	Y	136 ± 3	Y	69 ± 6	—	...
595	—	...	N	...	N	...
599	N	...	—	...	—	...
605	N	...	—	...	—	...
608	N	...	Y	38 ± 18	—	...
616	N	...	—	...	—	...
617	Y	24 ± 14	Y	49 ± 12	—	...
621	N	...	—	...	—	...
649	N	...	—	...	—	...
658	N	...	—	...	—	...
665	N	...	—	...	—	...

TABLE 4 — *Continued*

ID	1.3 cm Variable?	$(\Delta F/F)_{1.3cm}$	3.6 cm Variable?	$(\Delta F/F)_{3.6cm}$	6 cm Variable?	$(\Delta F/F)_{6cm}$
668	N	...	—	...	—	...
690	N	...	—	...	—	...
715	Y	92 ± 24	—	...	—	...
730	Y	51 ± 9	Y	50 ± 6	Y	47 ± 11
737	Y	905 ± 487	—	...	—	...
760	N	...	—	...	—	...
786	N	...	—	...	—	...
821	N	...	—	...	—	...
835	N	...	—	...	—	...
842	N	...	—	...	—	...
848	N	...	—	...	—	...
859	N	...	—	...	—	...
862	N	...	—	...	—	...
891	N	...	—	...	—	...
897	N	...	—	...	—	...

FIG. 7.— *Continued*

FIG. 8.— *Continued*

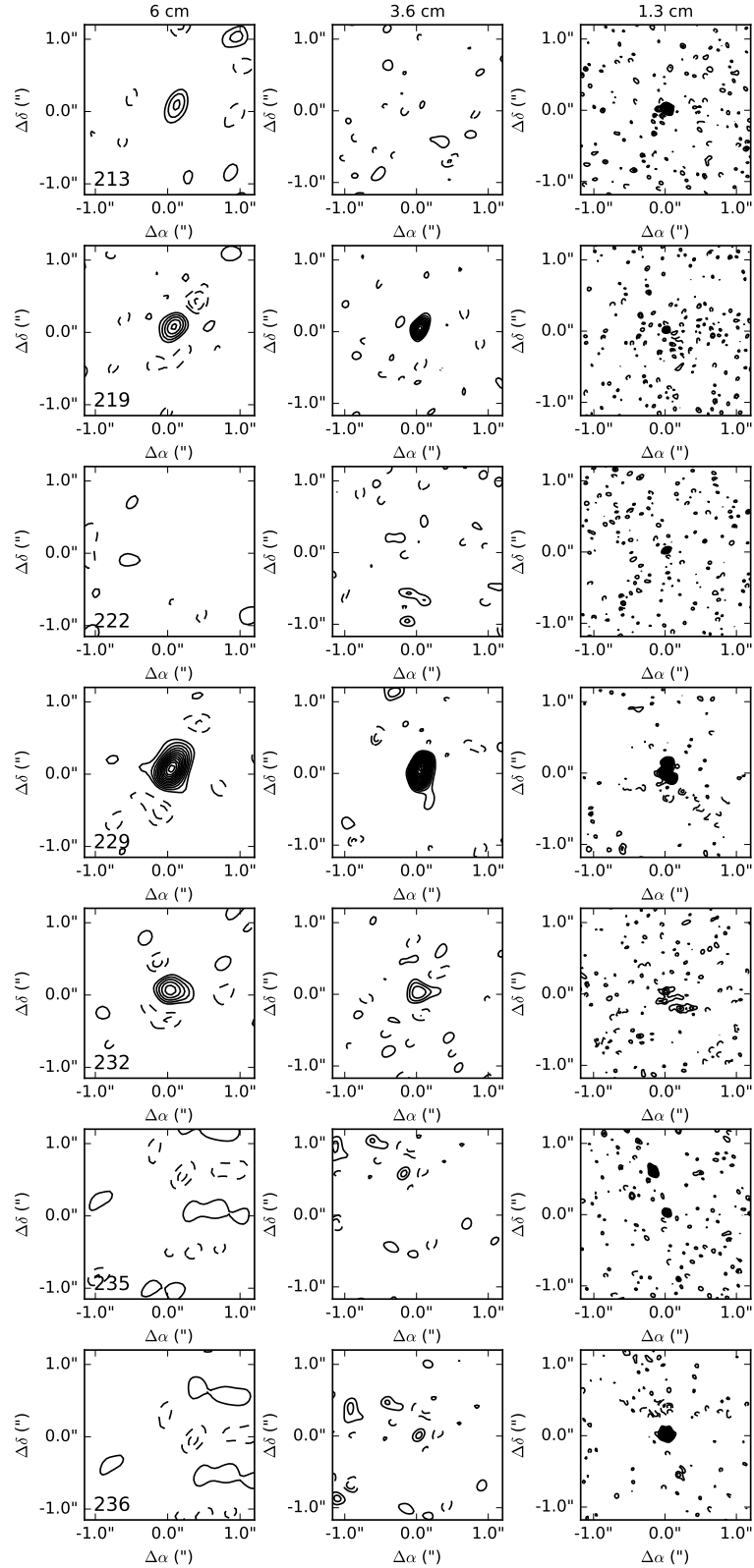
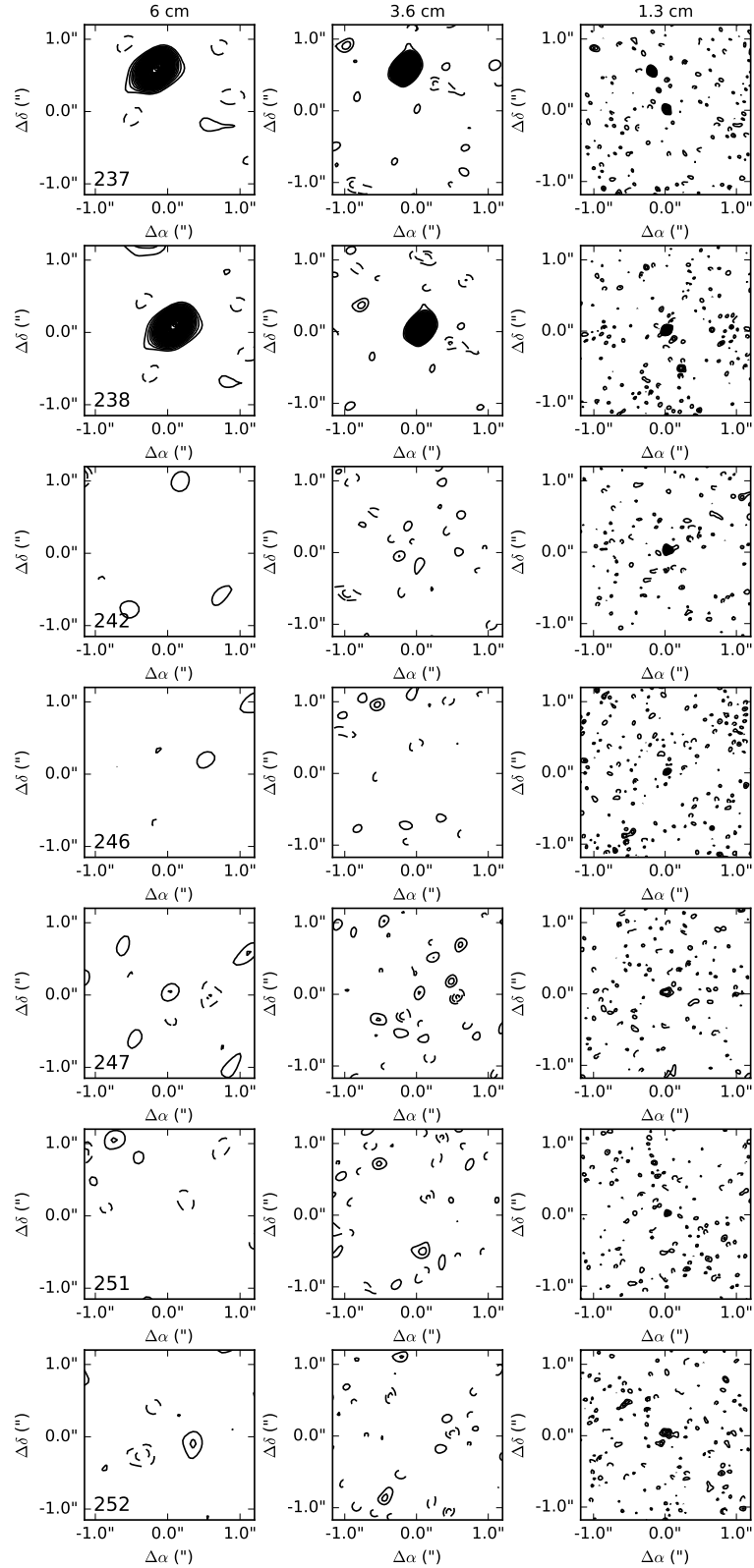
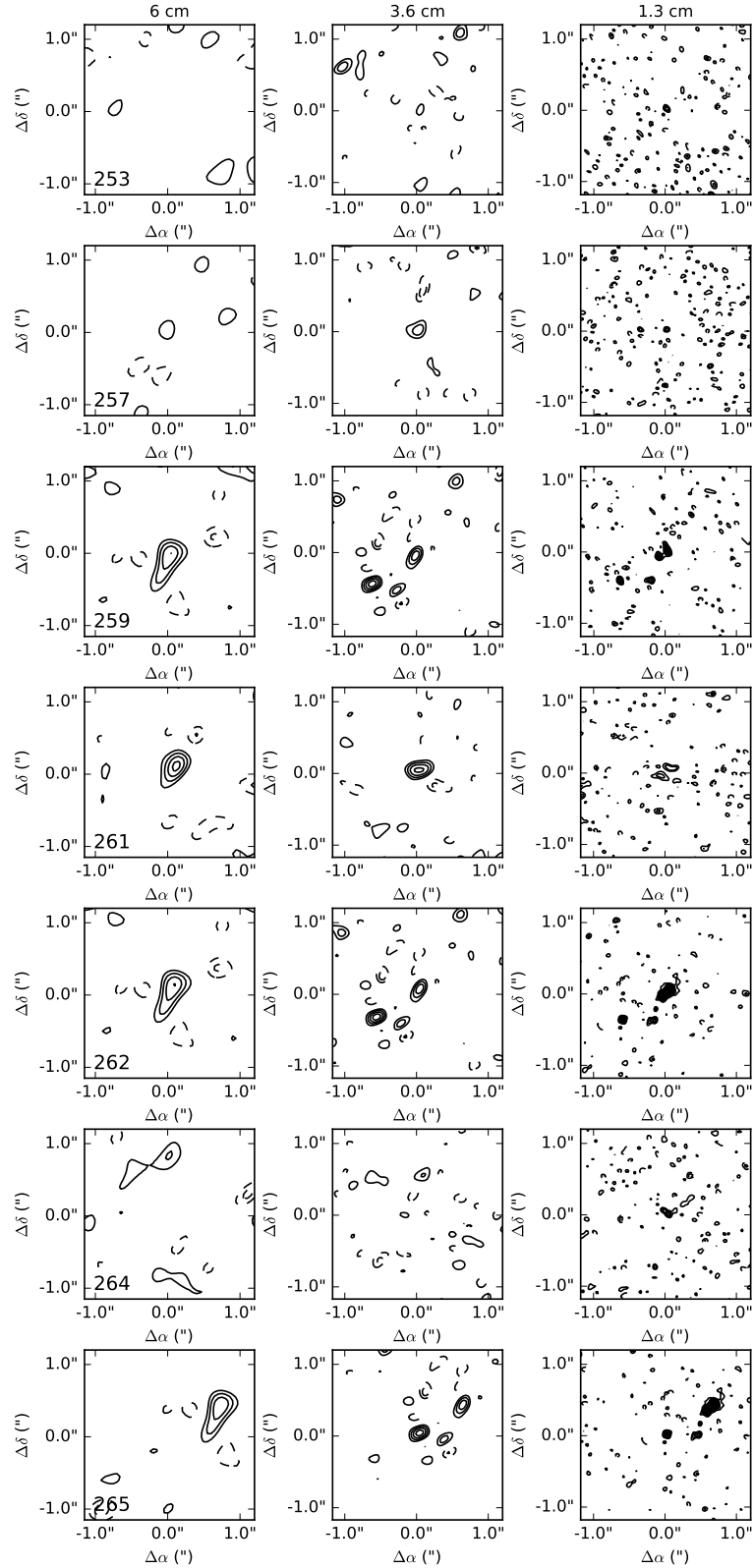
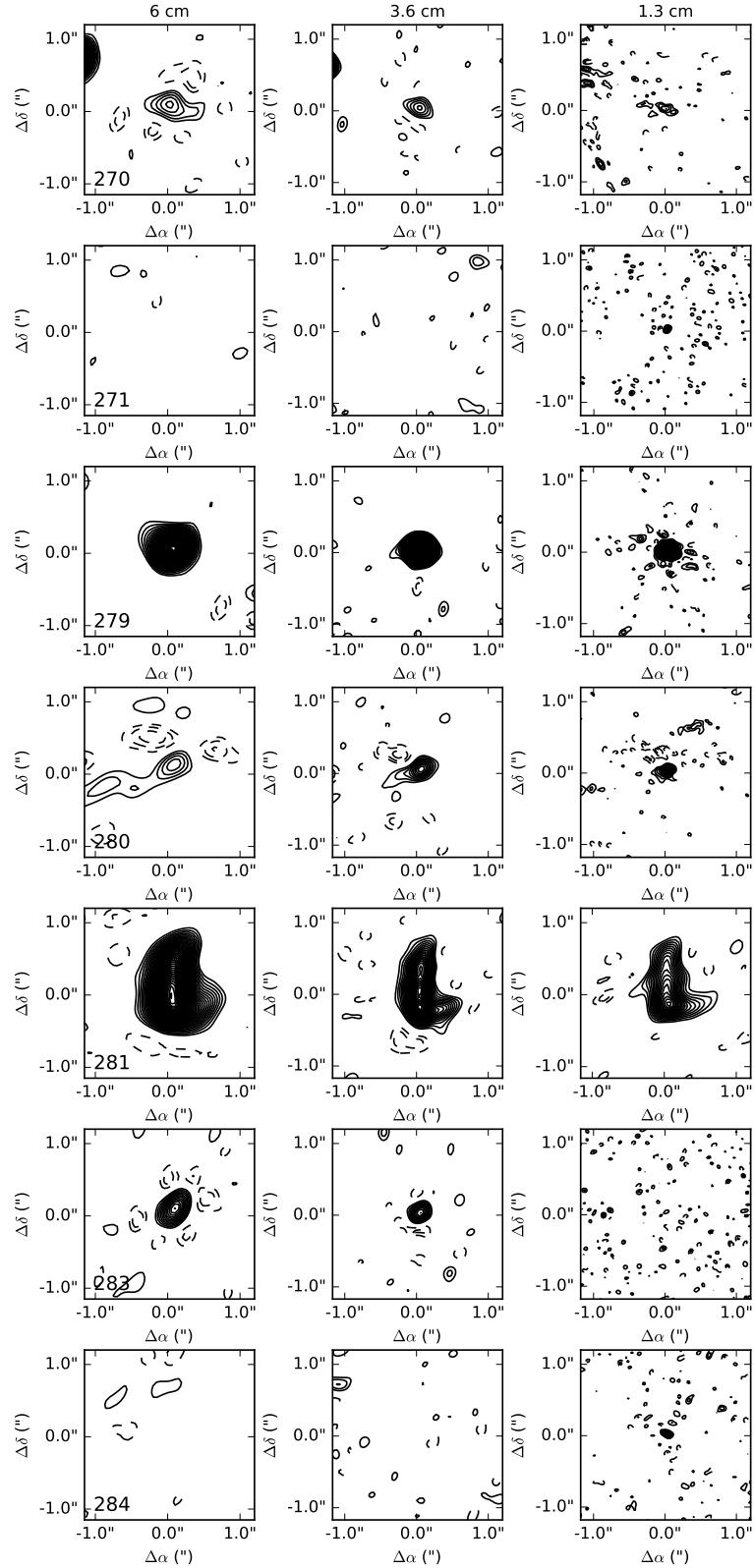
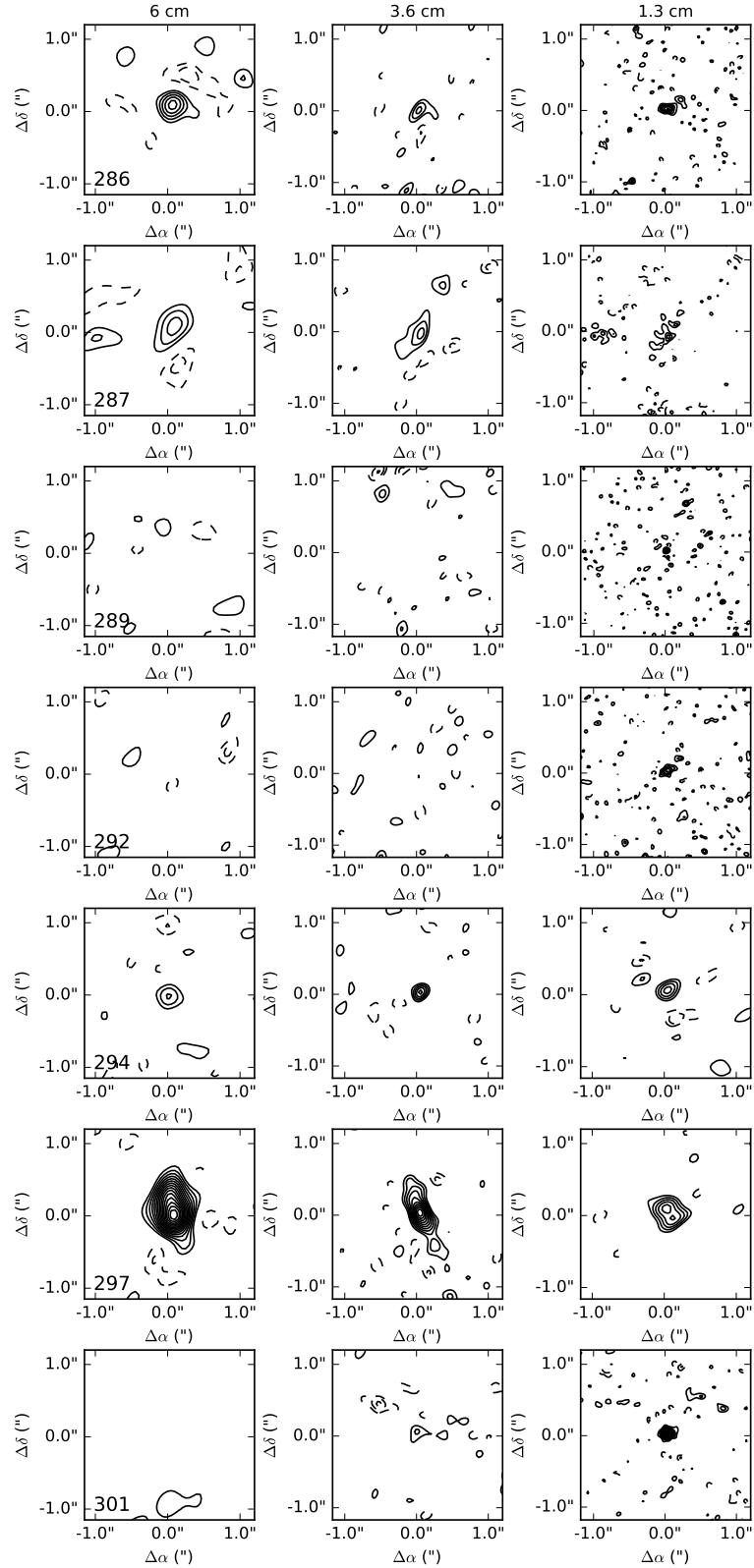


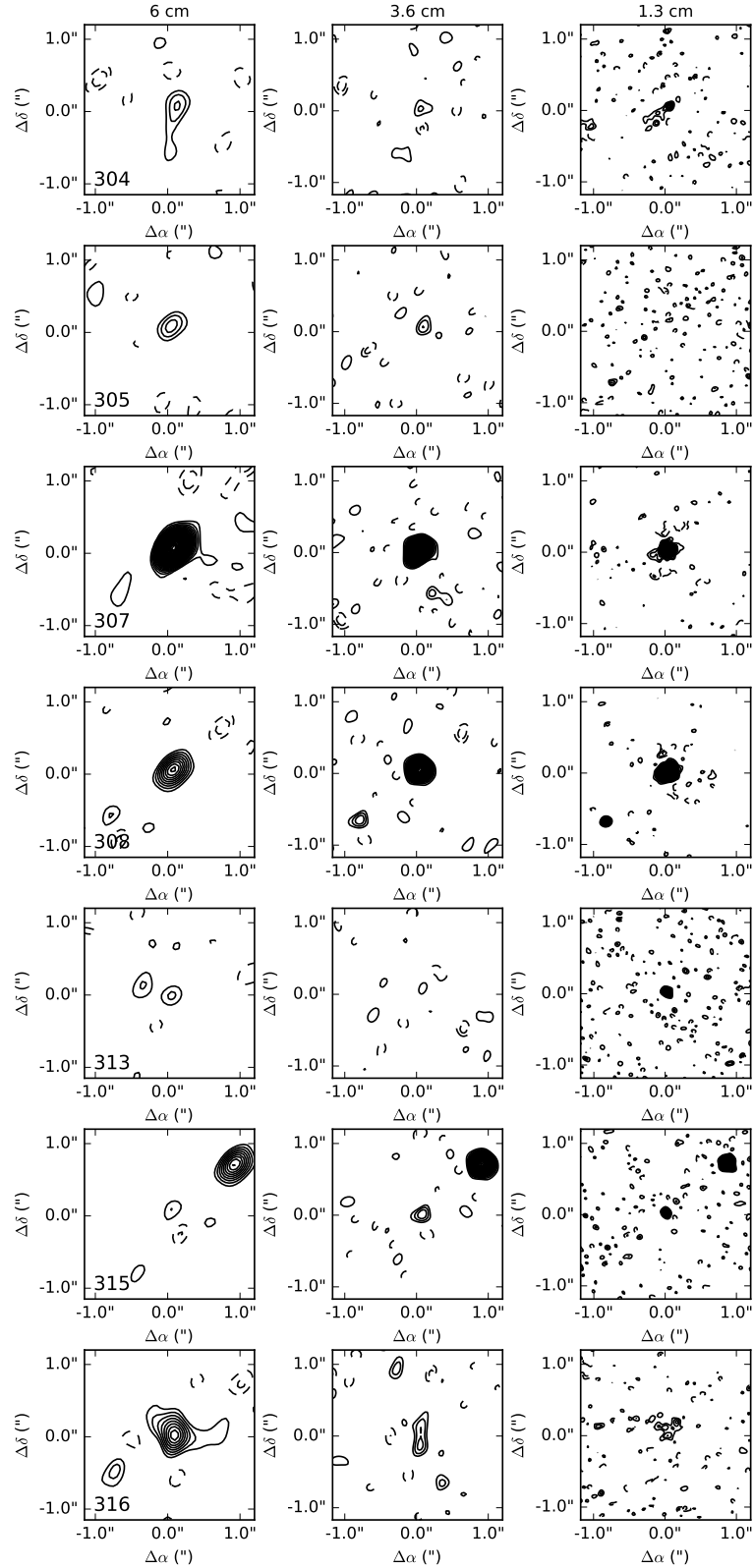
FIG. 9.—Continued

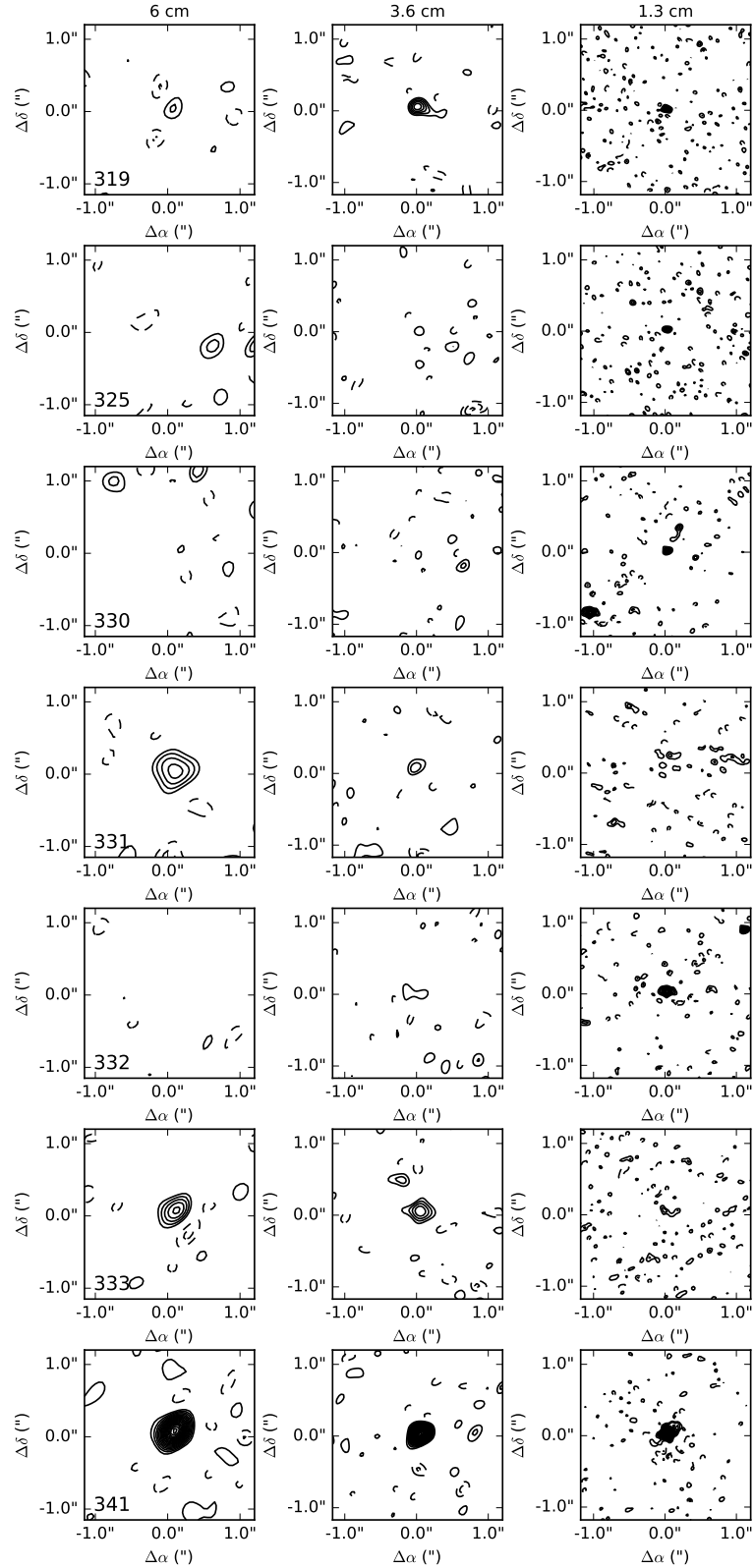
FIG. 10.— *Continued*

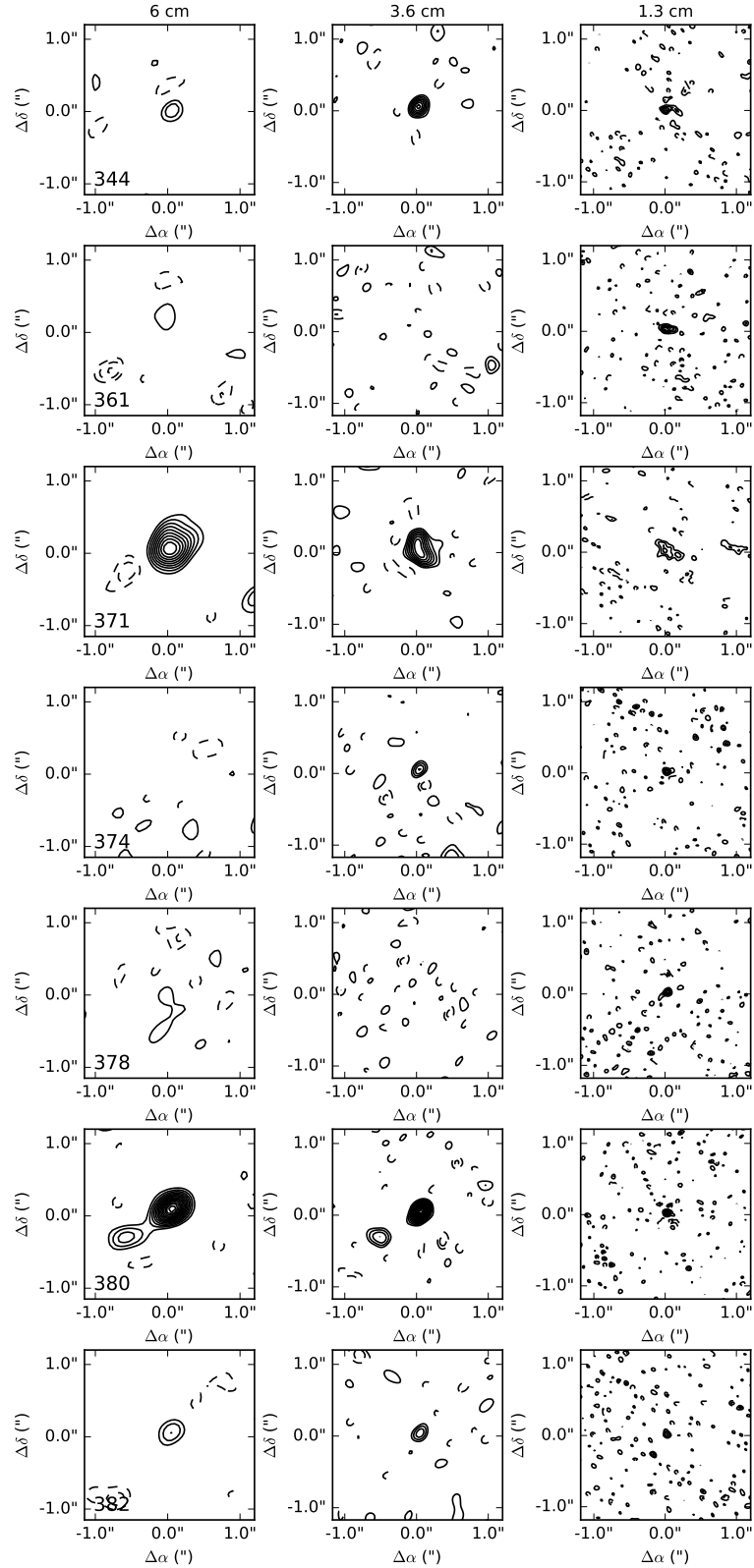
FIG. 11.— *Continued*

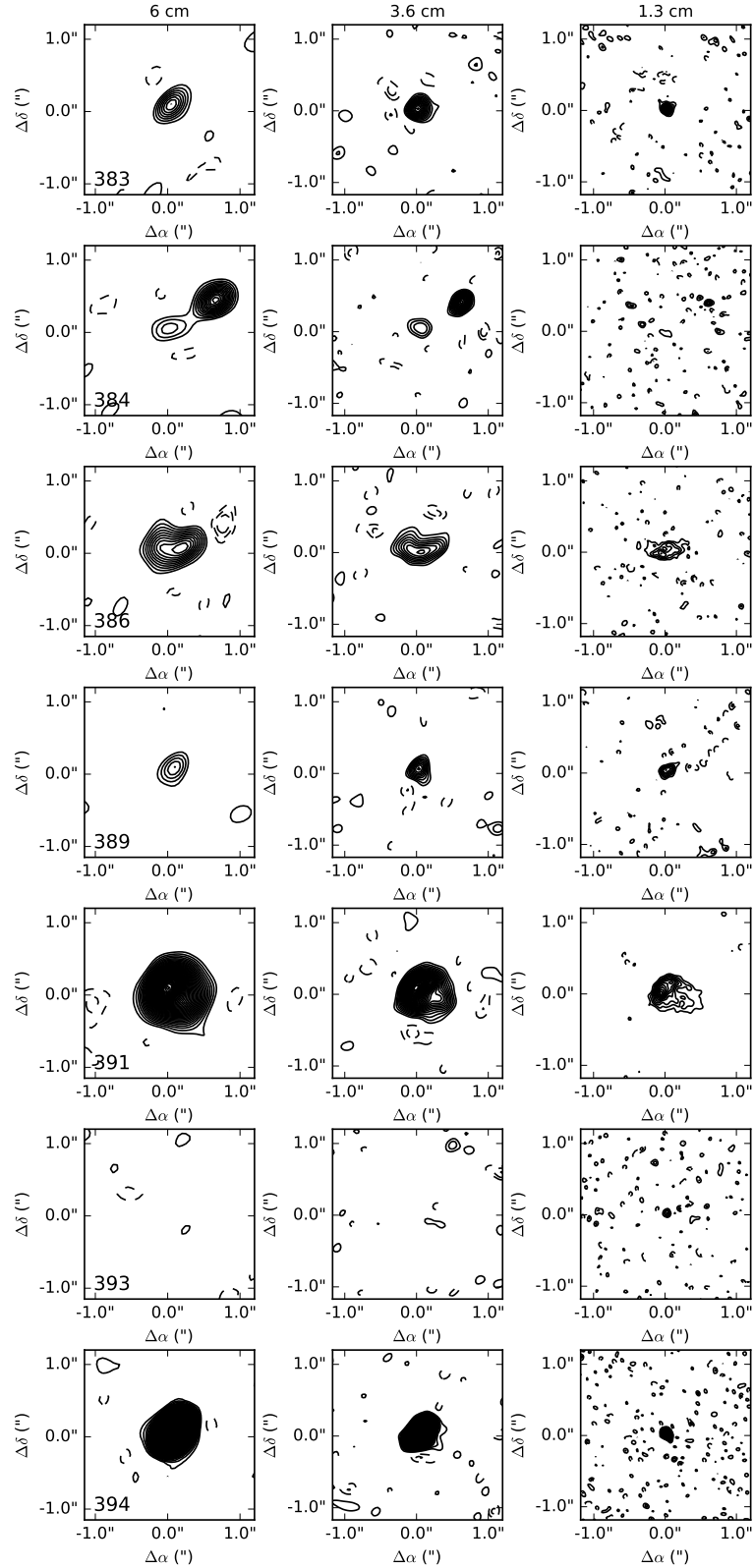
FIG. 12.— *Continued*

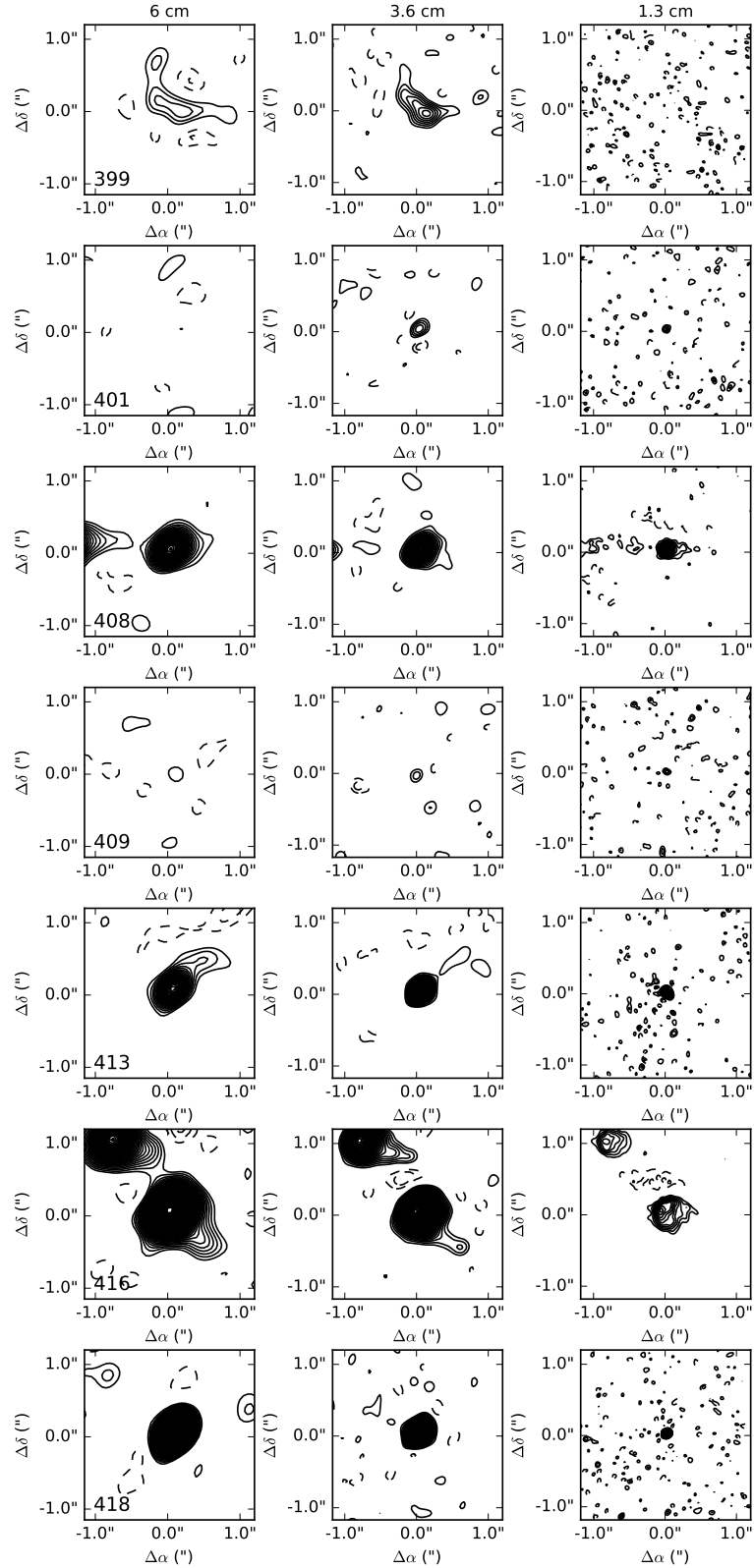
FIG. 13.— *Continued*

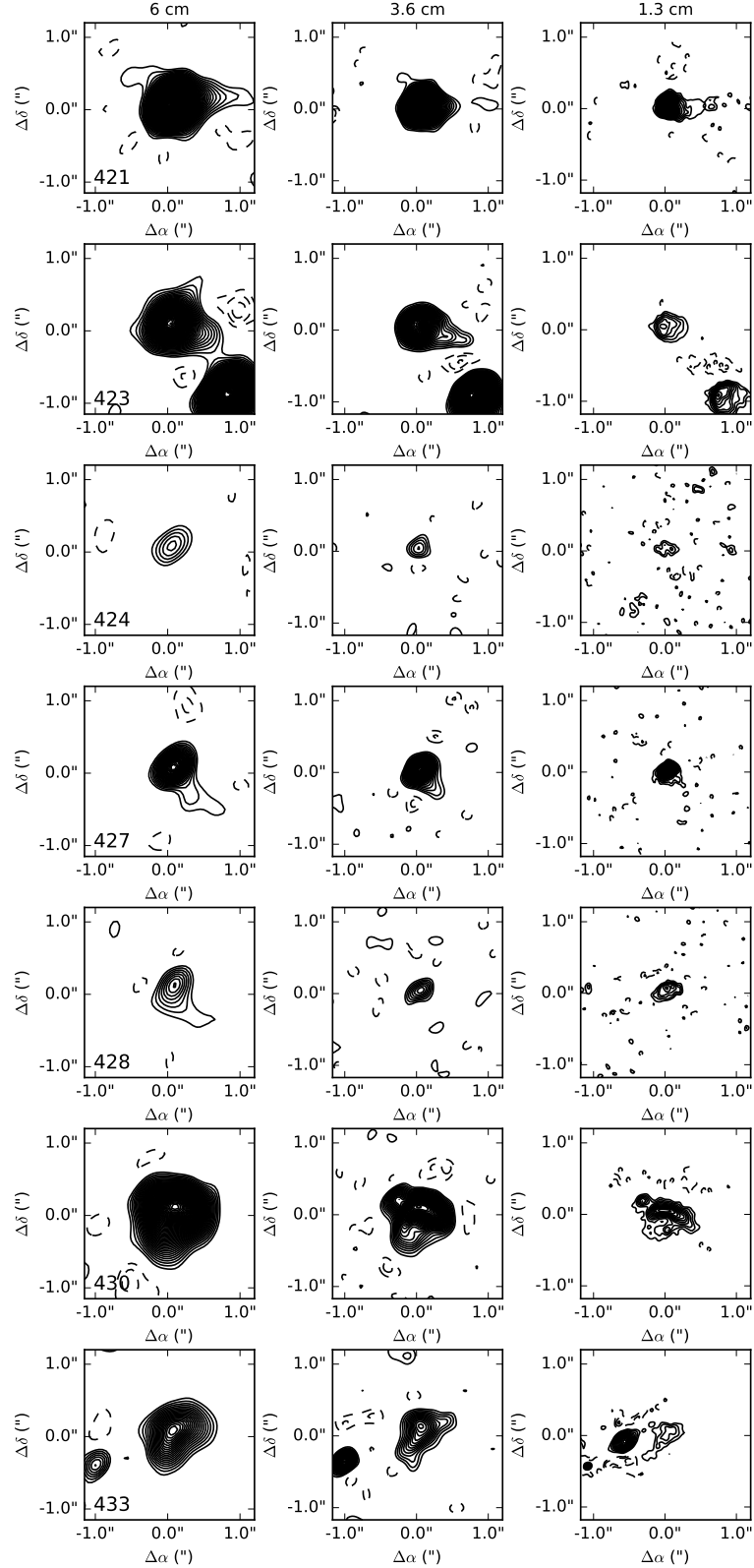
FIG. 14.— *Continued*

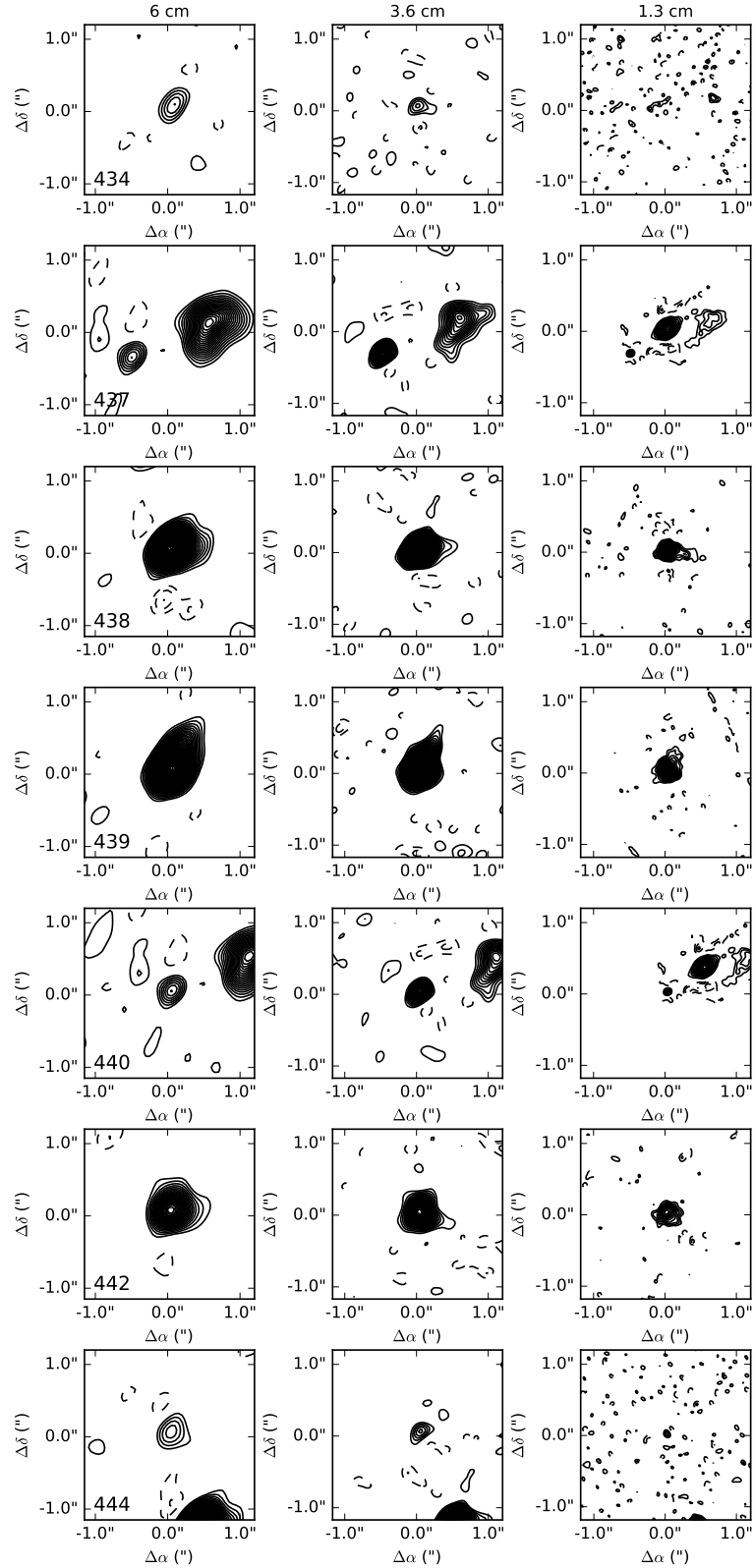
FIG. 15.— *Continued*

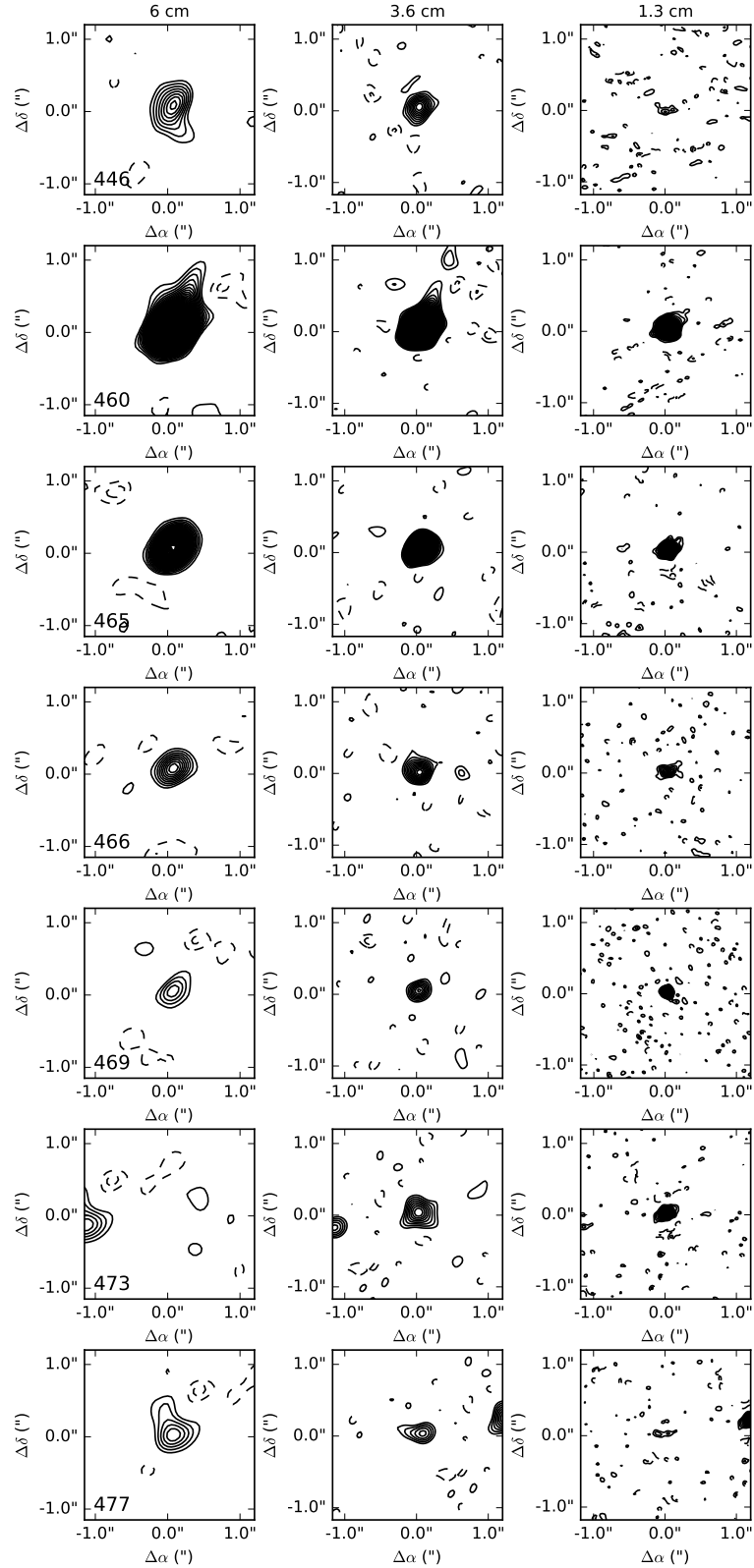
FIG. 16.— *Continued*

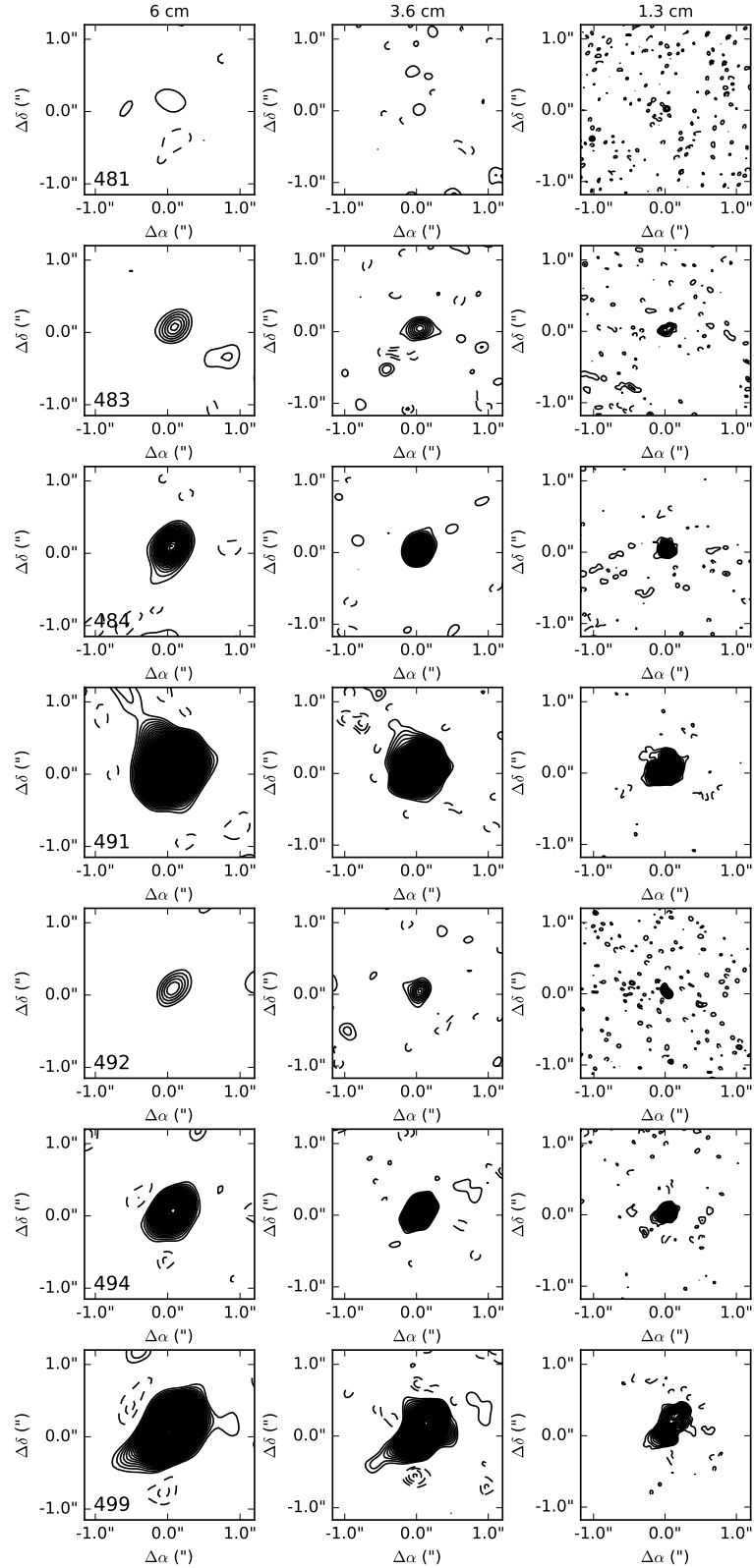
FIG. 17.— *Continued*

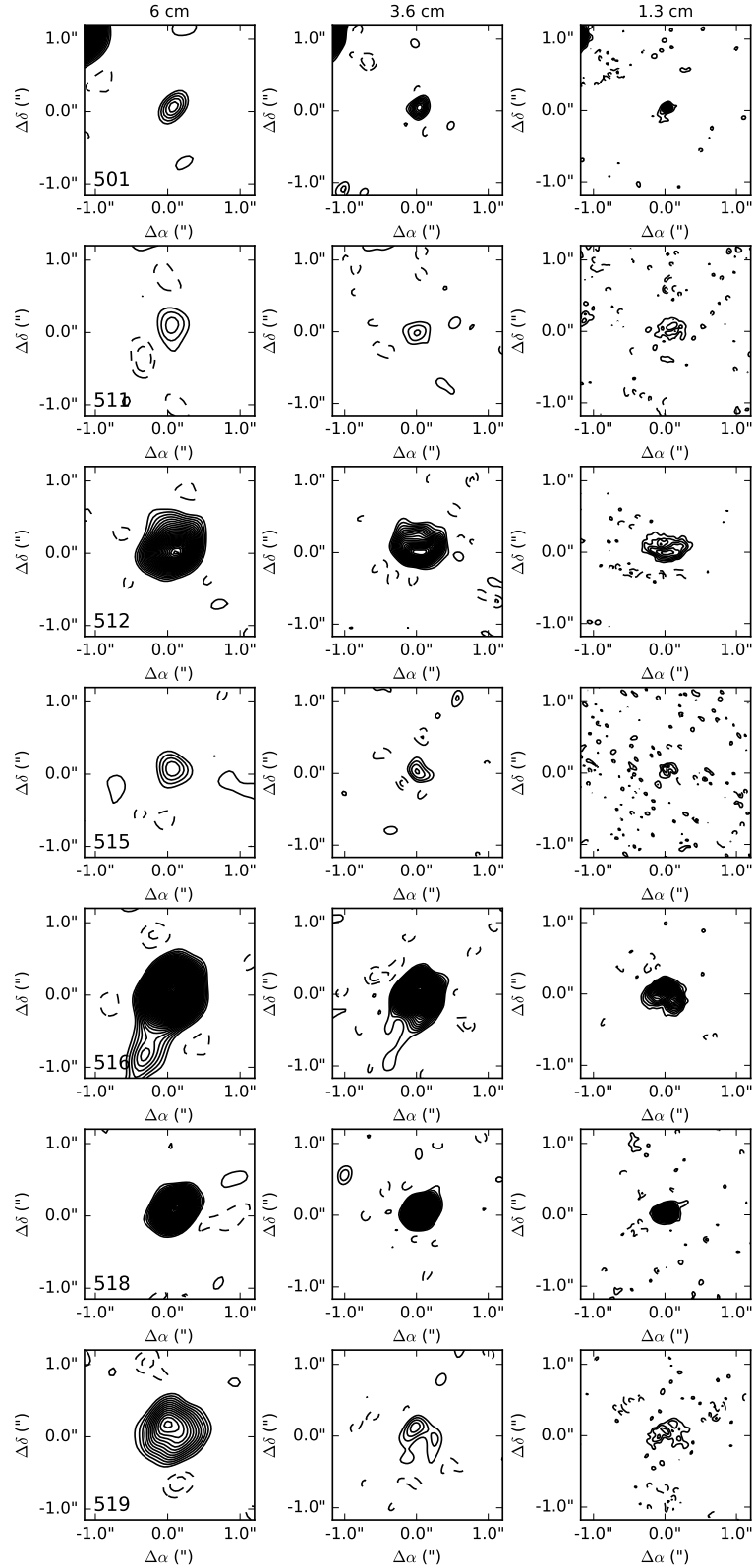
FIG. 18.— *Continued*

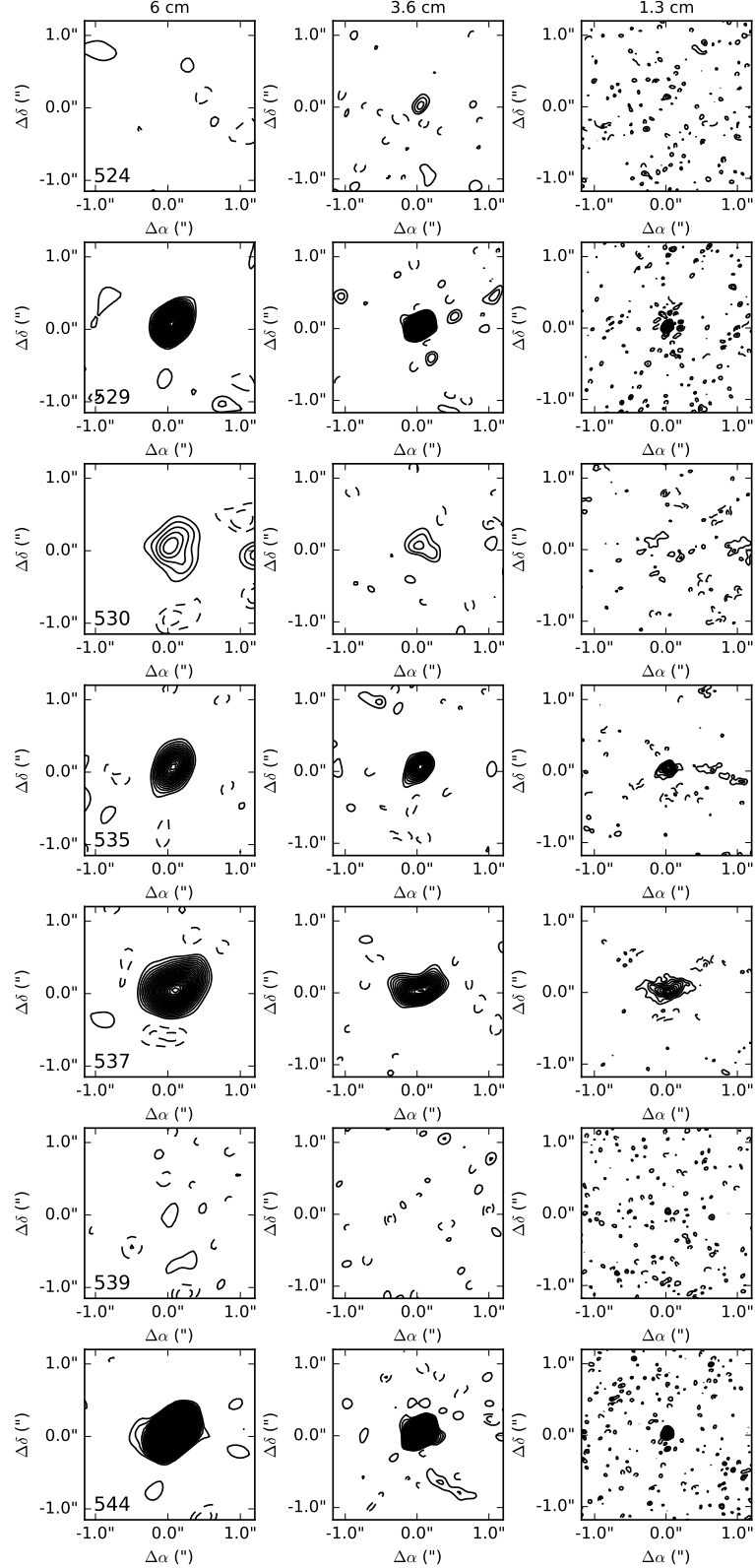
FIG. 19.— *Continued*

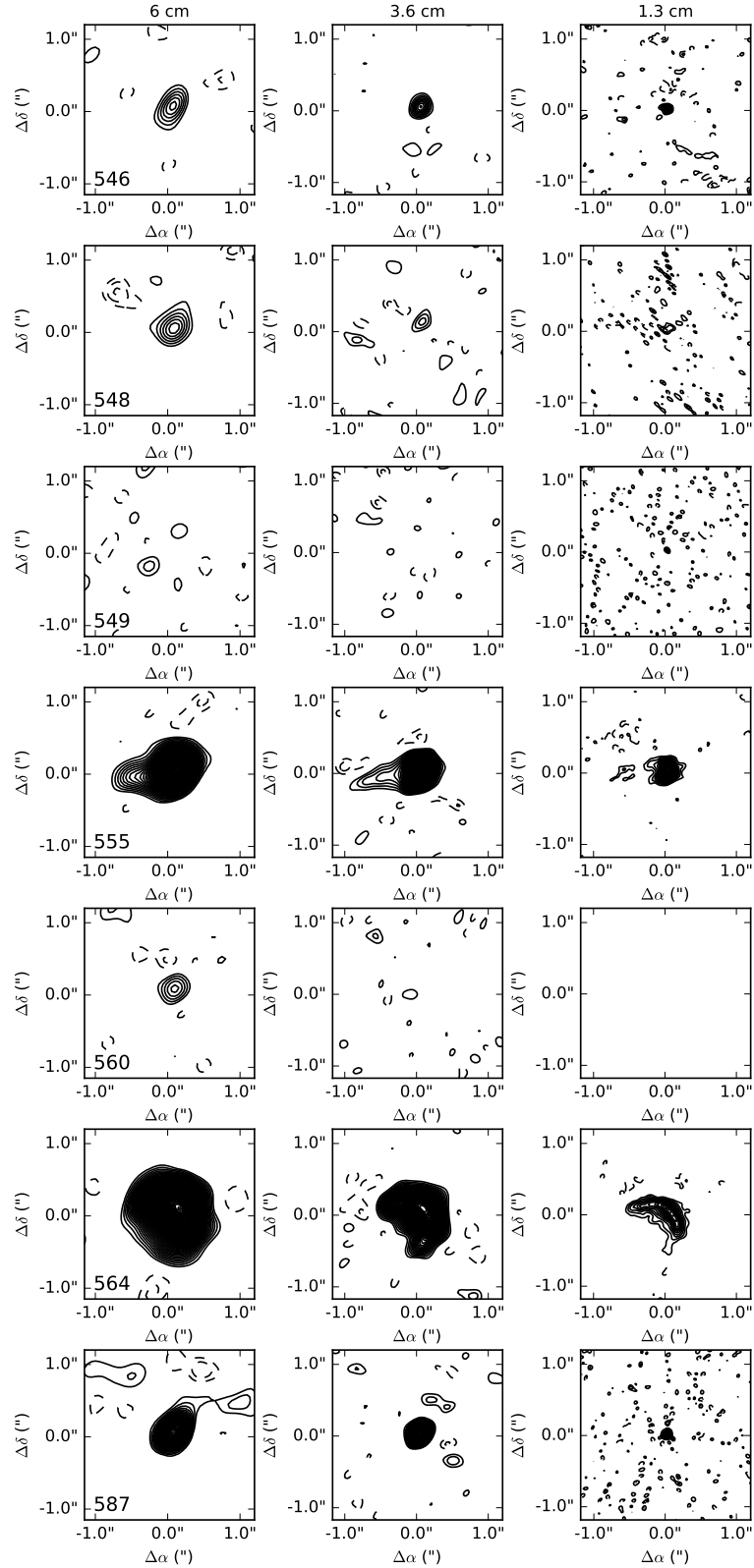
FIG. 20.— *Continued*

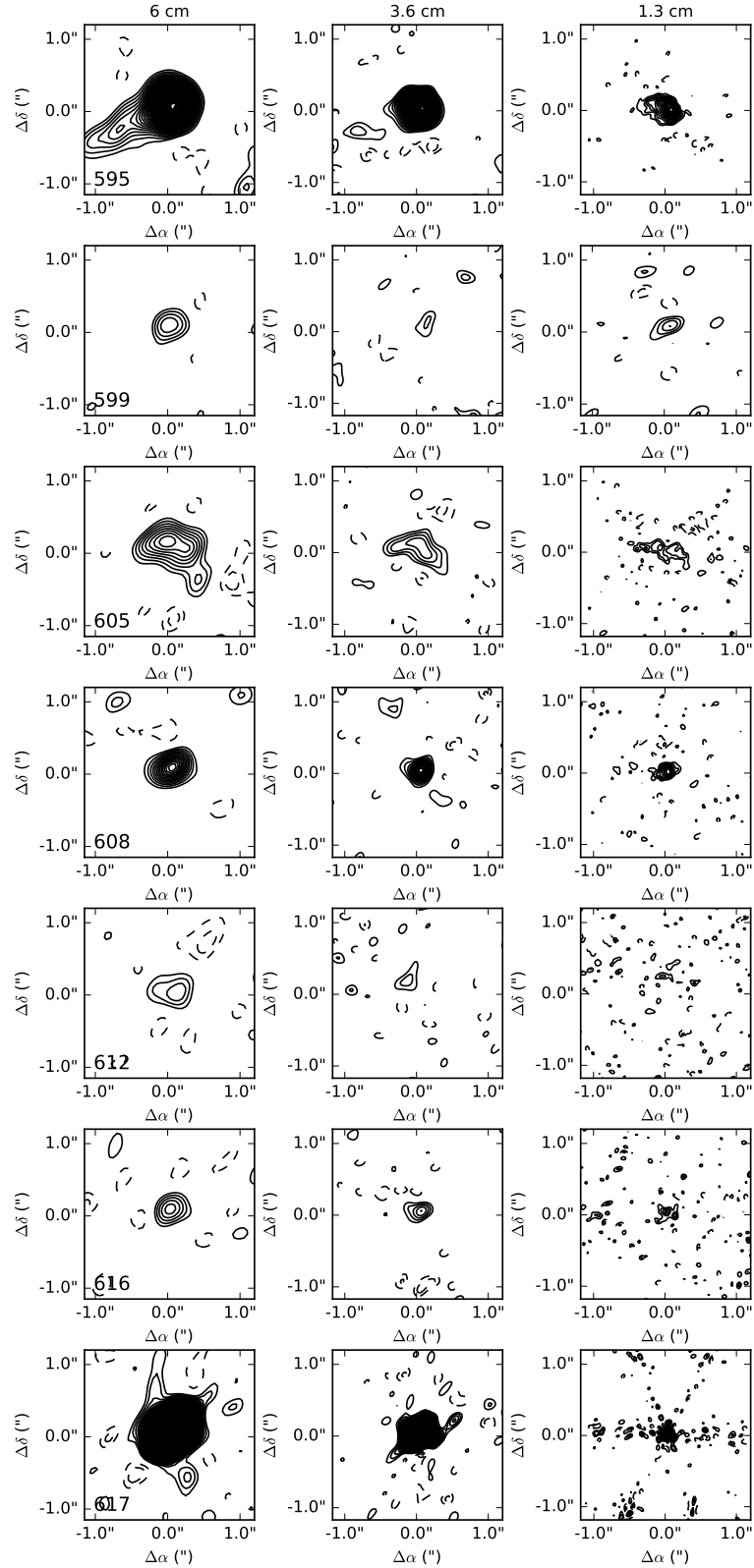
FIG. 21.— *Continued*

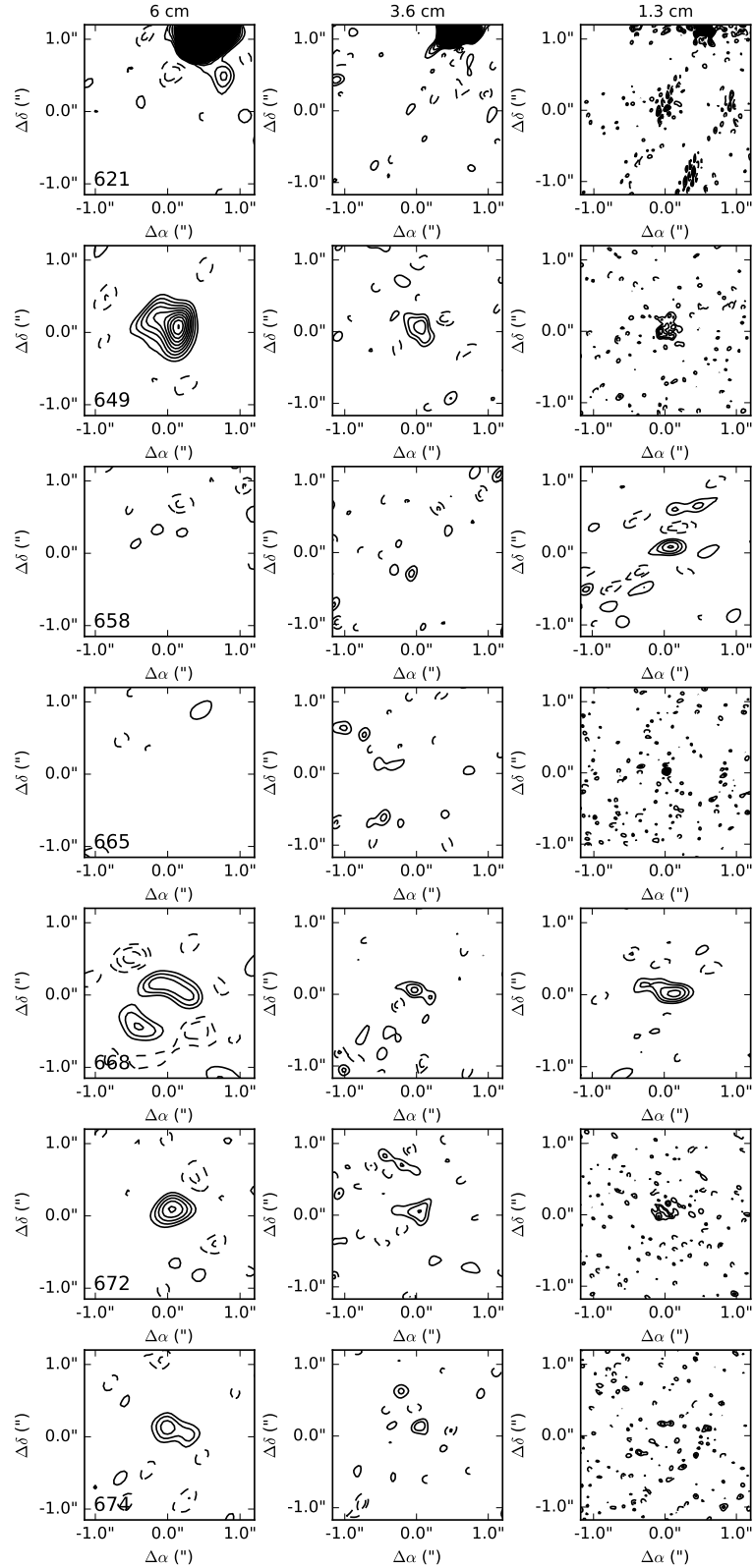
FIG. 22.— *Continued*

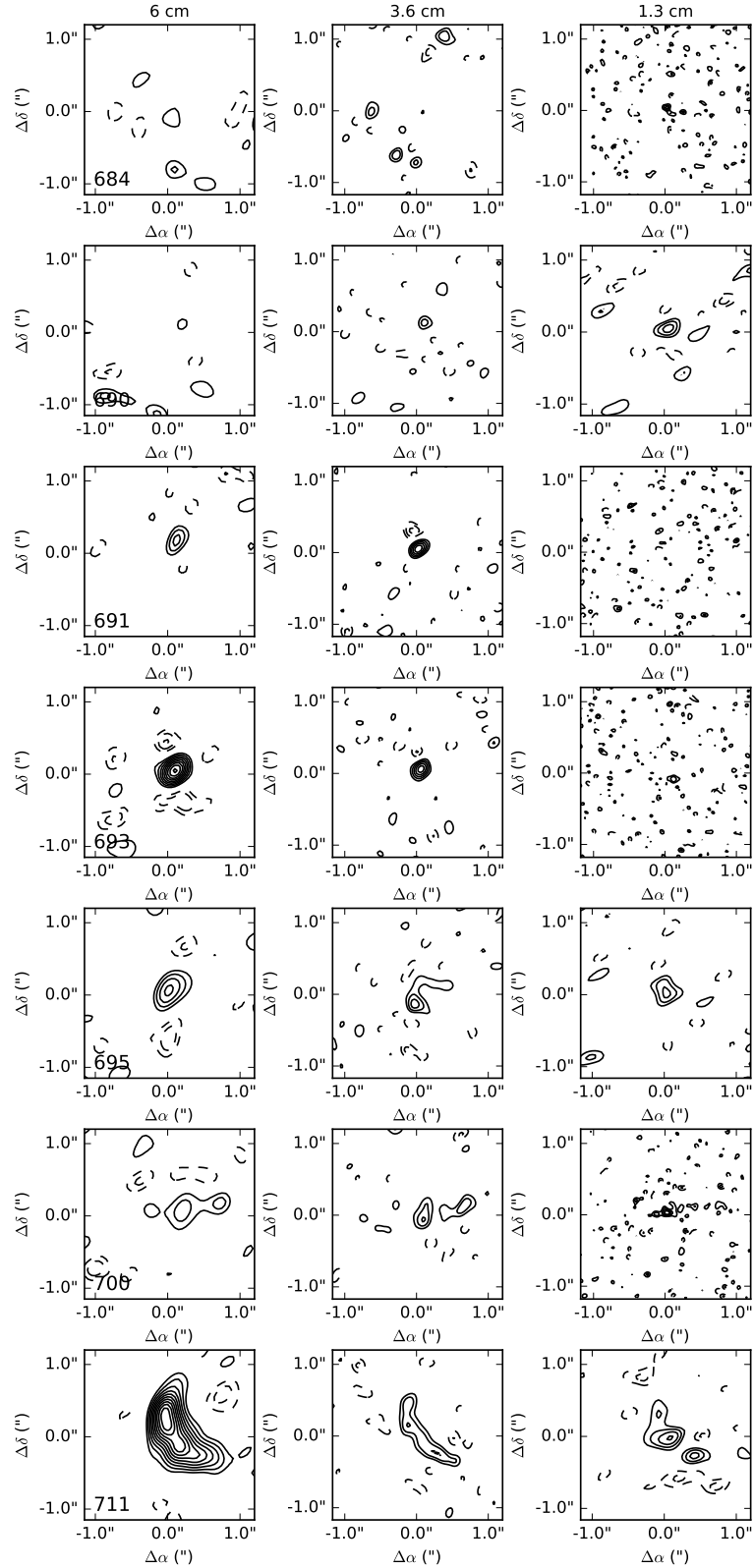
FIG. 23.— *Continued*

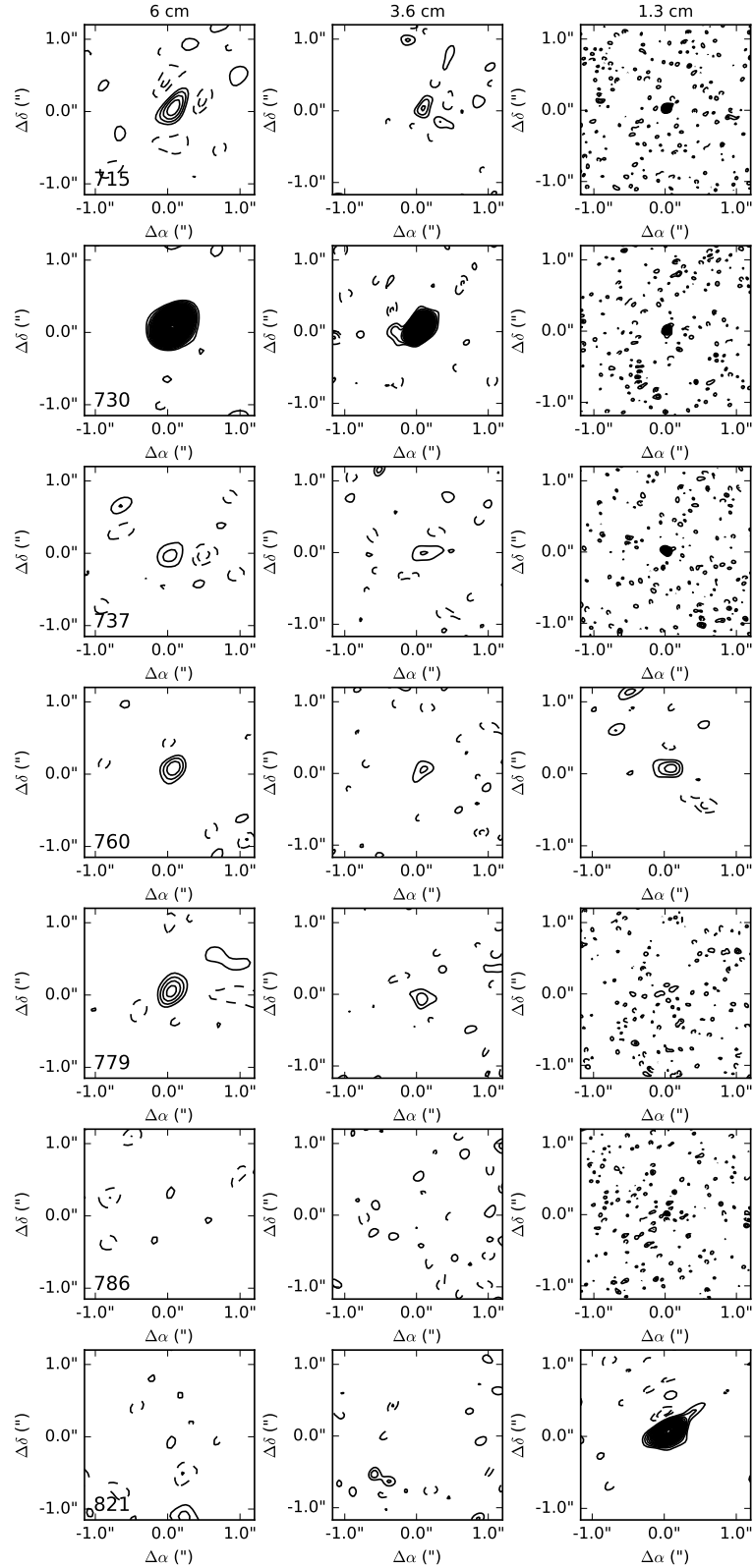
FIG. 24.— *Continued*

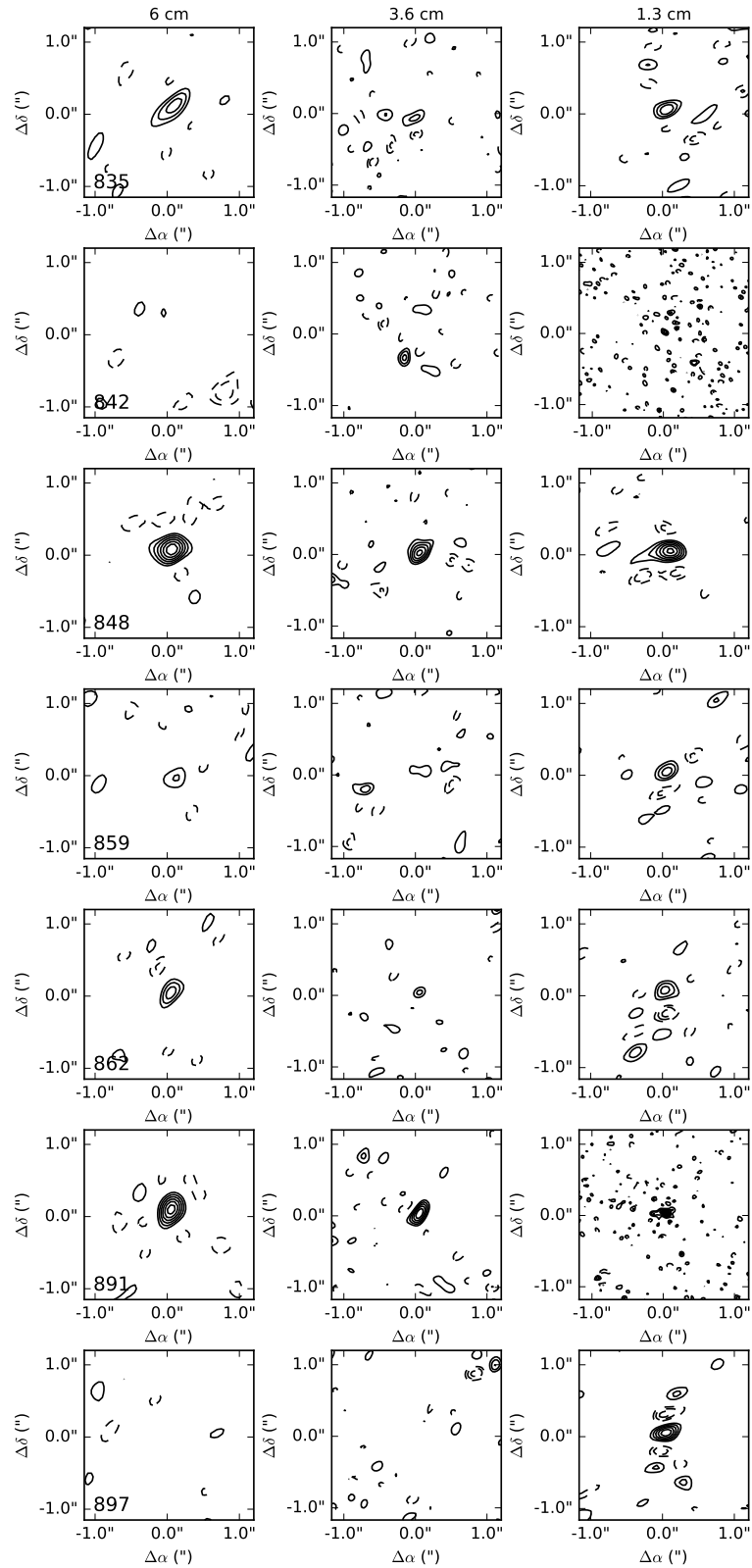
FIG. 25.— *Continued*

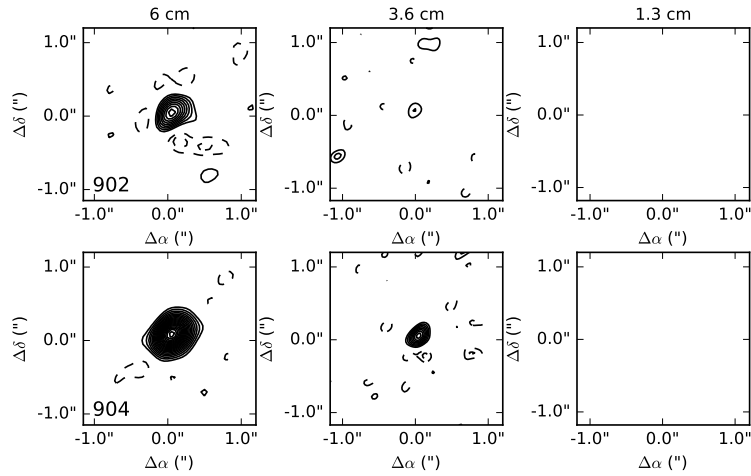
FIG. 26.— *Continued*

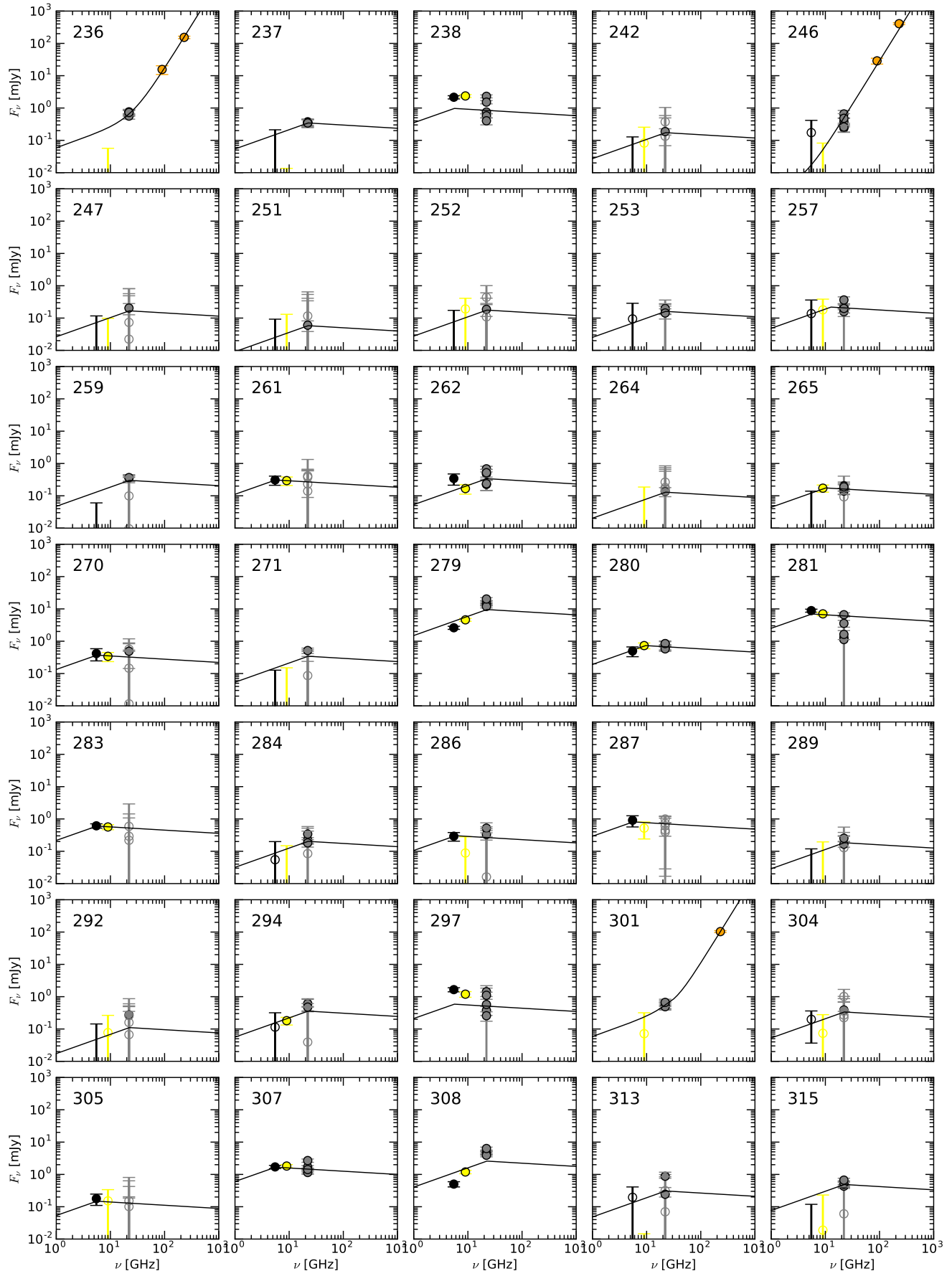
FIG. 27.— *Continued*

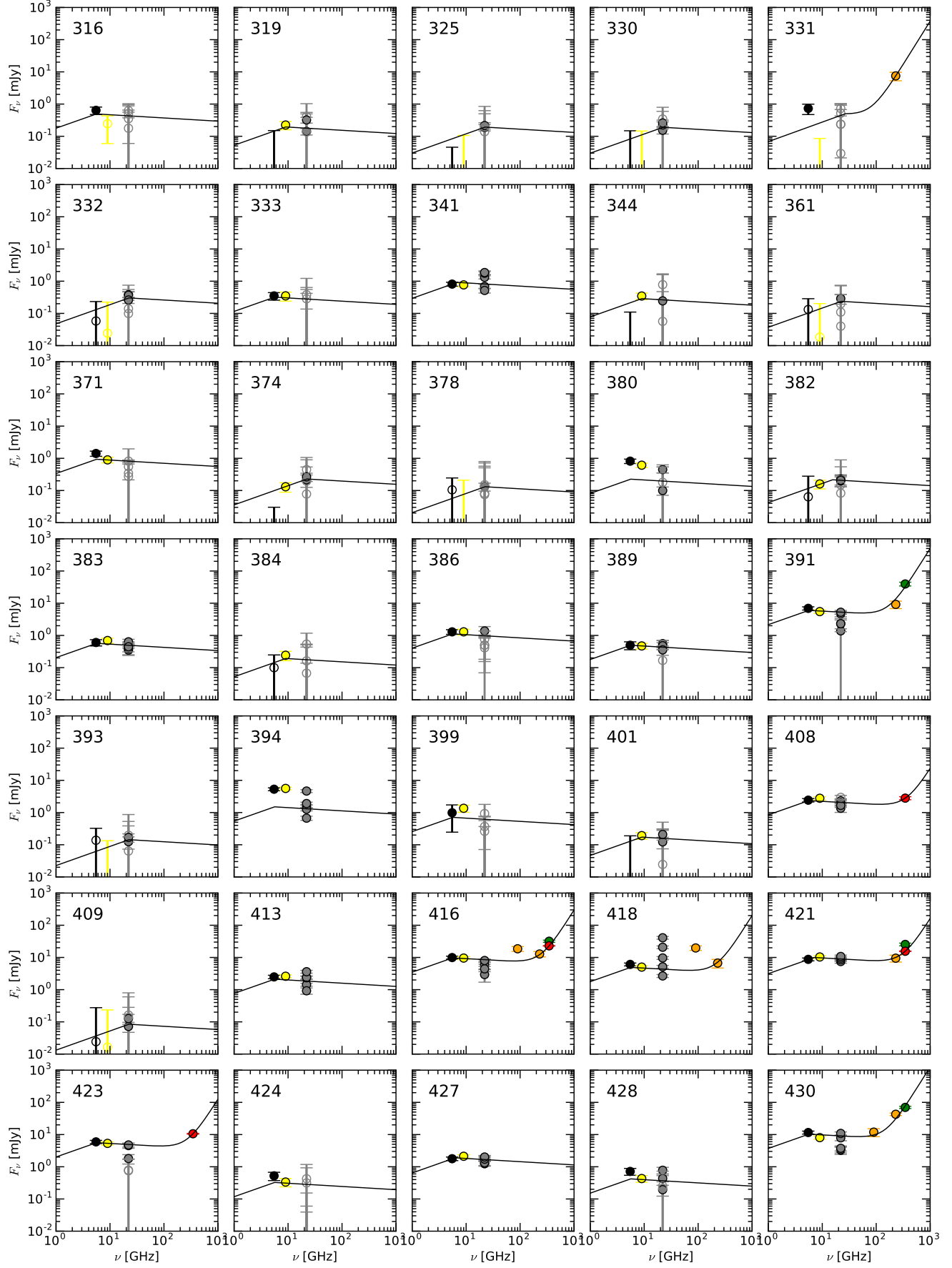
FIG. 28.— *Continued*

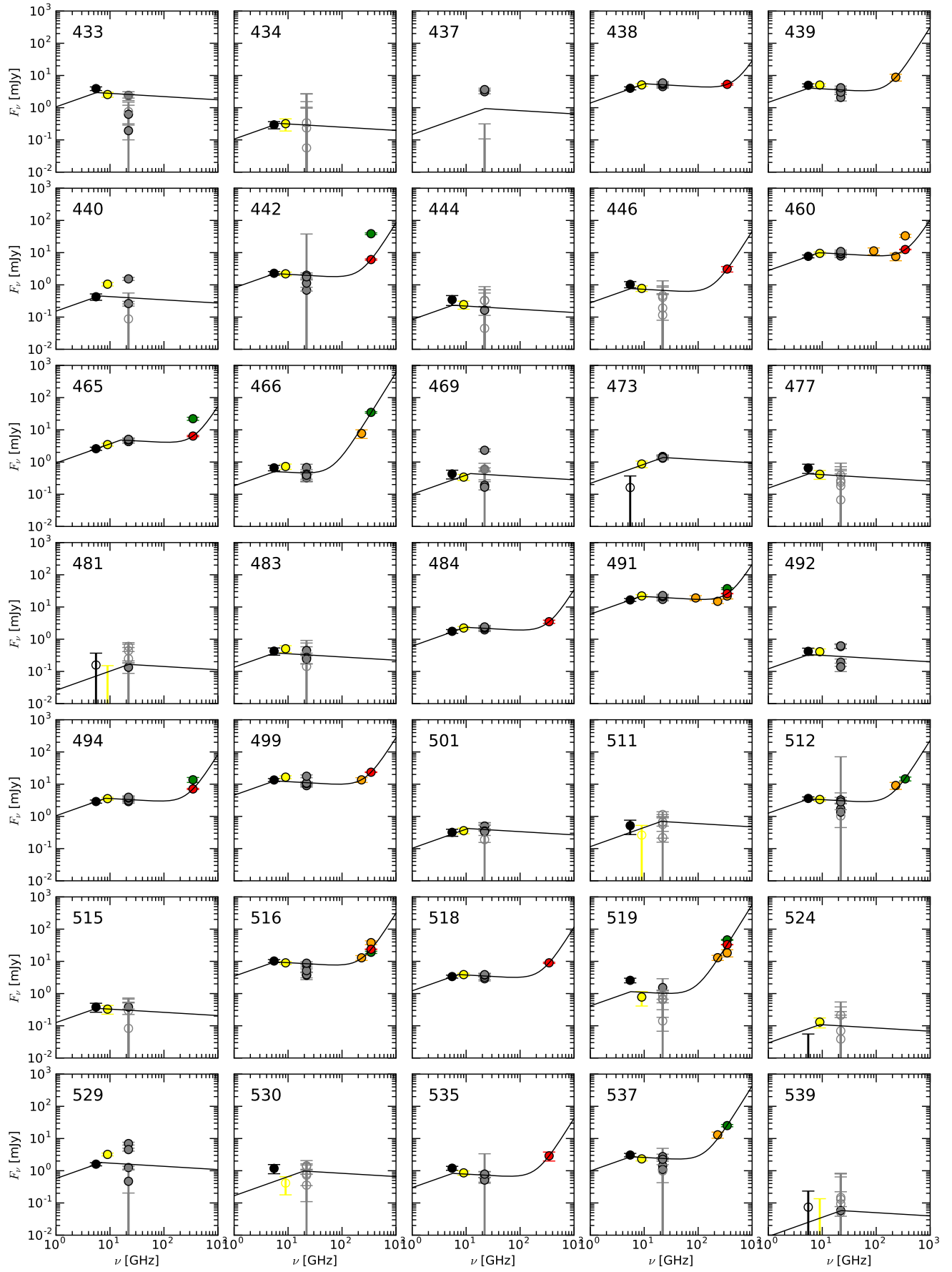
FIG. 29.— *Continued*

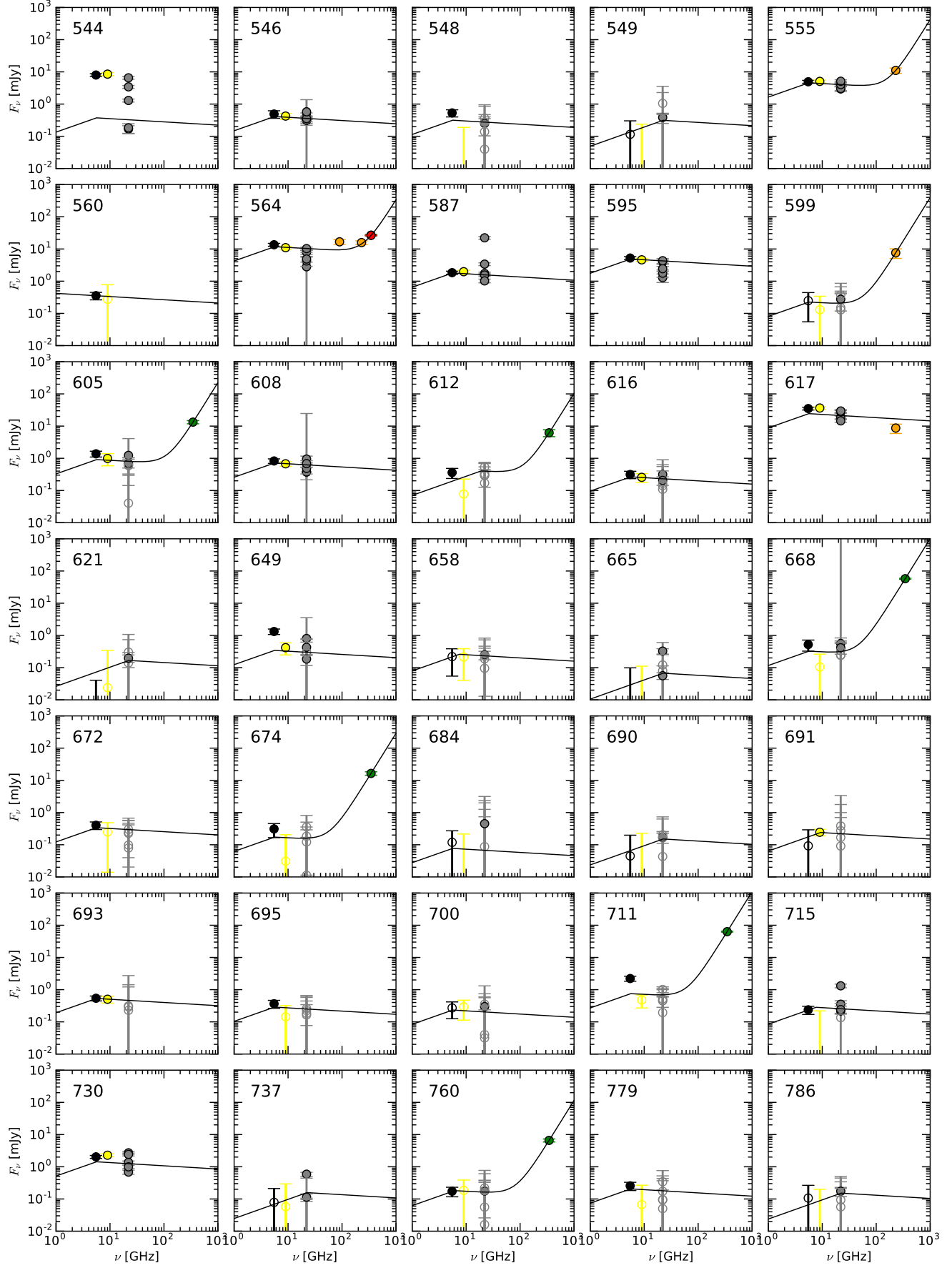
FIG. 30.— *Continued*

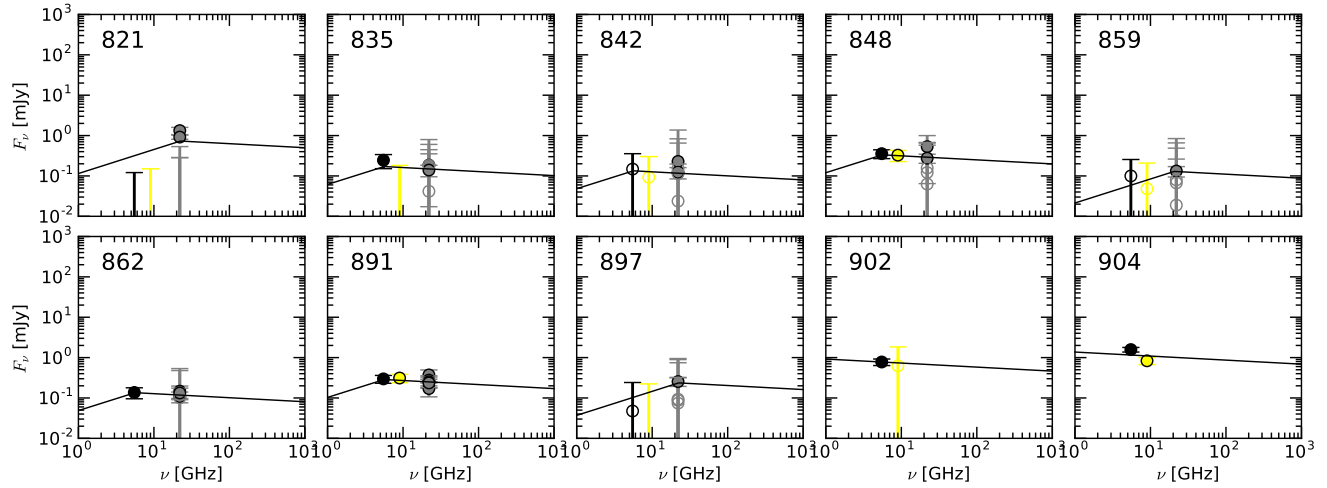
FIG. 31.— *Continued*

FIG. 32.— *Continued*

FIG. 33.— *Continued*

FIG. 34.— *Continued*

FIG. 35.— *Continued*

FIG. 36.— *Continued*